DESIGN MODIFICATIONS OF DYNAMICALLY LOADED STRUCTURES USING STRUCTURAL OPTIMIZATION

AIZZAT SAZALI BIN YAHAYA RASHID

FACULTY OF ENGINEERING
UNIVERSITY OF MALAYA
KUALA LUMPUR

2014

DESIGN MODIFICATIONS OF DYNAMICALLY LOADED STRUCTURES USING STRUCTURAL OPTIMIZATION

AIZZAT SAZALI BIN YAHAYA RASHID

DISSERTATION SUBMITTED IN FULFILMENT OF THE REQUIREMENTS FOR THE DEGREE OF MASTER OF ENGINEERING SCIENCE

FACULTY OF ENGINEERING
UNIVERSITY OF MALAYA
KUALA LUMPUR

2014

Original Literary Work Declaration

Name of the candidate: **Aizzat Sazali Bin Yahaya Rashid**
Registration/Matric No: **KGA100027**
Name of the Degree: **Master of Engineering Science (M. Eng. Sc.)**
Title of Dissertation: **Design Modifications of Dynamically Loaded Structures Using Structural Optimization**

Field of Study: **Mechanical Engineering**

I do solemnly and sincerely declare that:
(1) I am the sole author /writer of this work;
(2) This work is original;
(3) Any use of any work in which copyright exists was done by way of fair dealings and any expert or extract from, or reference to or reproduction of any copyright work has been disclosed expressly and sufficiently and the title of the Work and its authorship has been acknowledged in this Work;
(4) I do not have any actual knowledge nor do I ought reasonably to know that the making of this work constitutes an infringement of any copyright work;
(5) I, hereby assign all and every rights in the copyrights to this Work to the University of Malaya (UM), who henceforth shall be owner of the copyright in this Work and that any reproduction or use in any form or by any means whatsoever is prohibited without the written consent of UM having been first had and obtained actual knowledge;
(6) I am fully aware that if in the course of making this Work I have infringed any copyright whether internationally or otherwise, I may be subject to legal action or any other action as may be determined by UM.

Candidate's Signature Date:

Subscribed and solemnly declared before,

Witness Signature: Date:

Name:
Designation:

Abstract

The main aim of this study is to introduce modifications or reinforcements to the design of dynamically loaded structures by using structural optimization method. Two conditions of structural dynamic modification using structural optimization were examined, namely SDM for existing structure, and SDM at conceptual stage. The study aims at assessing the efficacy of structural optimization approach in ascertaining optimum solutions in SDM compared to the conventional approach employing Finite Element Analysis (FEA). Modal analysis was employed to find the natural frequencies and the corresponding mode shapes experimentally using Experimental Modal Analysis (EMA) and Operating Deflection Shape (ODS) while computationally using Finite Element Method (FEM). For the existing structure, it is found that the frequency of the first mode of the test rig is lower than the normal operating frequency which is about 20 Hz, so improvements were made to maximize the first mode. The process resulted in shifting the frequency to about 16-18 Hz which is still below the recommended value. For the structure in conceptual stage, the first torsion and first bending mode of a Body-in-white (BIW) of a compact 5-door hatchback were set to be above 40 and 60 Hz, respectively, using structural optimization. The process was successful in satisfying the objective of increasing the frequencies but with certain drawbacks such as added mass. In addition, different methods of optimization were also utilized such as changing the order of approach or performing two types of optimization simultaneously to demonstrate better results. Conclusively, structural optimization was a viable method of improving the dynamic characteristics of structures without trial and error process or previous experience.

Abstrak

Tujuan utama kajian ini adalah untuk memperkenalkan pengubahsuaian atau pengukuhan kepada rekabentuk binaan dibawah bebanan dinamik dengan menggunakan kaedah pengoptimuman struktur. Dua keadaan pengubahsuaian dinamik struktur (SDM) menggunakan pengoptimuman struktur telah diperiksa, iaitu SDM untuk struktur sedia ada, dan SDM di peringkat konseptual. Kajian ini ditujukan bagi menaksir kemujaraban kaedah pengoptimuman struktur dalam menentukan penyelesaian optimum untuk SDM berbanding dengan pendekatan konvensional menggunakan Analisis Unsur Terhingga (FEA). Analisis modal telah dijalankan untuk mencari frekuensi semulajadi dan bentuk mod sepadan dengan menggunakan kaedah Analisis Modal Eksperimen (EMA) dan Bentuk Pesongan Operasi (ODS) secara eksperimen manakala dengan menggunakan Kaedah Unsur Terhingga (FEM) secara komputer. Untuk struktur sedia ada, didapati bahawa frekuensi mod pertama bagi pelantar ujian adalah lebih rendah daripada kekerapan operasi normal iaitu kira-kira 20 Hz, jadi pembaikan dibuat untuk memaksimumkan mod pertama. Proses ini menyebabkan peralihan kekerapan sehingga kira-kira 16-18 Hz yang masih di bawah nilai yang disyorkan. Untuk struktur di peringkat konseptual, mod pertama kilasan dan lenturan bagi struktur ‘Body-in-white’ (BIW) sebuah kompak ‘hatchback’ 5-pintu telah ditetapkan untuk masing-masing berada di atas 40 dan 60 Hz dengan menggunakan pengoptimuman struktur. Proses ini telah berjaya memenuhi objektif meningkatkan frekuensi tetapi dengan kelemahan tertentu seperti penambahan berat. Di samping itu, kaedah pengoptimuman yang berbeza juga digunakan seperti menukar susunan pendekatan atau melaksanakan dua jenis pengoptimuman serentak untuk menunjukkan hasil yang lebih baik. Dengan itu, pengoptimuman struktur adalah suatu kaedah yang berdaya maju untuk

meningkatkan ciri-ciri dinamik struktur tanpa penggunaan kaedah cubajaya atau pengalaman terdahulu.

Table of Contents

List of Figures

List of Tables

List of Symbols and Abbreviations

DOF	Degree of Freedom
EMA	Experimental Modal Analysis
ODS	Operating Deflection Shape
FEA	Finite Element Analysis
FEM	Finite Element Method
MP	Mathematical Programming
OC	Optimality Criteria
NLP	Non-Linear Programming
GA	Genetic Algorithm
SDM	Structural Dynamic Modifications
SIMP	Solid Isotropic Material with Penalization
FRF	Frequency Response Function
FFT	Fast Fourier Transform
VI	Virtual Instrument
DAQ	Data Acquisition
CAD	Computer Aided Design
RPM	Rotation-per-minute
BIW	Body-in-white

Chapter 1: Introduction

Structures, either statically or dynamically loaded, will always have to be monitored to prevent failures that could affect the health and safety of the people around them. It is very important to understand the physics behind the designs such as the dynamic characteristics. In industry, machinery structures must be properly designed to withstand static as well as dynamic loads. Structure under dynamic loading will cause vibrations, either desirable or undesirable.

Devices using string to produce sound is an example of desirable vibration. On the other hand, an example of unwanted vibrations is such as excitations caused by rotating imbalances in machinery which is mainly caused by the dynamic characteristics of the structure. These types of vibrations are usually the cause of a number of problems such as unwanted noise, wear and tear of machinery components such as bearings, uncomfortable motion, and structural failure. A popular example of structural failure due to vibrations is the collapse of the Tacoma Narrow Bridge because of resonance.

There are several ways of minimizing unwanted vibrations such as shifting the natural frequency, isolating the source, attaching vibration absorber or increase damping. Therefore by understanding the nature of these vibrations, a more reliable design for a structure can be realized before undergoing manufacturing and construction. In order to achieve this, the design can first be virtually examined and developed to fulfill the requirements of structures capable of withstanding dynamic loads. It is also possible to introduce modifications and reinforcements onto an already built structure but other problems such as manufacturability of components, costs due to design modifications, maintenance downtime, materials and labors may arise.

The introduction of structural optimization approaches as a method for Structural Dynamic Modifications (SDM) may help in obtaining a much better dynamically loaded structure than the conventional method of trial and error. This method should be able to be employed for structure in most design stage including completed structures that already exists.

1.1 Modal Analysis

In the context of this research, the natural frequency and the corresponding mode shapes, which are part of the dynamic characteristics, were analyzed. The characteristics depend on material properties (mass, stiffness, and damping), geometric properties, and boundary conditions. The mode shape is the overall shape as the structure vibrates at each natural frequency and is divided into rigid and flexible modes. Rigid modes occur when the structure appear undistorted and consist of three translational and three rotational modes. Flexible modes are when the structure deformed due to the vibration such as bending and torsion modes.

The fundamental frequency for both bending and torsion mode are the basic of dynamic characteristics for most structure and can be extracted using modal analysis. This could be done experimentally using experimental modal analysis (EMA) or computationally by using Finite Element Analysis (FEA). Once these dynamics characteristics have been obtained, the behavior of the structure could be predicted quite accurately. Moreover, operating deflection shape (ODS) measurement was also done to determine the behavior of the structure under operating conditions. The main concern of this research is to shift the natural frequency in order to reduce the possibility of resonance.

First, the computational analysis employs Finite Element Method (FEM) and then using the result from experimental analysis (both EMA and ODS) to validate the accuracy of the

model. After validating, the model can then be used as the basis of the structural optimization analysis. The model will go through a series of optimization process and design manipulation to satisfy the given objective.

1.2 Structural Optimization

The conventional method of trying to obtain a good design for a structure would be to use FEA to create models where it can be analyzed first computationally with any fabrication. Then, when a suitable design was found, the structure would be realized and experimental analysis was applied to confirm the design. This would take significant amount of time and experience to accomplish because of the trial-and-error method employed. Therefore, by alternatively using structural optimization approach, both parameters can be reduced in order to determine the desired design. The optimization criterion (design variable, objective and constraints) needs to be established beforehand to make sure the process can run efficiently. The optimization processes that would be used are topology and size optimizations.

1.3 Aim and Objectives

This project aims at ascertaining the optimum designs for structures that can withstand the dynamic loading by employing structural optimization technique as the SDM. The effectiveness of employing the technique will be assessed for design modifications of existing structures as well as for virtual design modifications in the early design cycle (conceptual design stage). This would show that the method is applicable at important stages of structure design. The objectives are:

- To investigate the dynamic characteristics of a structure through experimental and computational methods.

- To determine optimum designs of dynamically loaded structures using topology and size optimization on two different types of structures.
- To evaluate structural optimization strategies that is best suited for structures under dynamic loading based on the type of structure and/or other suitable factor.

1.4 Research Scope

In order to accomplish the aim, the research will be divided into two; one using an existing structure and one with a structure still in the design stage. Both will undergo modal analysis to determine the structure's natural frequencies and their corresponding mode shape. The values from the result were analyzed first in regards to the design, the operating frequency and other factors. Once these characteristics have been determined, structures will undergo several structural optimization strategies which consider factors such as weights, design complexity and manufacturing constraints.

Specific parts of the structure were used as the domain of the procedure while the frequency, mass, volume and other properties were applied as the objective or constraints. A number of optimization strategies will be considered to shift the natural frequency of the structures to comply with the set conditions. Structural optimization processes such as topology and size optimization will be employed and critically examined to ascertain the best strategy. Finally, by comparing the results obtained, different innovative strategies were introduced by combining the processes to further improve the outcomes.

1.5 Chapter Summary

The early chapters will explain the development of the process of experimentation in finding and improving the dynamic characteristics of a structure. Chapter 2 first describes the previous work done with respect to structures under dynamic loading. This is then

followed by works on structural modification using the traditional way such as trial and error and the modern way such as using structural optimization. It shows the progress of the modification process from static loaded to dynamic loaded structures.

Chapter 3 shows the methodology used to incorporate structural optimization as a means for modification. The different structures demonstrated the varying process needed depending on the type and availability such as existing structure and structure still in conceptual stage. The optimization technique would also be adjusted to take into account any possible adjustment to the design of the structure such as the manufacturability of components. These alterations to the process were monitored throughout the study to maintain the possibility of an alternate variation to find better results.

The results and discussions of the whole study are shown in Chapter 4 and Chapter 5, respectively. In Chapter 4, each model and optimization approach yielded fair results that were recorded and analyzed accordingly. The values for the main responses were shown such as the mass, volume, natural frequencies and the corresponding mode shapes. The next chapter mostly discusses the design of the structure and how to improve on the outcomes. Chapter 5 also introduces possible new approach that captures the innovation of using structural optimization while still preserving the basic methods.

The final chapter compares all the previous results obtained and analyzes the positives and negatives of each approach and concludes the whole study. Future work that can be extrapolated from the end result was also discussed in this chapter.

Chapter 2: Literature Review

2.1 Dynamic Characteristics

Dynamic characteristics are usually used as a straightforward way to understand the behavior of the structure under dynamic loading (Bower, 2010). Initially for most structure undergoing dynamic loading, it is essential to know the natural frequency and the corresponding mode. The mode will show how the structure will react under certain external excitation (Thorby, 2008). In industrial applications, these characteristics needs to be tested and analyzed for most moving machinery before it is used (Hermans & Van der Auweraer, 1999). By understanding the modes, the durability of the structure can be realized before any load is applied. Durability under dynamic loading is directly connected to the mode shape and predicting the shape of failure for any structure is a very important task (Thorby, 2008). Basically, the mass and stiffness of the build needs to be at a certain range for any structure to carry out its work.

2.1.1 Modal Analysis and Structural Modifications

Modal analysis should be used in order to determine the natural frequency and the mode shapes of a structure. This could be done experimentally such as using Experimental Modal Analysis (EMA) (Maia & Montalvão e Silva, 1997) and Operating Deflection Shape (ODS) (Richardson, 1997) analysis or computationally such as using Finite Element Method (FEM) (Liu & Quek, 2003). Both of these methods would need to be compared to each other for validation purposes. These types of analysis could also be used to modify a structure under vibrations (Ramsey, 1983). Structural failure due to vibrations has been a growing problem in complex machines and operations. Failures such as wear and fatigue may happen due to the vibrations either desired or undesired (O'Connor & Kleyner, 2012).

A number of different methods for modifications have been introduced previously called structural dynamic modifications and are very much needed currently in industry because of the demands for higher performance of equipments and machineries (Kundra, 2000).

2.1.2 Dynamic Applications

The two structures used in this research are the experimental rig and the body-in-white (BIW) of a sedan car. These two structures offer different perspective in terms of optimizing because of the stage of design each is in whether in the development stage (BIW) or an existing structure (experimental rig). In such cases like the BIW, the modification of the body would also need to factor in the ride (Xu, Yi, & Huang, 2006), handling (Lu & DePoyster, 2002), and safety of the user. The vibration may be induced by a number of factors such as engine vibrations, road conditions, suspension system etc (Kim & Kim, 2005). This occurs because of the power delivered through uneven roads, engine movement, and suspension will result in resonance effect in a broad frequency band. The input force from the road and the engine can be used to define the frequency domain allocation of resonances expected in the system. By knowing the frequency band of the structure, the design can be modified to change the frequency when the structure resonates. Free-free boundary condition is used for consistency between results and the high repeatability offered such as established by (Zheng, Guo, Zhang, & Hou, 2001) when determining the global body stiffness of a structure with a modal analysis test.

Within the context of dynamic considerations, the ride and comfort of the users is also a factor for an effective design of the BIW structure. The comfort quantifications depended on the vibration of the body (Enblom, 2006). Besides the body, the damping coefficient and natural frequency of seats also affect the ride quality (Fan & Zhao, 2009). Furthermore,

the handling of the car will also be influenced by the dynamic behavior of the body. The condition of the body attachments are directly associated with the suspension system to help in giving the car the best control (Ahmadian, 2010).

Resonance can also be an important factor relating to the dynamic response. Other than control and comfort, failures can also occur depending on the behavior of the body (Billah & Scanlan, 1991). In order to prevent this type of failures, a system to accurately monitor the frequency of vibrating machines is needed. Condition monitoring such as using vibration signal analysis can help in determining the resonant and natural frequency of a structure (Renwick, 1984). More complex structures would also need non-stationary analysis for monitoring. Stationary approaches lack the ability to properly include the characteristic of individual events happening between components of the structure (Cempel & Tabaszewski, 2007). More recent development in successfully modeling a structure as real as possible is by using multi-body dynamics approach. Software such as MSC ADAMS can be applied to model and investigate the dynamic performance of components by comparing with practical results (Hale-Heighway, Murray, Douglas, & Gilmartin, 2002).

The reliability of the structure is usually optimized based on safety and also the life-cycle. On one hand, a design needs to be able to take into account failures that could arise from both short term and long term utilization. Structures under dynamic loading will undergo fatigue and by taking this into account, it is possible to predict the damage distribution such as by understanding the relation between the natural frequency and the mode shapes. On the other hand, the fatigue life of a component in a design can be used as a defining variable when predicting the life-cycle of a structure (Haiba, Barton, Brooks, & Levesley,

2002) Ongoing or post-failure maintenance of the structure can also be one of the objectives for optimization (L. P. Huang & Yue, 2009). The cost and time of maintenance should be minimized for an optimum design.

Additionally, by employing structural optimization the service life of the structure can also be verified. With an optimized design, failures can be reduced or prevented and that would lengthen the service life of the structure. Prediction of failures such as where crack will grow in the structure can also be used to strengthen the design. The complete life cycle of a structure is a very important aspect in the design of a machinery structure.

All these changes can be done by implementing a number of advanced objective and method such as design-dependant structures (Chen & Kikuchi, 2001) and computational form finding (Bletzinger & Ramm, 1993). There are a number of different set objectives for optimization. This project will firstly focus on the dynamic loading of a system and will therefore use optimization based on mass and stiffness of the structure. The dynamic characteristic of the system will be attained and used as the basis for the design and optimization of the structure.

2.2 Structural Optimization

In layman's term, structural optimization can be described as a technique to find the best possible design for a structure (Haftka, Gürdal, & Kamat, 1990). The optimization will be based on the objectives, constraints and variables set as the criteria. In recent years, industries have addressed the limitations or setbacks in production such as resources, technology, or environmental impact. So, new and more efficient method in designing was needed to properly address the matter. Hopefully with a better approach, structures with

high performance, low cost and lightweight can be produced. One such approach is by understanding the concept of optimization, where the process will seek to find the best optimal solution to engineering problems. In retrospect, structural optimization can be defined as tool to maximize efficiency by removing different constraints, such as the amount or availability of material (X. D. Huang & Xie, 2010). Optimum design is a very interesting subject which has been under extensive studies and research in terms of engineering problems. Engineering design was previously dealt based on the creativity and experience of the designer while employing trial and error processes. The process usually takes too much time and work to achieve still unguaranteed solutions.

In the present day, a focus on meeting a product functionality and quality in the highest regard while still maintaining or reducing the time and cost of production is of utmost importance. With the help of high end computers, the concept of engineering design has been revolutionized. So today, trial and error method can and should be replaced with scientific methods of rational design where researcher would use computational methods to calculate the optimum design. This is shown to be very effective such as using structural optimization.

First and foremost in any structural optimization process is to clearly define the objective of the design, design variables and constraints. These factors will influence the progression of a general structural optimization as it is a process to minimize (or maximize) the objective function by manipulating the design variable subject to geometrical and behavioral constraints. Examples of geometrical constraints are manufacturing constraints, availability of fabrication and member sizes while examples of behavioral constraints are mechanical properties, cost, weight and volume of structure, and natural frequency.

Mathematically, the general optimization problem (Haftka et al., 1990) can be expressed with the following for a single objective function, $f(x)$:

$$\begin{aligned} &\textbf{Minimize} && f(x) \\ &\textbf{Such That} && g_j(x) \geq 0, j = 1, \ldots, n_g \\ & && h_k(x) = 0, k = 1, \ldots, n_e \end{aligned} \qquad (1)$$

where x denotes a vector of the design variables. $h_k(x)$ denotes the equality constraints where it is used to when a constraint is set at a specific value while $g_j(x)$ is the inequality constraint and is used when the constraint needs to be at a certain limit.

The objective function can be classified and worked on depending on a set category. The design variables will need to be in range of the constraints to constitute a feasible domain. But if the variables violate any of the constraints, it will constitute as an infeasible domain. If the equality constraints, inequality constraints and objective function are linear relative to the design variable, the problem would be regarded as linear. If any of the three is not linear, than it is a non-linear problem. Most engineering problems however are usually non-linear problem because of the complexity of engineering design (Chu, 1997).

Structural Optimization can be separated into three types; size, shape and topology. The classification will depend mostly on the design variable and the objective (Ravindran, Reklaitis, & Ragsdell, 2006).

Firstly, for size optimization, the objective would be obviously to change the size parameters of a design in order to satisfy the objective. It is usually used at the initial design stage with either discrete or continuous design variables. For example, finding an optimal

thickness distribution of a plate or truss to minimize (or maximize) physical quantity such the stress, strain, or deflection. It also should be noted that size optimization is the simplest and the earliest form of structural optimization (Huang & Xie, 2010). The domain is also usually fixed for this type of optimization.

Then, computation methods of different approaches will be used to calculate and predict the new design or changes that is needed for the structure. A number of systematic methods in optimizing have been developed such as using a stochastic algorithm (Spall, 2003).

Alternatively, shape and topological optimization methods allow for changes in the geometrical domain of the design. In shape optimization, a set of control variables that will map the boundaries of the domains by defining the coordinates of the borders. The coordinates of these domains will be changed in order to achieve the objective function. The final shape can then be generated to satisfy the requirement of an optimal design (Haftka & Grandhi, 1986). Usually the domain used in shape optimization is not fixed but with a fixed topology unlike in size optimization. Typically, shape optimization is used to find the best shape of the external boundary surfaces. Basically, this technique is employed to perform at preliminary design stage. It was also used in the automotive industry, aerospace technology, and electromechanical, electromagnetic, and acoustic devices. One example is by using software such as MSC Nastran to solve shape design problems and generate optimized complex shapes of two and three-dimensional engineering components (Holzleitner & Mahmoud, 1999).

Finally, topology optimization is usually done as the other two may result in sub-optimal results. Therefore, topology optimization is generally implemented on an already defined design domain. It is used to determine the characteristics of a model such as the condition

or form of the domain and the shape of holes. Unlike the other two types, the initial design domain of a structure should be universal, such as rectangular plates. The unknowns of the problem are the physical shape, size and connectivity of the model but are represented by distributed functions which will be defined under a fixed domain. Topology optimization is commonly known to be the most complex of the version of optimization. The geometrical domain is generally defined and the algorithm will create a negated area in the whole system that would help in the materials distribution for an optimum design (Bendsoe & Rodrigues, 1991). This type of optimization problem is generally done in terms of a maximum stiffness approach. Therefore, a minimum weight topology optimization method would use stress constraints formulation in which a transferred stress constraint would not be able to completely embody the constraint requirements. A popular new concept was introduced called topological sensitivity, which was widely used in structural optimization after it was further developed into what is called topological gradient by (Cea, Garreau, Guillaume, & Masmoudi, 2000). The method basically admits an arbitrary starting point of a structure and then shows all the necessary topology changes while incorporating shape optimization. Various approaches are then used to update the structural changes in terms of topology such as using homogenization methods (Bendsøe & Sigmund, 2003). This method is done by not removing actual material from the structure but by changing the element density according the optimization criteria.

Besides homogenization methods, there are other methods of doing topology optimization such as the power-law approach (SIMP), evolutionary approach, the soft-kill hard-kill methods etc. The SIMP method is basically making the design variables the utilizing constant material properties of elements and also the relative element densities raised based on the property of the solid material (Duysinx & Bendsoe, 1998).This power-law approach

has to be combined with some constraints or a filtering technique. Evolutionary method is done by eliminating and adding elements at each iteration having a low value of criterion functions, such as the dynamic compliance or some other response parameters (Huang & Xie, 2010). There is also a proposed method where all elements of stress constraints will be replaced with constraints with the most active potential and a generalized average stress constraint (Rong, Liang, Guo, & Mu, 2008).

There are many approaches to solve the issue using structural optimization can be categorized into classic calculus methods and numerical methods. The use of calculus in optimization was first introduced in the 17th century. Michell (1904) researched on finding the optimal topology of trusses using calculus which led to the renowned Michell-type structures. The two different but closely related type of calculus used in optimization are differential calculus and calculus of variations.

Differential calculus dictates that the condition for extreme values can be extracted from the first order partial derivatives where the function regarding the design variable is zero. This is a very straightforward approach in which only direct application such as through unconstrained optimization problems is viable.

On the other hand, calculus of variation addresses the generalization of the differentiation theory. An objective function is proposed to be expressed by a definite integral of a function which is defined by an unknown function and other derivatives (Haftka et al., 1990). The unknown function is directly related to the design variable and the optimization process is to form the unknown function instead of individual extreme values of the variables. The required condition for the extremum is the first order of variation to be zero. By taking into account of the boundary conditions, the resulting equation is the well-known

Euler-Lagrange equation. Although the application of this approach is moderately restricted, it is a crucial addition in the development of optimization methods. It shows the fundamental significance of the mathematical nature of optimization and also in delivering lower bound optimums to be compared with alternative methods.

As for numerical methods, it is highly considered to be the fundamental for designing real structures. It can be classified into three categories; direct minimization method such as mathematical programming, indirect methods such as optimality criteria and genetic algorithm methods.

One of the most popular optimum search techniques is by using mathematical programming (Miro, Pozo, Guillen-Gosalbez, Egea, & Jimenez, 2012). The technique is a stage-by-stage search method involving iterative process that includes a step differentiating the value of the objective function and its gradient in terms of the design variables and the calculation of the change in the design variable that would reduce the objective function. The methods was solely used in linear problems in the past, but since 1960, many algorithms of non-linear programming have been developed such nonlinear programming (NLP) (Schmit, 1960), feasible direction (Ruszczynski, 1980), gradient projection (Gulyaev & Markovskaya, 1982), and penalty function method (Yagawa, Aizawa, & Ando, 1981). Concurrently, there are studies where approximation techniques that utilize the standard linear programming are used to address non-linear problems, such as sequential linear programming (Arora, 1993). Mathematical programming is very useful because it can be employed in most optimization problems, but the drawback is that as the number of design variables and constraints increases, the computing cost becomes expensive.

The minimality of the objective function has to follow a condition which is called the optimality criteria and can be derived using principles of mechanics or variation methods. Optimality criteria method was methodically formulated by in the 1960s (Prager, 1968). Later, the method was numerically developed and became widely accepted as a structural optimization method. Different form of optimality criterion is required for different types of optimization. One type of optimality criteria method is by using rigorous mathematical statements such as the Kuhn-Tucker conditions (Haftka et al., 1990).

Subsequently, genetic algorithm was introduced in the 1970s where it uses genetic process of reproduction, crossover and mutation (Jenkins, 1991). Genetic algorithm follows a set of procedures:

- Creating an initial population of designs randomly
- Evaluating the fitness of individual design to a certain function
- Reproducing the fittest members and allowing them to cross among themselves
- Developing new generation of members having higher degree of desirable characteristics than the parent
- Repeating until near optimum solution is reached

Genetic algorithm is getting more recognition as an optimization method because of its reliability and robustness.

2.3 Optimization Related to Dynamic Problems

Using optimization to improve the dynamic behavior of a structure is very important such as minimizing the noise and vibration in a design (Kim & Kim, 2005). In similar case like this, the dynamic behavior of the system is treated as an object of the optimization process

and not as a constraint (Ma, Cheng, & Kikuchi, 1994). Nevertheless, it is very challenging to apply optimization method as it is difficult to develop sensible combinations of objective functions and constraints. Even though, the main idea of structural optimization is to obtain an optimal layout of a load bearing structure, traditionally, structural designers used to develop the designs according to the stiffness necessities while control designers will work on to lessen the dynamic response of the structure (Ou & Kikuchi, 1996).

Optimization related to vibration problems follows some common aim in concept. The first is to increase a specified structural eigenvalues to reach a maximum. Secondly, the intention is maximize the gap between the specified structural eigenvector from a given frequency. The third and final aim is to optimize a structure to obtain a prescribed eigenvalue (Ma et al., 1994). Eigenvalue optimization is important for the design of structures that are dependent on dynamic loads. Structures with high fundamental eigenvalues tend to be significantly stiff for all loads and will therefore results in design with good static stiffness (Bendsøe & Sigmund, 2003).

The existing method that is widely accepted to improve the dynamic characteristics of a structure is Structural Dynamic Modifications (SDM). There are slight differences between SDM and structural optimization on dynamic problems. Main difference is that SDM only address the modification of existing structure for the next design cycle. Though structural optimization can also be used to improve existing structure, the major advantage is that it can be used at the initial design stage.

In this research, only two types of optimization were used; size optimization and topology optimization. Furthermore, the structure used will either be in the design stage or an already

existing structure. Therefore, the approach will need to meet each condition properly so that the result can be as accurate as possible.

For topology optimization, some work has been done such as by Diaz & Kikuchi (1992) who considered using topology optimization with reference to eigenvalues of vibration. The natural frequency was maximized and strategy to find the optimum shape and topology was the concept of the work. Others have tried defining the mean eigenvalue equivalent to the multiple eigenvalues of a structure and then by utilizing optimal material distribution, the problem will arrive at the desired eigenvalue (Ma et al., 1994). There are also some works that were done with structures subjected to periodic loading such as the minimization of vibration due to the loads (Jog, 2002). Structural modification conventionally was done by understanding the behavior of the structure under certain loading and modifying based on the numerical result such as done by Ebrahimi, Esfahanian, & Ziaei-Rad (2013) and Kim, Kim, Shin, & Lee (2010).

Most of the works previously mentioned were done in the design stage; therefore, manufacturability was not as important. For that reason, one of the conditions of the optimization is to take into account the manufacturability of the new structure and its parts to be suitable for the industry.

Chapter 3: Methodology

This research starts with finding and understanding the dynamic characteristics, primarily the natural frequency and the corresponding mode shapes of a structure. This is done by using experimental method and computational method depending on the structure used. Two different structures would be used for the analysis. The first model is an existing experimental rig consisting of a pedestal and a motor (referred to as the **experimental rig** onwards). The second model is of a body-in-white structure of a compact 5-door hatchback in design stage (referred to as the **BIW** onwards). The results obtained from the dynamic analysis will be recorded and studied by comparing with the dynamic behavior of the structure.

Depending on the result, certain development will be introduced to satisfy the objective which is to improve the dynamic characteristics of the models. The development of the methods would take into account the design stage each structure is currently in to differentiate the nature of the approaches. Structural optimization will be used with various approaches to obtain the optimum design and configuration of the structure without thoroughly relying on the knowledge of the user. The optimization result obtained will then be compared to each other and further analyzed to understand more on the optimization processes.

3.1 Experimental Rig

The rig consists of an induction motor resting at the top of a rectangle pedestal with 4 L-shaped legs (Figure 3.1). The motor, when it is running, generates the main vibration that may cause unwanted reactions of the structure. The motor is the only source of dynamic loading in this structure. The rotation-per-minute (RPM) of the motor which is bolted onto

the top of the rig solely affects the operating frequency of the structure. However, the motor will only be represented as a rigid body when executing the modal analysis.

Since this rig is already a functioning structure, the optimization methods would need to include other important factors that could devalue its effectiveness such as redesigning and fabricating the structure from the ground up. It would be much more efficient to maintain the original design and introduce means of only reinforcing the structure.

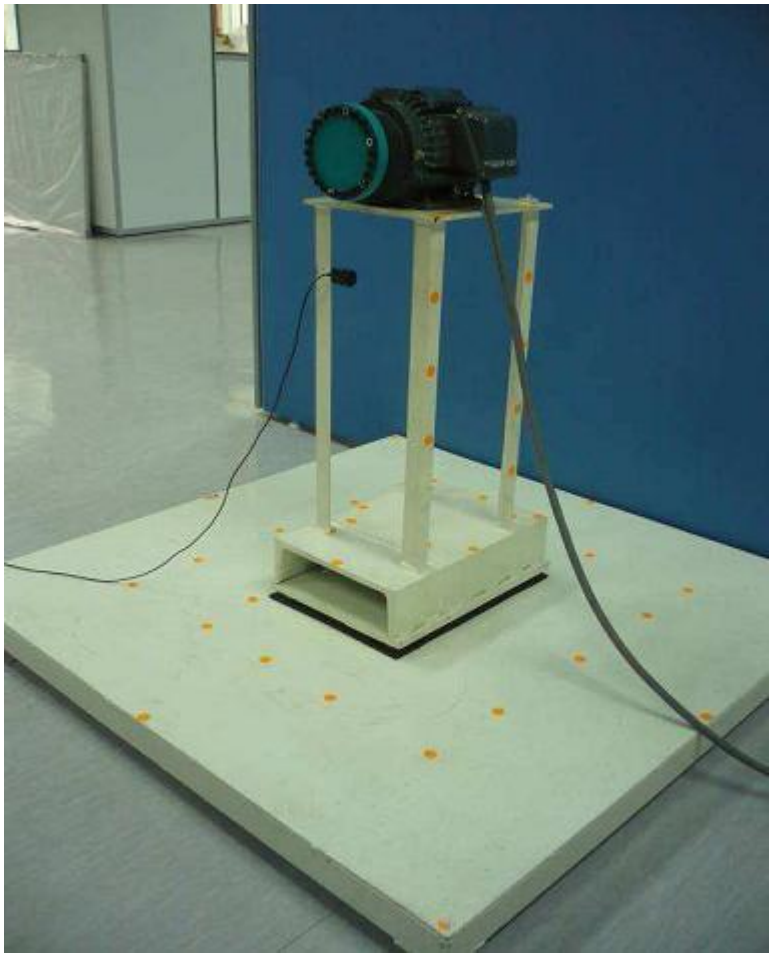

Figure 3.1: Experimental Rig Pedestal with Motor

These responses can be reduced by comprehending the nature of the structure under certain load. The reason this structure will be used is to show the effect of the structural optimization on an existing structure. There are certain conventions that will need to be conducted when a structure undergo any analysis involving modeling such as both

computational and experimental method needs to be within a certain accuracy to validate the reliability of the model (Schedlinski et al., 2005). The dynamic characteristics of the structure will be analyzed experimentally by using experimental modal analysis (EMA) and operational deflection shape analysis (ODS) to show the natural frequencies and the mode shapes.

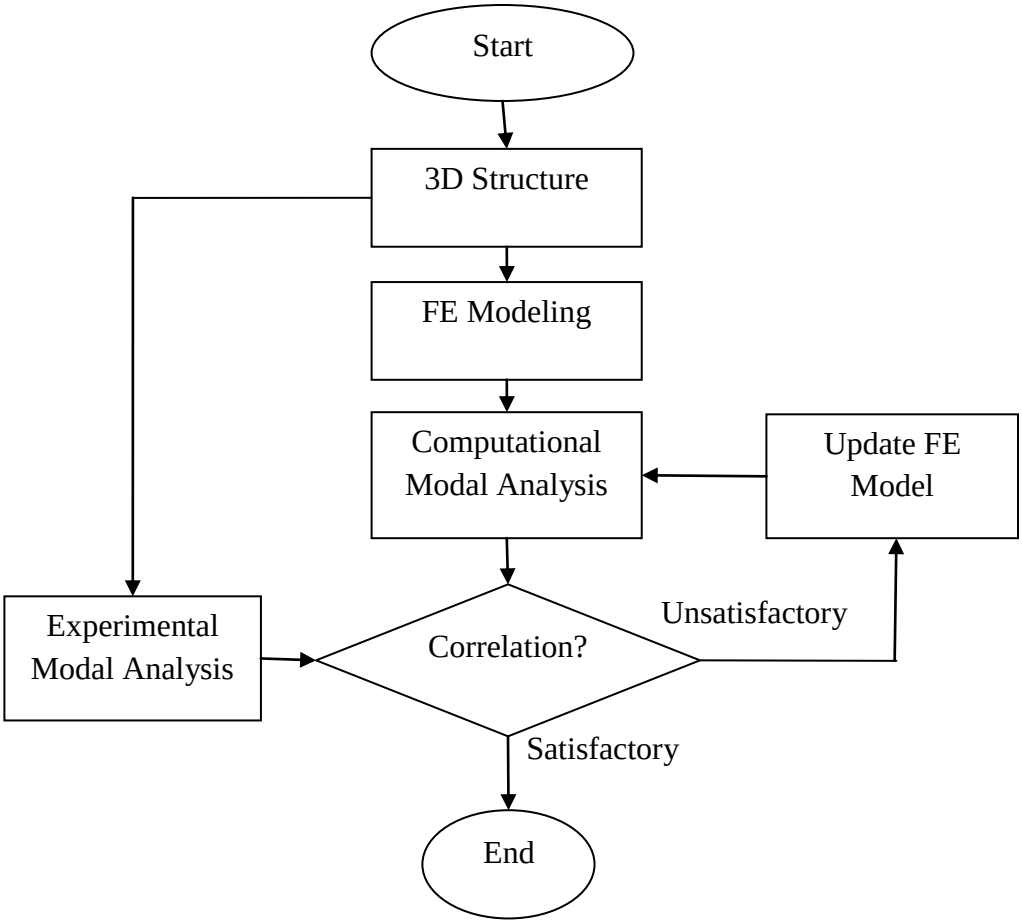

Figure 3.2: Experimental Rig Model Validation Strategy

3.1.1 Modal Analysis

Firstly, in order to perform experimental modal analysis (EMA), the structure is excited typically with an impact hammer to create a known excitation, and the corresponding response is measured simultaneously by a sensor (Maia & Montalvão e Silva, 1997). There are at least four different approaches in performing EMA that can be used (Brandt, 2011).

The approaches differ in terms of number of acquisition channels and excitation source available. For this research, single input/multiple output approach will be used because of the availability of a 4-channel data acquisition system. An impact hammer will be used for the fixed reference point and direction, while the acceleration will be measured using tri-axial accelerometer roving along the measurement points.

Based on these excitation and response data, the frequency response function (FRF) can be determined, which expresses the structural response to an applied excitation as a function of frequency (Cawley, 1986). System natural frequencies, modal damping and mode shapes can therefore be estimated from the FRF. Most often, the system is assumed to be linear and time invariant although this is not necessary. FRF is typically used to describe the relation between the input and output of the system.

The FRF can be estimated by transforming the data from time domain to frequency domain using Fourier transform. The best way would be to use fast Fourier Transform (FFT) algorithm which is based on limited time history and assuming that the waveform would repeat itself over time. By doing this, the theoretical advantages of Fourier transform can be implemented in the digital signal processing.

The EMA will be conducted on the real structure in three main steps:

1) Modeling of the structural geometry
    a) Measurement points are located on the structure
    b) The structure is modeled using Vibrant Technology ME'scope VES
2) Data acquisition using FRF-analyzer VI

a) Obtain and record FRF readings from measured impact force and response from the points

3) Viewing and processing results

a) Import readings from FRF-analyzer VI to ME'scope VES

b) Determine the natural frequencies and view the animation of the corresponding mode shapes

The measurement points will be decided by observing the measured positions of the impact force, response acceleration and constraints. Check every measurement points to make sure that the accelerometer would fit in between the points. The cable of the accelerometer will also need to be ensured to not experience excessive bending due to the limited space that will cause noise and affect the measurement. The points can then be labeled with numbered stickers while the dimensions and the coordinates can be measured using a ruler and a measuring tape.

This is followed by the modeling of the structure using ME'scope VES, which is a post-processing software, using the measured dimensions. The points will also be numbered according to the aforementioned labels. Then, check the model to ensure the consistency of the representation in the x, y, and z coordinates. The pedestal will then be modeled using 72 measurement points, as shown in Figure 3.3.

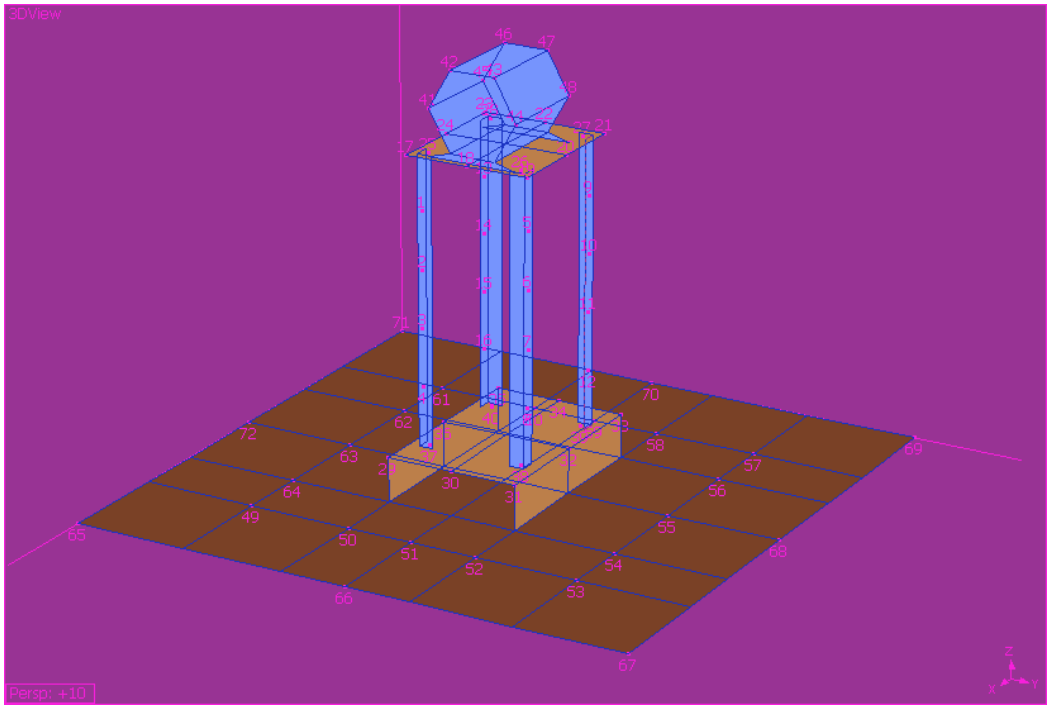

Figure 3.3: Experimental Rig Model in ME'scope VES with Measurement Points

Set up the data acquisition system by connecting the physical hardware, i.e accelerometer, impact hammer, analog input module. Using the data acquisition software LabVIEW, a modal analysis virtual instrument (VI) will be developed which serves as a conventional FFT analyzer for EMA (Jamal & Pichlik, 1999). The VI consists of a front panel; the user interface for control and indicators, and a block diagram. The initial configurations for the block diagram are; sampling frequency = 2000 Hz, Number of samples of DAQ = 14000, threshold value = 10 N, trigger samples number = 10000, and number of averages = 5 (Table 3.1).

The windowing options will be set to 'rectangular' for input and 'exponential-decaying' for output response. The tri-axial accelerometer will be attached to the measurement points. It is then followed by configuring the front panel settings such as the file path for the results, the degree of freedom (DOF) and the 'response x (-1) button of the VI. Thus the DOF for the first measurement can then be set as 2X:1Y[1], 2Y:1Y[1], 2Z:1Y[1] while the DOF for

the second set is 3X:1Y[2], 3Y:1Y[2], 3Z:1Y[2]. Switch on the 'response x (-1) to inverse the sign of the response signal acquired. This should be done to maintain the consistency of the sign of the response signal.

Table 3.1: Initial Configurations in Block Diagram of FRF-analyzer

Module	Parameter	Features
DAQ	Sampling Rate	Number of digitized reading sampled in one second from analog data
	No. of samples	Number of samples to be read
	Sensitivity	Calibrated sensitivity of accelerometer and hammer
Trigger	Threshold Value	Data will only be taken for FRF starting from when impact force exceed this value
	No. of samples	Number of output samples for FRF calculation
FRF	No. of averages	Number of averages needed for FRF calculation

Next, a fixed impact point will be given an impulse force by the impact hammer. Record the displayed average magnitude, phase and coherence of the FRF upon completion. The time domain impulsive force will then be checked to ensure that double knock did not occur. The FFT impulsive force will also be checked to give smooth curve over the frequency span, and also the values of coherence must be high (>0.5) at frequencies of interest. The result of the measurements will only be accepted when all requirements; no double knock, smooth curve and high coherence, are met. Repeat the measurement until the number of averages reach as per the settings. The whole analysis will then be repeated by moving the tri-axial accelerometer at all the different measurement points with the same steps.

Finally the FRF measurement files can then be imported to ME'scope VES for results viewing and processing. All FRF measurements will be overlaid together in a single graph

to get a clearer view of the FRF peaks. The measurements will be assigned according to the measurement points of the model. Display the mode shape in the animation by dragging the peak-cursor frequency band to contain one of the peaks in the overlaid FRF curves, which indicates one of the resonance frequencies of the structure. Any discrepancies observed in the animation such as certain points not moving or illogical point move, the measurements will be taken again at that particular point. These mode shapes will correspond to the averaged peak frequencies contained within the band, which can be interpreted as the natural frequencies. Therefore, all the natural frequency and the corresponding mode shapes under the proposed frequency can be obtained from the analysis.

Secondly, operating deflection shape (ODS) analysis will be used to monitor the actual condition of a system under actual operation. This is a better approximate to be used than EMA due to the fact that the measurements are taken during the operating condition of the machine, hence it better signifies the actual response of the system under normal operation. ODS can be defined in several ways (Richardson, 1997) but in this research, the ODS is defined as a complex valued function whose magnitude and phase equals the magnitude of the FFT of the response and the phase of the cross-spectrum between reference and response points.

A minimum of 2 channel data acquisition system are required to perform the analysis. One accelerometer will be fixed at a certain fixed point as the reference point and direction with another accelerometer roved along the measurement points. Thus the magnitude of the FRF reading signifies the true response amplitude of the particular measurement point and the phase of the FRF signifies the phase difference of roving acceleration relative to the

reference acceleration. The points will then be measured in x, y, and z direction so the number of FRF measurements will be three times the number of points used.

It should be stressed that there are significant differences between EMA and ODS analysis. EMA was used specifically to determine modal parameters such as natural frequencies, mode shapes and modal damping of a system, while ODS analysis was used to show the actual response of the system under operating condition. By doing both analysis, a more comprehensive understanding of the dynamic characteristics of the system in question can be shown.

ODS analysis consists of three main steps as described below:

1) Modeling of the structural geometry
    a) Measurement points are located on the structure
    b) The structure is modeled using ME'scope VES according to the dimension
2) Data Acquisition using ODS FRF-analyzer VI
    a) Obtain and record the FRF readings from the measured reference and roving response acceleration for all measurement points
3) Viewing and processing results
    a) Import the FRF readings acquired from the VI into ME'scope VES
    b) Animate and view the structure response at operating frequency

The same model that was created in ME'scope VES as in the EMA can be used for this analysis. The same measurement points will also be used for the ODS analysis. The data acquisition system will be set up similar to the previous analysis such as connecting the same physical hardware.

The virtual instrument developed in LabVIEW environment will also be set up with a front panel and a block diagram. The initial configuration for the block diagram is also very similar to the FRF analyzer VI for EMA. The settings will be set as sampling frequency = 2000 Hz, number of samples of DAQ = 14000, threshold value = 1 m/s^2, number of samples of trigger = 10000. The windowing option to be used is 'hanning' for both the reference and the roving response. The motor will then start and allowed to run at operating speed. The 'hanning' window is used to ensure that the assumed waveform is continuous because the motor was running at a steady state and the vibration is continuous. A uni-axial accelerometer will be attached to a reference measurement point while a tri-axial accelerometer will be attached to a roving measurement point. Set the front panel settings with the same setting as the EMA. The ODS-FRF readings for both magnitude and phase can then be extracted from the graph displays.

The analysis will then be repeated by attaching the tri-axial accelerometer at the other measurement points while leaving the reference uni-axial accelerometer at a constant position. This step should be repeated until the shifted tri-axial accelerometer has covered all the measurement points. Finally, the ODS-FRF will be imported into ME'scope VES to be viewed and processed. The structure can then be animated by dragging the frequency cursor to the operating frequency.

After both experimental methods are complete, Finite element analysis (FEA) will be executed to computationally ascertain the dynamic characteristics of the structure using Radioss solver on Altair Hyperworks. This will be done with real eigenvalue analysis in four main steps:

1) Measure and Generate 3D representation of the structure

a) Measure all the dimensions from the real structure

b) Create a computer aided design (CAD) model of the structure using Solidworks

2) Import and Mesh the finite element model

a) Import a surface file (IGES) from the CAD model

b) Mesh the model using 2D or 3D elements

3) Apply properties/conditions and solve the analysis

a) Apply material properties accordingly

b) Apply constraints at the corners of the base

c) Apply Real Eigenvalue extraction condition (EIGRL)

4) View and analyze result

a) Check the value of the natural frequencies and the mode shape of the structure

Create the model using Solidworks with the dimensions acquired from the real structure. It is then imported to FEA using the IGES file that will only include the surface information of the design. Therefore more work needs to be done in the FEA such as creating solid models from the surfaces and making sure that the structure is reliable.

The solid will be created using the bounded surface option. The surfaces are chosen as the sides that will create a bounded area with the solid inside. To perfectly simulate the structure, it was initially separated into 5 smaller components; base, hollow base, legs, motor base, and motor. These components will then be connected using spot-welds. Mesh all the components using 3-D tetra elements. Then, create the spot-welds using the 1-D spot-weld option by connecting the surfaces that are in contact. The element type used for the welds is CWELD, a mesh-independent connector element. The material to be used

throughout the whole model is of structural steel, so the properties will be applied onto all the elements. The material is set as isotropic with a Young modulus of 200 GN m^{-2}, Poisson ratio of 0.3 and density of 6700 kg m^{-3}.

Another model will also be created without the spot welds to show the validity of a simpler model. The model will be created as a whole rigid body without any connecting elements. The main reason is to illustrate the negligibility of the welds in this type of structure and will also help in the structural optimization process. Modeling without the connector will aid the optimization by needing relatively less computation power without significantly reducing accuracy.

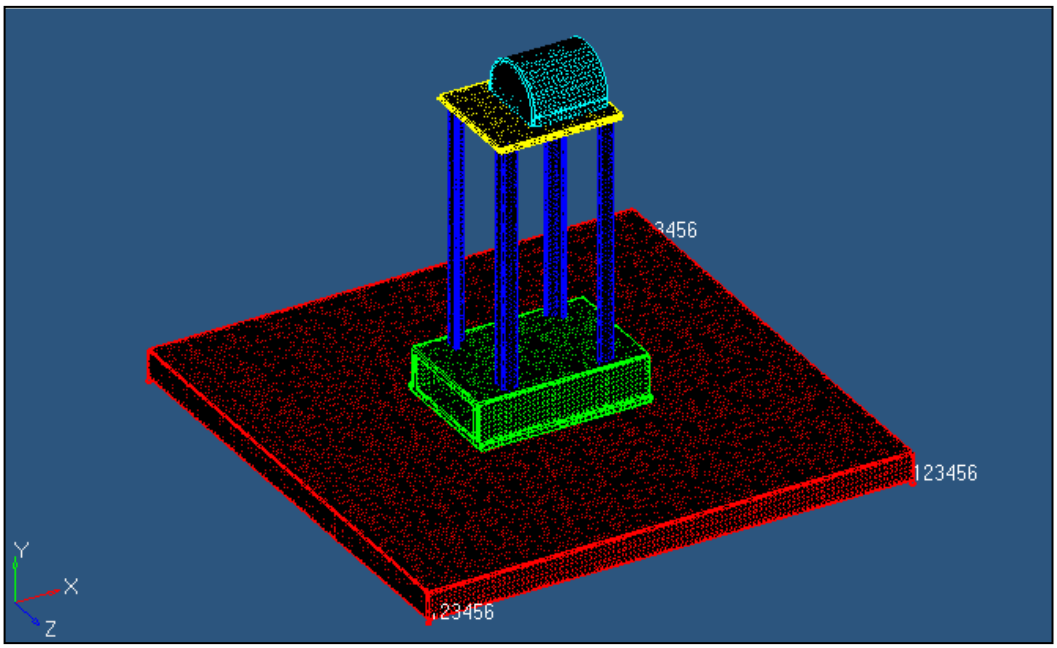

Figure 3.4: Meshed Model of Experimental Rig by Parts

After meshing the whole model, 19152 solid elements and 291 weld elements were created (Figure 3.4). The quality of all the elements will then be checked and will be redone if not of certain standard. After all the elements are faultless, the loading conditions can then be implemented.

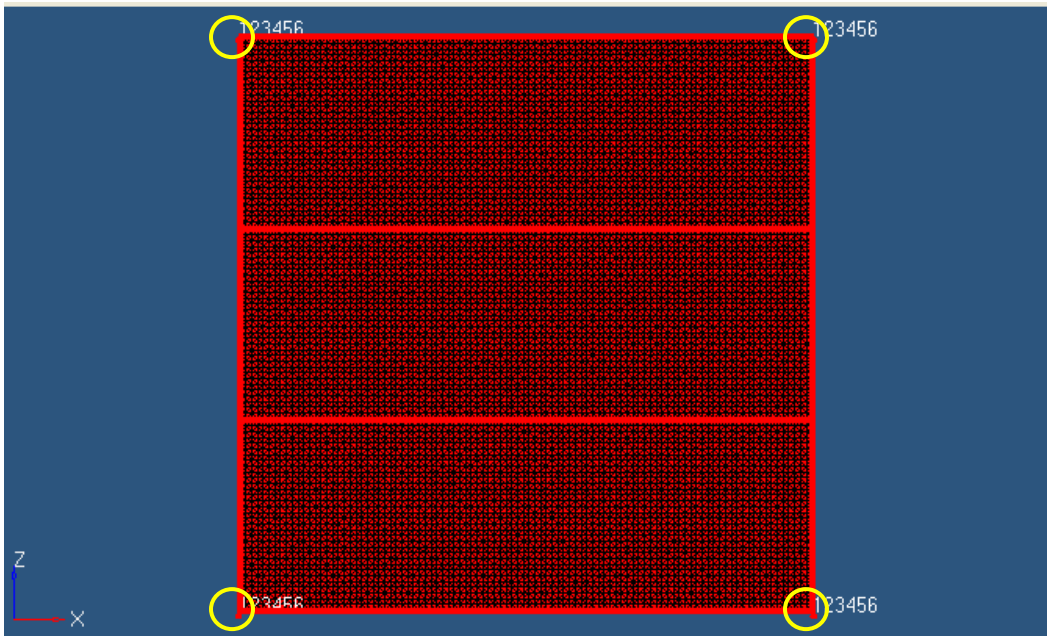

Figure 3.5: Boundary Constraints Positions

Two types of loads will be applied; eigenvalue analysis conditions and boundary constraints. For the eigenvalue condition, the numbers of modes will be set as 6 and the maximum value of frequency will be 100 Hz. This would mean that only the first 6 modes that are less than 100 Hz would be recorded. The static constraints will then be applied at the four corners of the base (Figure 3.5). All 6 degree of freedoms is set at 0 so that the base will be properly secured.

Finally, with all the elements and conditions applied, the model can now be solved using the Radioss solver. The outputs from the analysis will then be analyzed using Altair Hyperview for the simulation and the data will be recorded. Therefore, to achieve the same result with a less time-consuming analysis will be to simply make the structure a whole rigid build without the use of connectors. By using this, the accuracy may decrease a little but may save a lot of time.

Hence, create the model as a whole rigid structure and apply the same methods as before except without the spot-welds. While the number of elements used should be about the

same, weld elements will not be used. The result of both of the analysis will be compared to the result from EMA. From the results, the main focus will be on the first two modes; the bending modes of front-to-back and left-to-right while the other modes will be used only to validate the simulation.

3.1.2 Structural Optimization

After all the modal results have been collected, the structure can now go into the process of improvement. The structural optimization will be done using the FEA model as the basic structure. To obtain the optimization result, four main steps would need to be set up first before the analysis can be done. First of all, the designable variable for the optimization will be set depending on the domain where any modifications would need to be done. The variable for this model are the solid elements but the space would depend on the different processes of optimization. Secondly, the optimization responses need to be set up. The responses are the factor that will control the outcome of the optimization. Third, from the responses, the objective and constraints of the optimization should be set up. The objective is the maximization or minimization of the response while factoring in the constraints of other responses that were put in place. Finally, the analysis can be performed after setting up the optimization controls. The usual controls used are such as objective tolerance, number of iterations, additional methods etc.

The main responses used for the optimization will be the volume of the whole structure and the natural frequency. The Altair Optistruct solver uses density method where the density of the elements can be changed within a range according to the need of the elements at particular positions. The volume/mass of the whole structure should be minimized in order to decrease the material and in turn reduce cost. The complexity of the design is also an

important factor in the optimization process that will affect the manufacturability in terms of cost and time.

Generally, topology optimization will be conducted to find the fundamental new design for the structure. The drawback of topology is that it will only show the changes in the domain in terms of geometry without the focus on dimensions. Therefore, size optimization is needed to verify the new dimension of the design obtained from topology optimization. Both optimization processes use the same method except for the design variable. The variable for topology is the element densities while the thickness of the parts will be used in size optimization.

As mentioned before, the rig is known as an existing structure where the physical form is present to be studied upon. Hence, necessary option and restriction will be imposed regarding the optimization to properly assess the analysis. One such implication is where the improvement can be done by only adding reinforcements to an already built structure or modifying some or the whole original structure altogether. This establishes the preferred designable space and chosen design variable used to reflect the optimization approach.

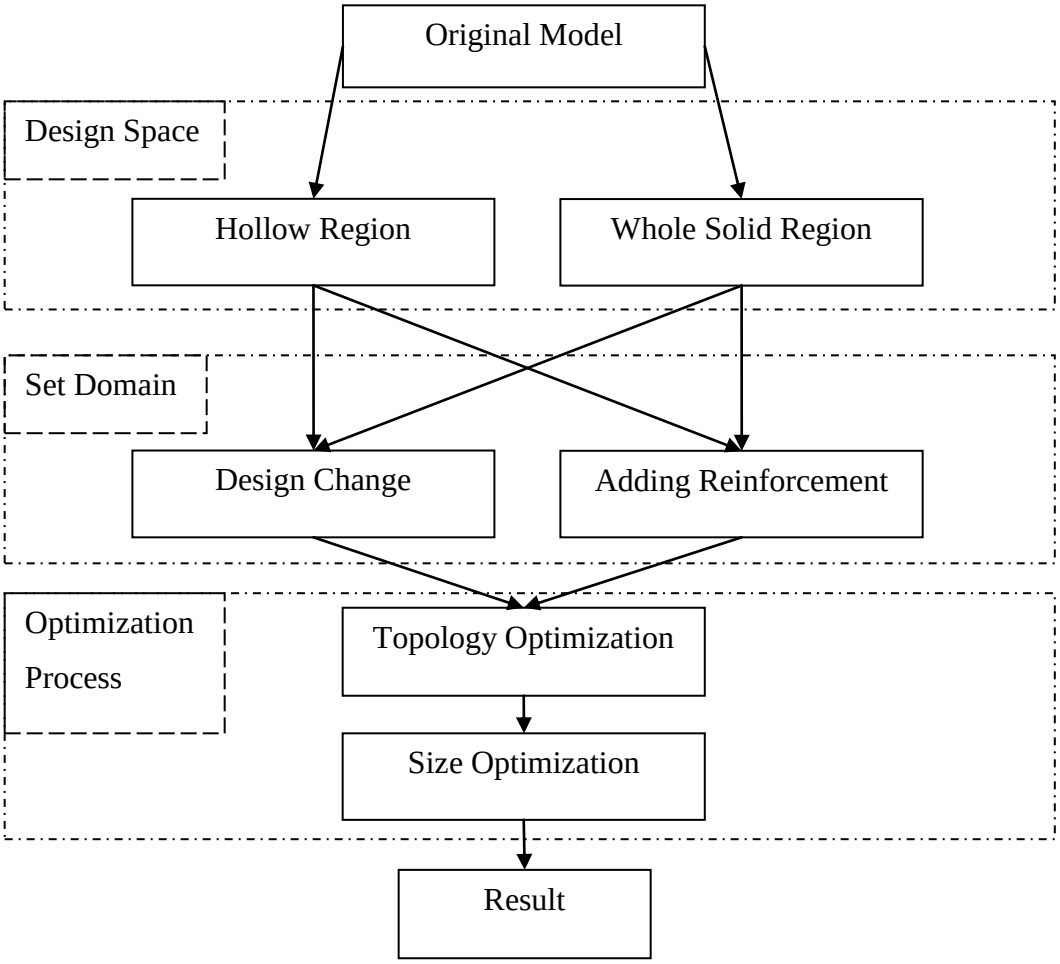

Figure 3.6: Structural Optimization Strategy

Two different designable spaces will be used as the basis of the optimization. The first is using a whole solid beam replacing the legs original position while the second is using a hollow beam with the same thickness of the legs. This should completely cover the basis for where new or additional materials may be adjoined for the optimization. It will also show the different result that may surface from using slightly different initial designable space.

The hollow region would justify the topology optimization of the structure with constant thickness in between the support. The whole solid region will be used to expectantly

introduce internal reinforcements such as a strut that connects across two diagonal legs laterally.

The optimization criteria for this structure will be mainly based on the natural frequencies obtained from the modal analysis. The objective will be to maximize the natural frequency for one specific mode while satisfying constraints such as the frequency for other modes and volume of the structure. Some controls will be applied for the optimization mainly for the objective tolerance and number of iterations where it was set to 0.0001 and 100, respectively.

Besides that, the optimization method will also be divided into two. For the first method, the optimization will be conducted to change the design of the structure without any regards to the original design. For the second, conduct the optimization with the intention of maintaining the original structure while adding materials for reinforcement.

The whole solid beam region is basically just a thick rectangle beam with 223 × 195 mm rectangle cross-section (Figure 3.7). This should significantly change the design of the structure from the original. By doing this, the new design from the optimization could have varying thickness along the beam or any internal material as support. The space can then change from the original by redrawing it in CAD and then meshed using quad elements in FEM. Primarily, the whole beam region will be cast as the design variable for the optimization.

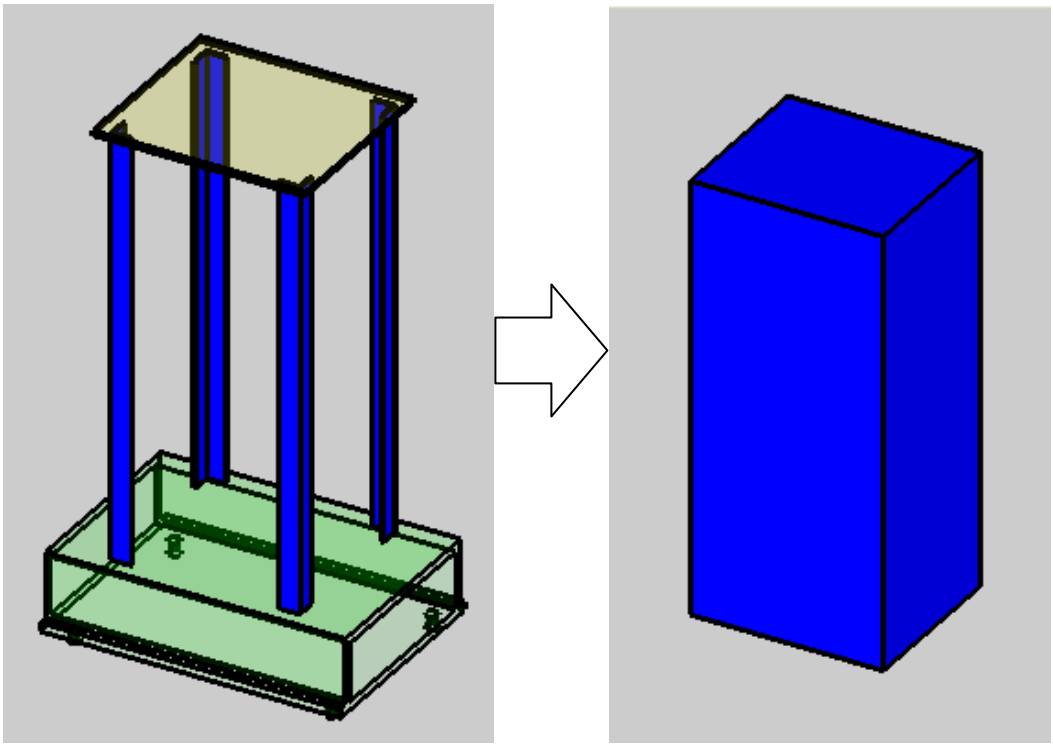

Figure 3.7: Whole Solid Region Model

The optimization will then run with the frequency of the first mode as the objective and the volume as the constraint. This would mean that the result will show the best design with the highest value of the natural frequency of the mode with the least volume of the whole structure.

Table 3.2: Topology Optimization Criteria

Variable	Element Density
Constraints	Volume
Objective	Maximize First Frequency

This is then followed by changing the design variable by still using the thick beam region but without taking into account the original legs position. By doing this, the legs would stay as a constant formation for the entire optimization run. Different result should be obtained where the original structure would still be used with some additional reinforcement added to it. The same objectives and constraints would be used for this process as the former (Table 3.2).

The optimization results will be viewed in Altair Hyperview where the contour of the element density can be controlled and evaluated. The result needs to be smoothed out before any new analysis can be performed. The contour result can then be extracted from the result and redrawn in CAD to produce the new design for the structure. These new designs will then be subjected to the same FEM modal analysis as mentioned in Chapter 3.1.1.

The final results from the all the optimization run will be compared to and analyzed. These results will show the significant distinction on the use of different response for the objective and the initial design variable used.

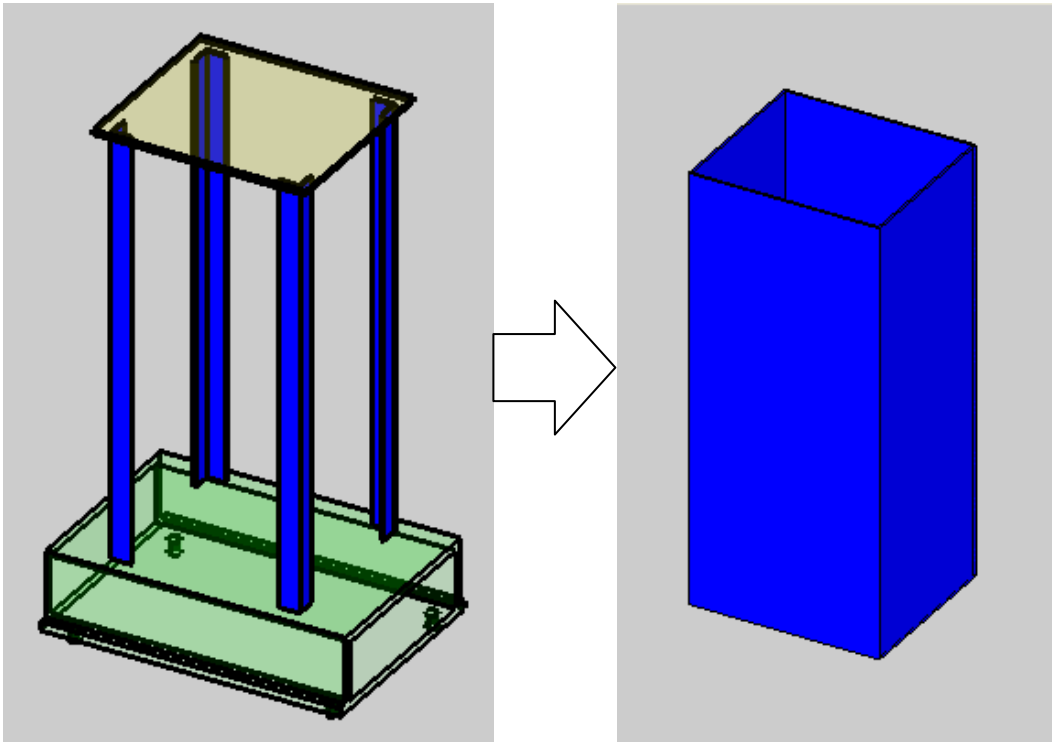

Figure 3.8: Hollow Region Model

Next, the analysis will be done using a hollow beam region which is basically a hollowed out beam of the same dimension from the previous case (Figure 3.8). The thickness of the sides is the same as the thickness of the legs which is 3 mm. This will be conducted with

the intention of doing an optimization with a constant thickness already set at the beginning of the process. By doing this, the result may show a slight difference because of the lack of inner material of the design space. This will also utilize CAD before importing it into FEM.

The optimization will also run with the same objectives and constraints set as the previous case (Table 3.2). The optimization will first be employed with the whole hollow beam region as the designable variable and followed by the beam with the legs as a non-designable variable.

The contour result should be studied before redesigning them using CAD. The new design will also undergo modal analysis using FEM. Every result from the hollow beam optimization will also be compared to each other and analyzed before comparing them with the result from the whole solid beam case. Finally, all results from both design space will undergo a comparison of the value of both the frequency and the volume so the best design and method could be determined.

3.2 Body-in-White (BIW)

Body-in-white of a car is the basic structure of only spot-welded components of the vehicle. This structure is in its development stage meaning that the final design is still undetermined. Therefore, the structural optimization methods to be introduced to improve the design could be more exploratory than in the previous structure. The design would not be limited by an already existing structure and can be modified further as long as it is within the boundaries of the material and mechanical properties. The dynamic characteristics of a body-in-white structure of a car are important in the design phase. Initially for most structure undergoing dynamic loading, it is essential to know the natural frequency and the corresponding mode (Thorby, 2008; Bower, 2010). The dynamic

behavior of a structure can be predicted by knowing the characteristics. By understanding how a structure would react under certain frequency, a number of improvements can be implemented to the design. In such cases like the BIW, the modification of the body would also need to factor in the ride (Xu et al., 2006), handling (Lu & DePoyster, 2002), and safety of the user. Failures could occur due to resonance, such as wear and fatigue, and should be avoided by monitoring the resonant and operating frequency of the structure (Billah & Scanlan, 1991).

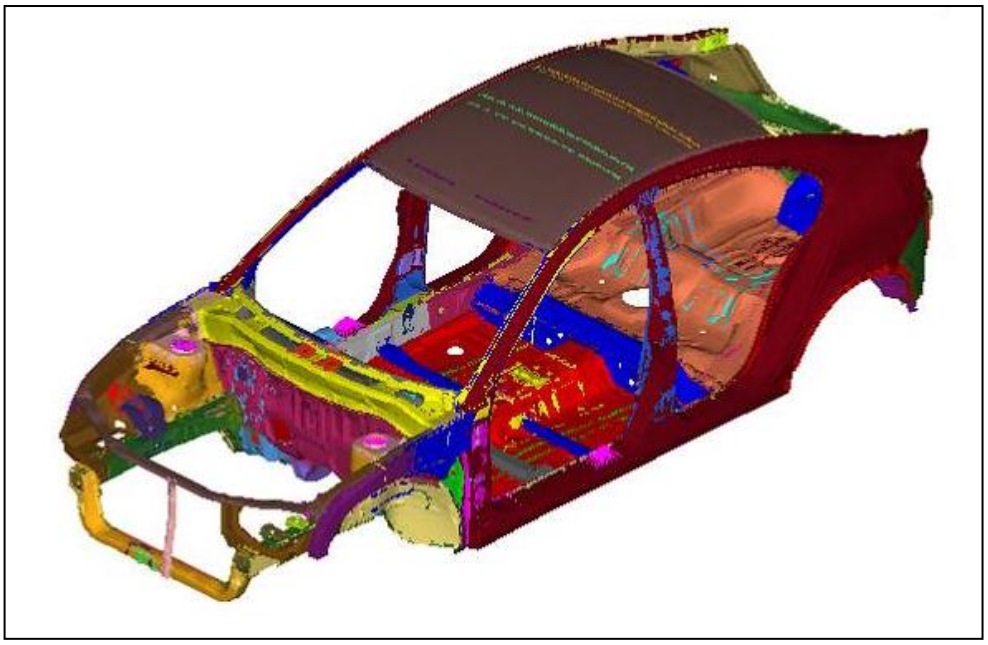

Figure 3.9: Original BIW Model (Source: Proton Berhad)

Free-free boundary condition will be used for consistency between results and the high repeatability offered such as established when determining the global body stiffness of a structure with a modal analysis test (Zheng et al., 2001). It is then compared to the operating frequency of the structure depending on the vibration that may be induced by a number of factors such as engine vibrations, road conditions, and suspension system (Kim & Kim, 2005).

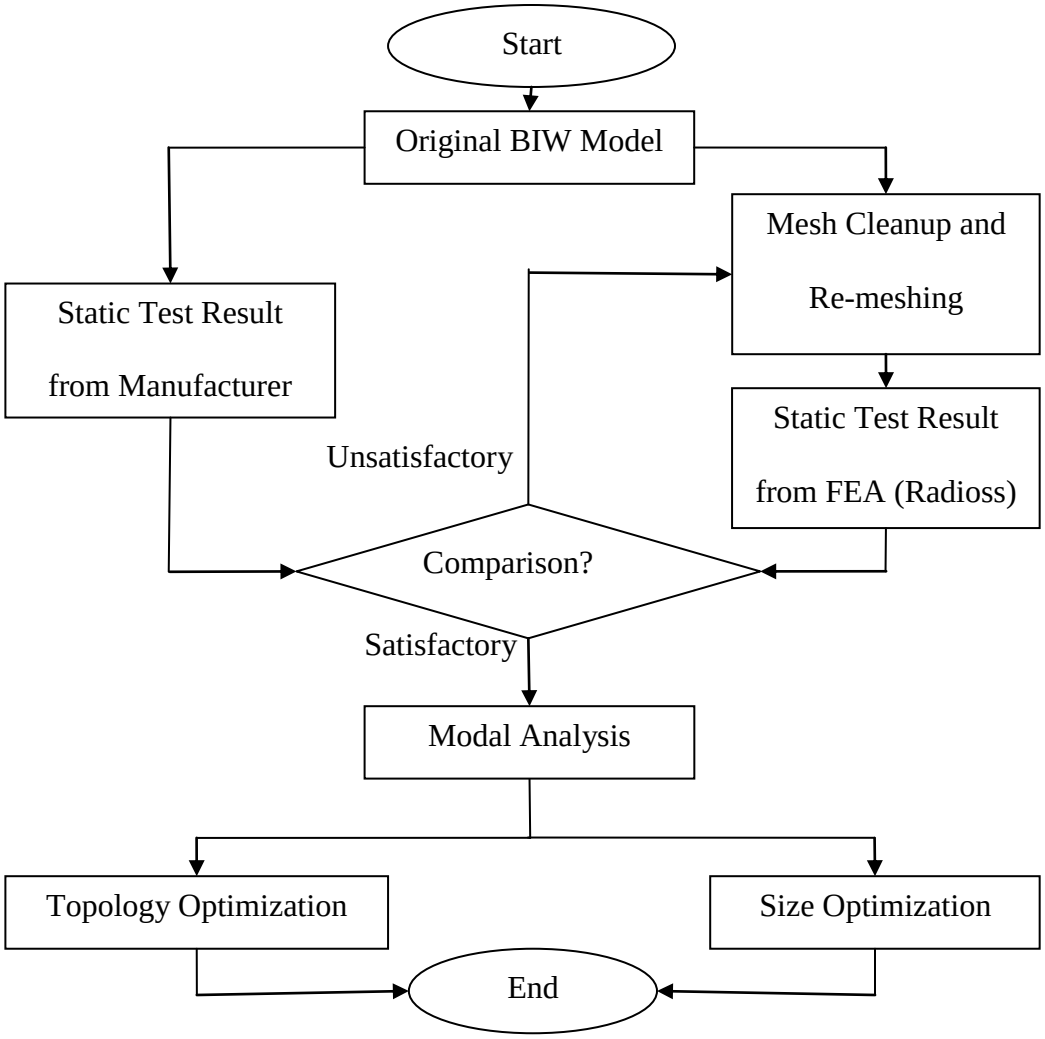

Figure 3.10: Validation Strategy for BIW Model

3.2.1 Modal Analysis

The model used for this paper is a compact 5-door hatchback with the BIW of the car shown in Figure 3.9. While the research mainly covers dynamic response of the structure, a static test can be used for validation purposes in regards to the other factors. The consistency of the analysis can be checked because the dynamic analysis used, which is a real eigenvalue analysis, will only rely on the mass and stiffness of the model same as in a simple static analysis.

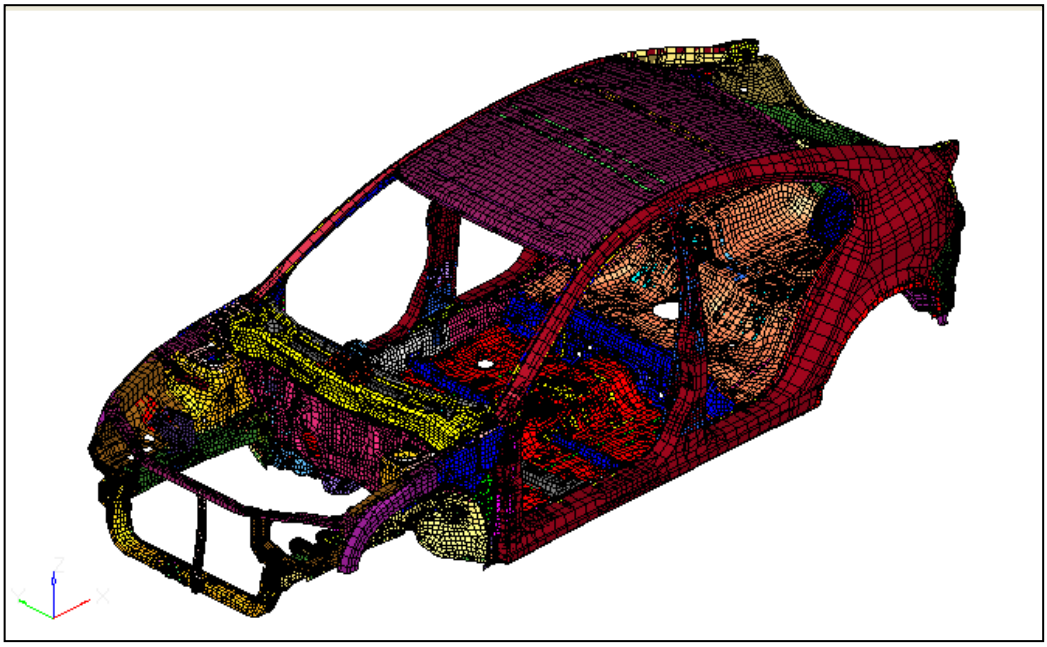

Figure 3.11: Meshed Model of BIW

The model given by the manufacturer is a Nastran model so it would need to be imported into Hypermesh before it can be used. The elements that will be used for this model are a mixed of tria and quad elements because of the complex shape of the build (Figure 3.11). The model only consists of 2-D elements unlike in the previous case. This is done to simplify the simulation and in turn reduce the time taken for the analysis. Some element cleanup has to be done because of the difference between the thresholds used for the different solvers. For this simulation, the elements need to be of certain standard that is set by the Radioss solver.

After the cleanup, both element and material properties will be applied onto the elements. Because shell elements will be used for this model, the thickness of the shell would need to be applied. The thickness depends on the real thickness of each components of the real structure. Besides that, the material used is aluminium so the property such as the Young's modulus, Poisson ratio and density were also assigned.

With the model set for analysis, static bending and torsion test will be conducted to show the rigidity of the structure in terms of static load. The test will be done by calculating the deflection of specific location on the body when the loads were applied. For torsion stiffness, the position of the wheel base will be used as the point of interest in the test. While for bending stiffness, the position of the side frame-door mechanisms will be assessed as the deflection point (Happian-Smith, 2002). The durability of the structure affects the crashworthiness for cars because of the deformation of the body under loading. Hence, it may also influence the New Car Assessment Program (NCAP) crash rating for the car. Once the model has been proven to reflect accurately between the solver used in the research and the solver used by the manufacturer, it can go through modal analysis to find the dynamic characteristics.

This will be followed by setting the loading conditions which is the real eigenvalue extraction data (EIGRL) to set for modal analysis. The number of modes will be set at 10 because the first 6 would be the rigid body modes. The flexible body modes, which are of importance in this study, starts from mode number 7. However, the only modes of interest are the first torsion and bending mode which should occur at mode 7 and 9, respectively. The natural frequency values at those modes will be extracted to be analyzed and optimized.

3.2.2 Structural Optimization

After the natural frequencies for the two modes are found, optimization of the structure can be done to improve both modes. Structure optimization will first be employed by using topology optimization with the mass of the structure as the objective. The added mass will be minimized as to satisfy development objectives such as, among others, a fuel-efficient

car. Consequently, the frequency of the first bending and torsion modes will be used as the constraint to suppress vibration (Sugahara, Kazato, Koganei, Sampei, & Nakaura, 2009). This is important as not to affect other factors contributing to the BIW design such as crashworthiness, components placements, and design space (Jang, Choi, & Choi, 2008). From the optimization, spots where reinforcement is needed can be established.

Table 3.3: Thickness of Components

Thickness (mm)	No. of Components
0.6	4
0.7	18
0.75	2
0.8	6
0.85	1
0.9	3
1.0	20
1.2	37
1.4	19
1.5	1
1.6	19
1.8	5
2.0	13
2.3	4
2.4	2
3.0	1
Total	155

The design variable for the optimization would be the thickness of the components whereby the basic design of the body would not be influenced by the alteration (Table 3.3). The change in thickness will only be set to increase so that the structural strength of the structure would not be compromised. Any decreases in thickness of any components have a high probability of reducing the structural stiffness (Reddy, 1999). Therefore, the thickness will be set to be able to change to 3.2 mm or 4 mm from its original thickness where the maximum thickness was 3 mm. The reason those values were chosen was because standard sheet metal used to reinforce body panel is between 0.2 mm to 1 mm (Duffy, 2009). The

responses used are the natural frequency for the two modes and the mass of the whole structure. The natural frequencies will then be set as the constraints and the mass will be set as the objective. The first torsion mode will be set to be above 40 Hz and the bending mode will be set to be above 60 Hz. These were the values given by the manufacturer where they have determined to be the most suitable frequency for a running vehicle to prevent most dynamic problems.

Table 3.4: Optimization Criteria Settings

Variable	Thickness of shell elements, T
Constraints	First torsion mode > 40 Hz First bending mode > 60 Hz
Objective	Minimize mass

Then, to contrast the result from the topology and the original in terms of manufacturability, the process will be repeated using size optimization. The criteria of the optimization will be the same as in the topology optimization except for the design variable (Table 3.4). In this approach, the thickness can increase between the original thickness and the maximum thickness while for topology the thickness can only be either the original or the maximum thickness. The thickness limit will be set to 3.2 mm and 4 mm same as in the previous study.

This will be followed by the rigidity analysis of the new designs according to the changes induced from the optimization process. Then, employ both static torsion and bending test onto all of the structure produced from the optimization. The analysis will show whether the modification introduced affects the structural rigidity of the structure. The result from the test will be evaluated against the result from the original structure, and if the rigidity decreases, the modifications may need to be reconsidered or readjusted. If it shows a better rigidity, then the new configuration can be deemed as a reliable change to the structure.

With the changes done using the implication from the optimization, both the frequency for torsion and bending modes should increase to the proposed value. Furthermore, there should also be an increase in the volume and mass of the structure, though it is of minimum value. The extra load is the result of trying to increase the value of the frequency without significant changes in the design. The location that needs reinforcement can then be extracted from the result for further investigation.

Chapter 4: Results

Firstly, the dynamic characteristics of each structure will be presented to understand the behavior under specific operating frequencies. Secondly, the optimum design of the structures will be introduced from the result of the structural optimization processes. These results should show that the structural optimization method could provide the optimum design of the structure rather than relying on the trial and error method that counted on the knowledge of the user, which can also be time-consuming. Although the structural optimization method may also involve lengthy setups, the compensation of having a controlled and a much more predictable timeline is a significant advantage.

4.1 Experimental Rig

For the experimental rig, because the structure is available in a laboratory and can be operated readily, the process of optimizing the structure requires both experimental and computational methods. The experimental approach would validate the accuracy of the model developed in the computational approach. The natural frequencies and the corresponding modes less than 100 Hz were extracted from both analyses and a comparison. This was done as any frequency over 100 Hz is already too excessive and impractical for the structure because of the limitation of the excitation frequency which comes from the motor that has an allowable frequency of about 50 Hz.

4.1.1 EMA and ODS

The model of the pedestal with the 72 measurement points as shown in Figure 3.3 was analyzed using EMA in the lateral (x), horizontal (y), and vertical (z) directions for each measurement points.

This analysis resulted in 216 FRF measurements which were overlaid together in a single graph (Figure 4.1). From the graph, it is obvious that there are two resonance peaks below 50 Hz, while a total of five modes below 70 Hz. The peaks above 70 Hz can be neglected since the maximum operating frequency of the motor is only 50 Hz. Therefore, it is sufficient to consider the modes with frequencies in the range of 10 to 70 Hz as shown.

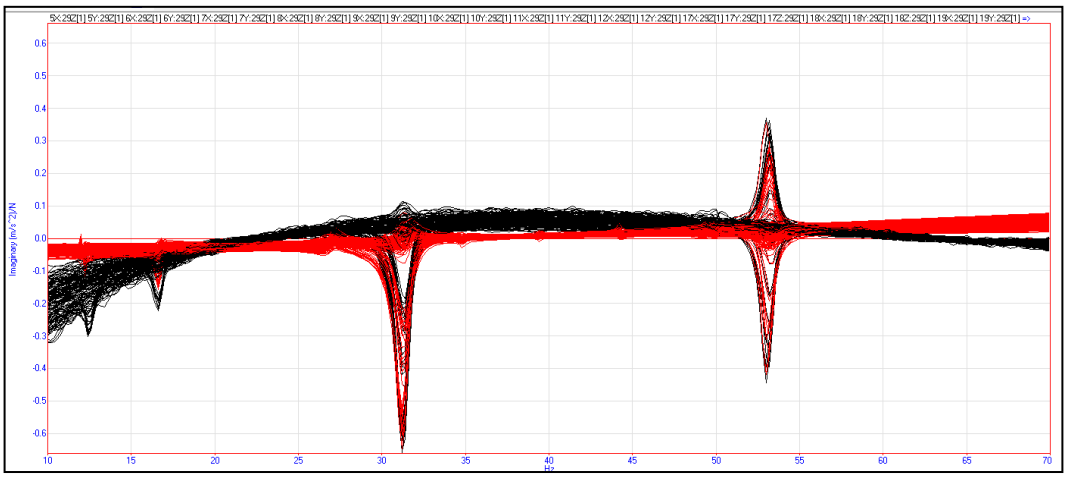

Figure 4.1: Curve Fitting FRF between 10 Hz and 70 Hz

The natural frequencies and the corresponding mode shapes were found by examining the model under the chosen frequencies. Peak cursor band fit was used to find the natural frequencies of the model.

As stated previously in Chapter 3, the rig consists of a motor, a motor base, pedestal made up of 4 L-shaped legs, a hollow base and a plate base. The deformation of the rig would then depend on the strength or the stiffness of each of these components. Therefore, because most of the components were made as a base to support the other components, the weakest part of the structure would deform first before the others such as the pedestal.

The first mode occurs at 12.1 Hz, with a shape of the model bending in the x-direction or from front-to-back as shown in Figure 4.2. The pedestal would sway front to back because of the lack in stiffness compared to the mass it is supporting. There is also a slight

deformation at the bottom of the legs where it connects with the base of the pedestal because of the bending due to the hollow nature of the part connecting the pedestal and the plate base.

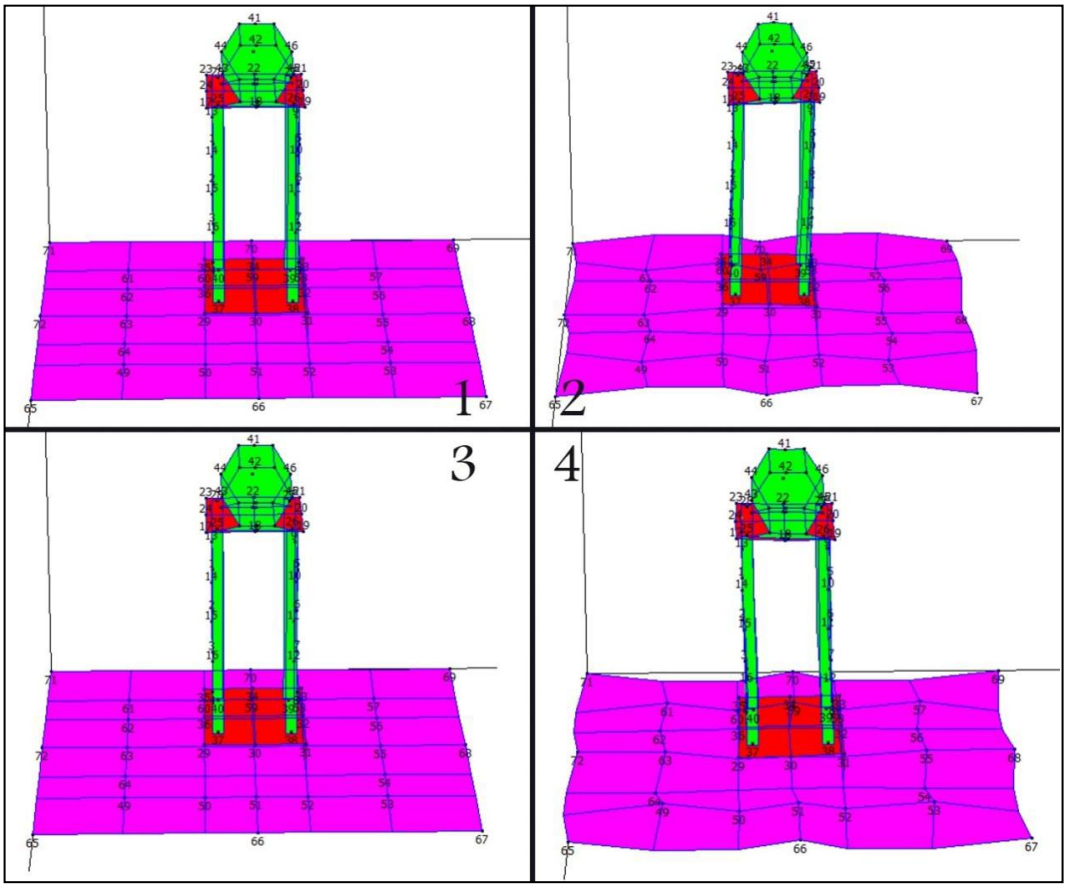

Figure 4.2: Mode 1 at 12.1 Hz

The second mode occurs at 16.7 Hz, where the pedestal bends dominantly in the y-direction or side-to-side as shown in Figure 4.3. The same behavior of the pedestal occurs here only at a different direction. The frequency is slightly higher because the hollow base is stiffer in the horizontal direction. The slight deformation is also evident at the same position because of the bending motion.

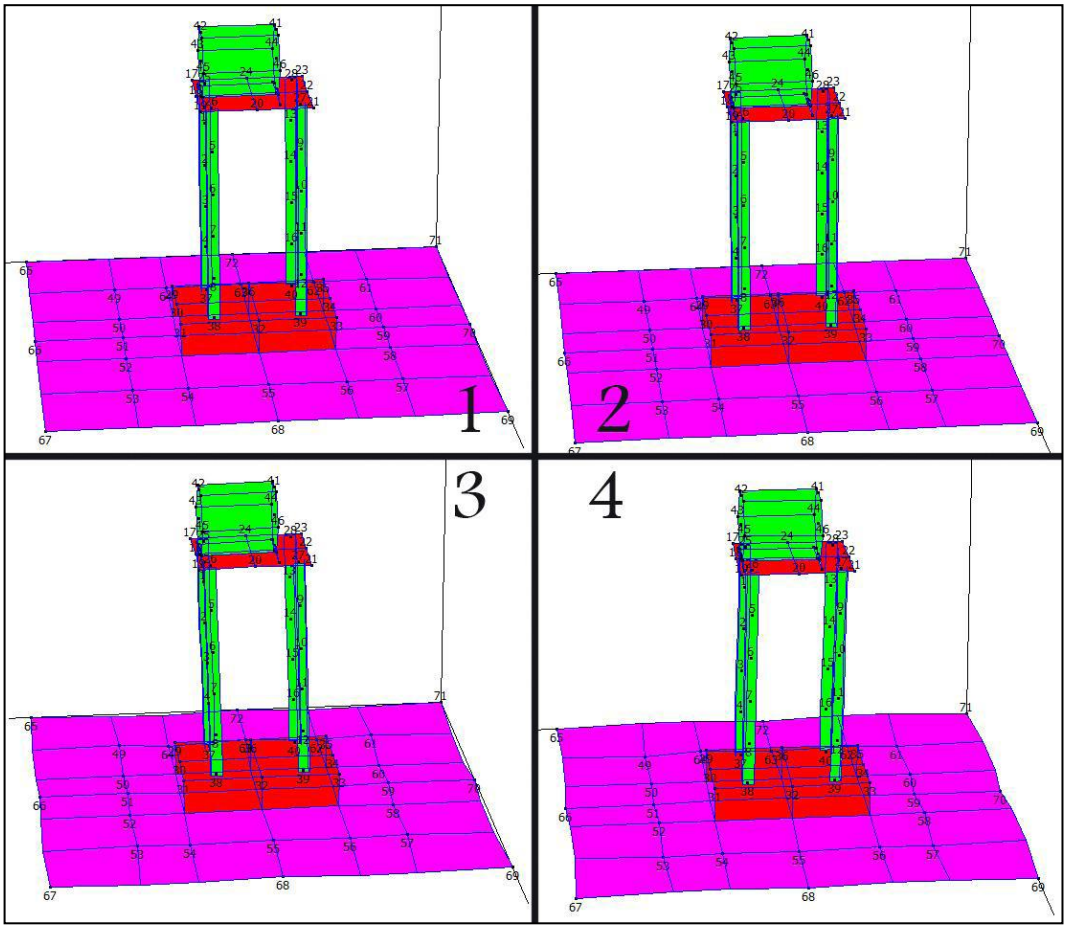

Figure 4.3: Mode 2 at 16.7 Hz

The third mode occurs at 31.4 Hz, where the deformation differs significantly from the two previous modes as shown in Figure 4.4. The pedestal stays mostly unaffected but the base has moved up and down or bounced from its initial location. This happens because the next possible part to deform after the pedestal is the plate base. The thickness of the plate is small compared to the whole structure resulting in a deflection because of the lack in stiffness.

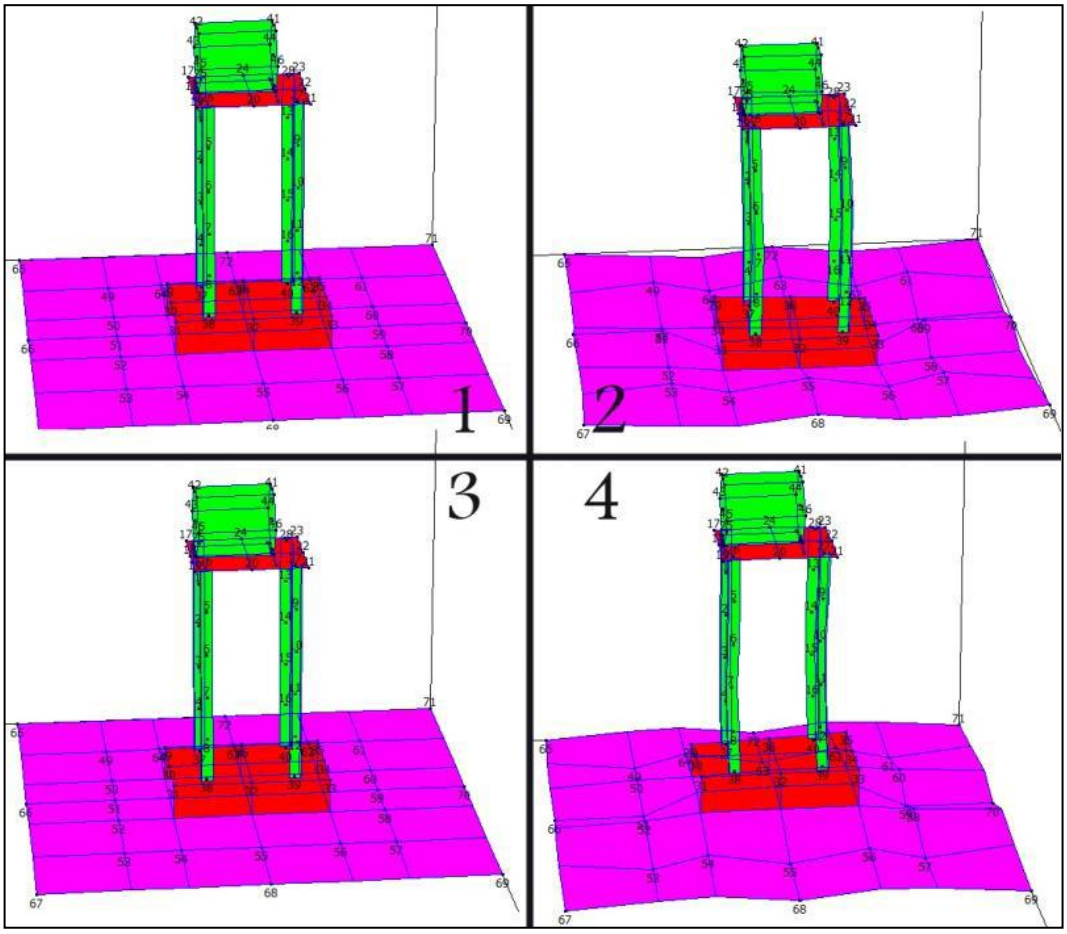

Figure 4.4: Mode 2 at 31.4 Hz

The next mode frequency is above 50 Hz. The fourth mode occurs at 53 Hz, which is the first torsion mode where the pedestal twists about z-axis as shown in Figure 4.5. The rotation originated from the legs or pedestal that simply deformed because of the weight of the motor encumbering the support structure. The deformation of the base is significantly smaller compared to the two previous modes.

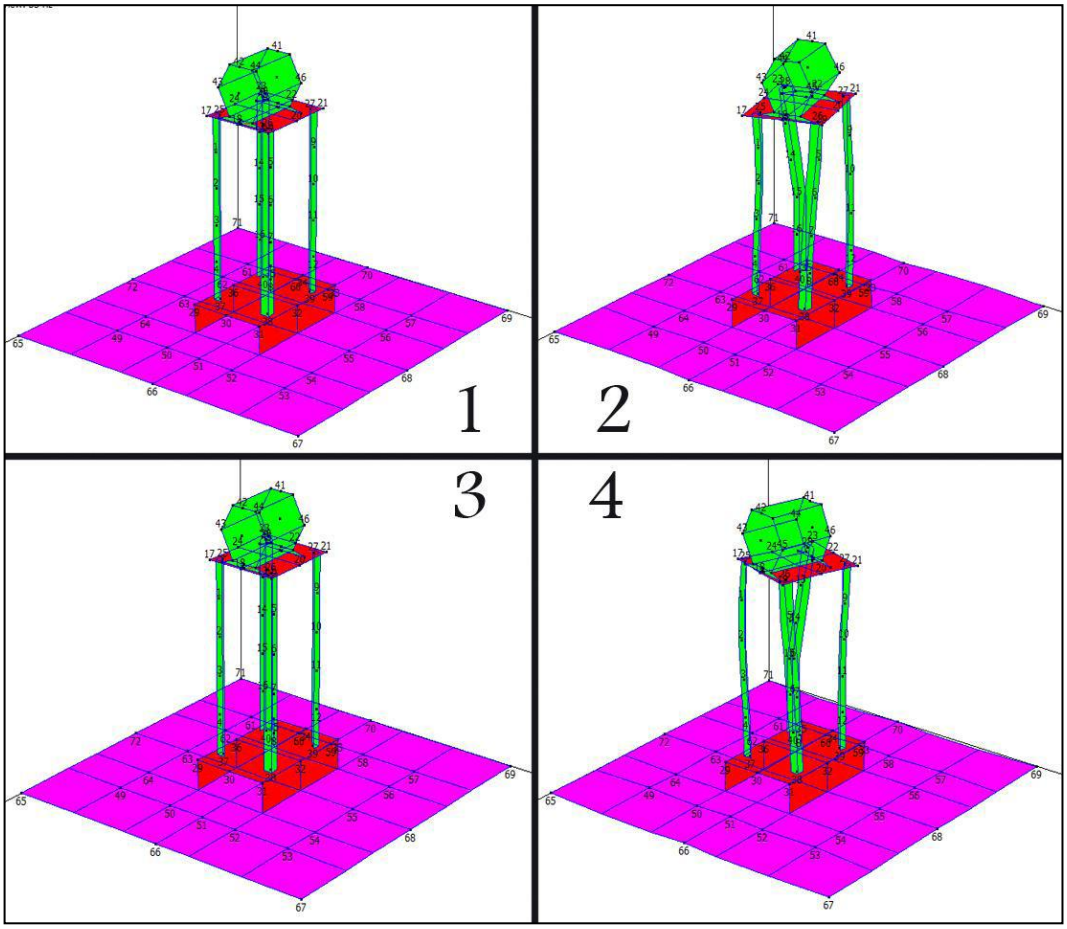

Figure 4.5: Mode 4 at 53 Hz

This is then followed by the result from the ODS analysis. The ODS was done to validate the natural frequency obtained from the EMA. The first mode at 12.1 Hz was used as the comparison for the resonance problem created by running the motor at 12.1 Hz. The analysis was also done at a non-resonant frequency of 8.0 Hz to show the differences occurring at resonance.

The ODS analysis at 12 Hz shown in Figure 4.6 can be seen to be significantly similar to the result in Figure 4.2. All 216 FRF readings from the measurement points were categorized according to the x, y, and z-direction (Figure 4.7). Note the obvious peak at 12 Hz especially in the y-direction, within the frequency 100 Hz.

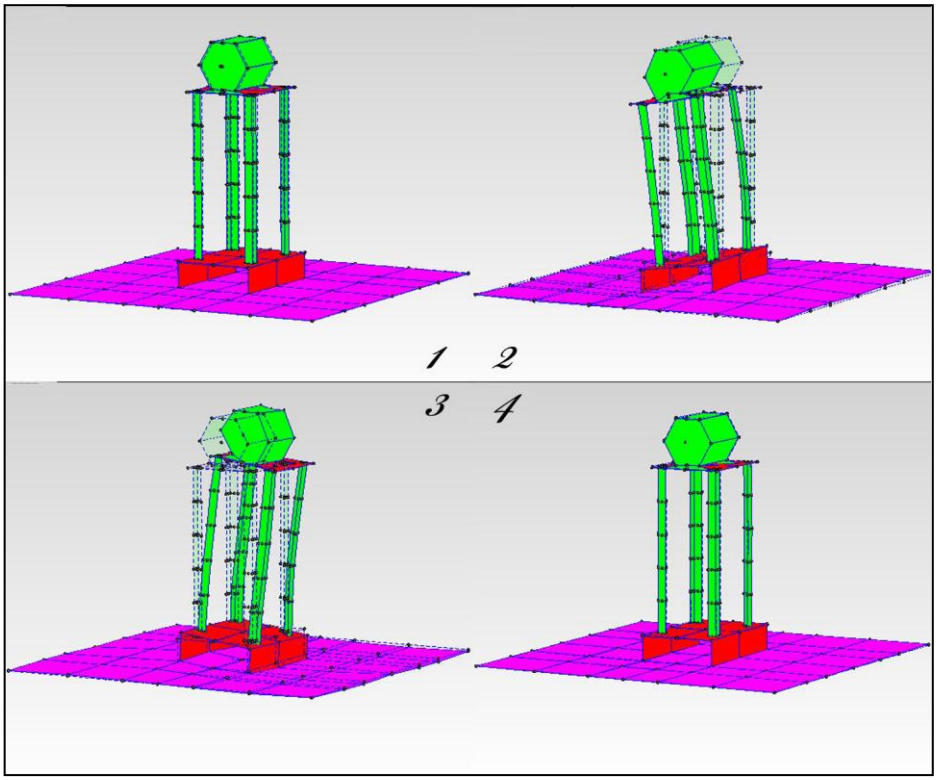

Figure 4.6: ODS of Structure at 12.1 Hz

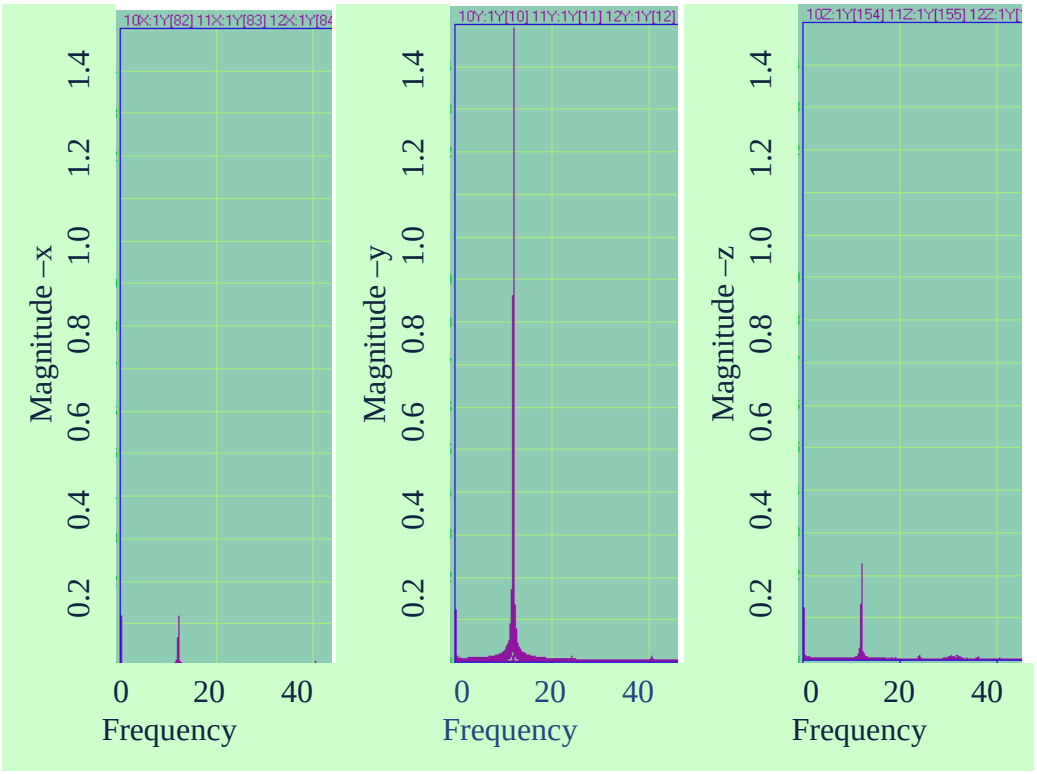

Figure 4.7: ODS FRF in x-, y-, and z- direction, at 12 Hz

The RMS values of all the readings were calculated and tabulated from 0 to 200 Hz. The values are representation of the energy content of the structure, so in the y-direction the energy content is about three times larger than in the x and z-direction (Table 4.1). Hence it can be concluded that resonance does occur at 12.1 Hz. In addition to RMS values, the vibration accelerations at several major points that experienced great motions compared to others were taken and the total accelerations were calculated (square root of the sum of squared acceleration in the three directions).

Table 4.1: RMS Value of x-, y-, and z-direction at 12 Hz

Direction	x	y	z
RMS (ms-2)	0.007472656	0.021125561	0.008326795

To further verify that resonance occur at certain frequencies, another ODS analysis was done at an assumed non-resonant frequency. The value used was 8.0 Hz which is 33% away from the first mode so that the frequency is in the range of non-resonance.

From Figure 4.8, it can be seen that the response shape is similar to the shape at 12.1 Hz. This is because the excitation force from the flywheel is rotating about x-axis, causing most motion in the y and z-direction. Therefore for a more comprehensive conclusion, the RMS values from the FRF of the 8.0 Hz can be compared to the values from the 12.1 Hz.

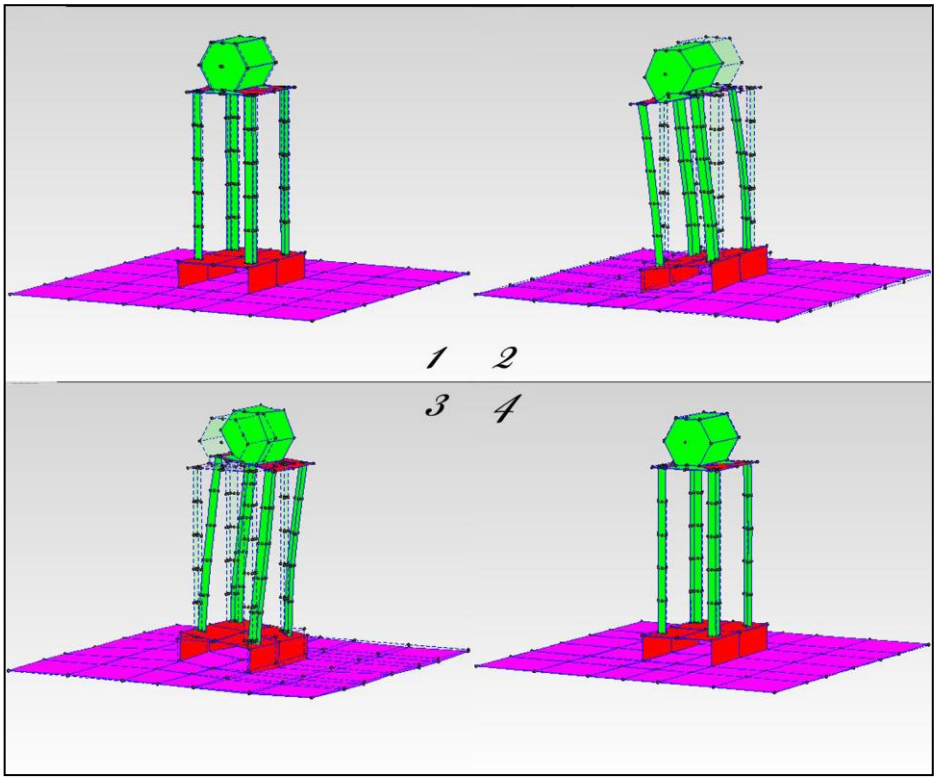

Figure 4.8: ODS of Structure at 8 Hz

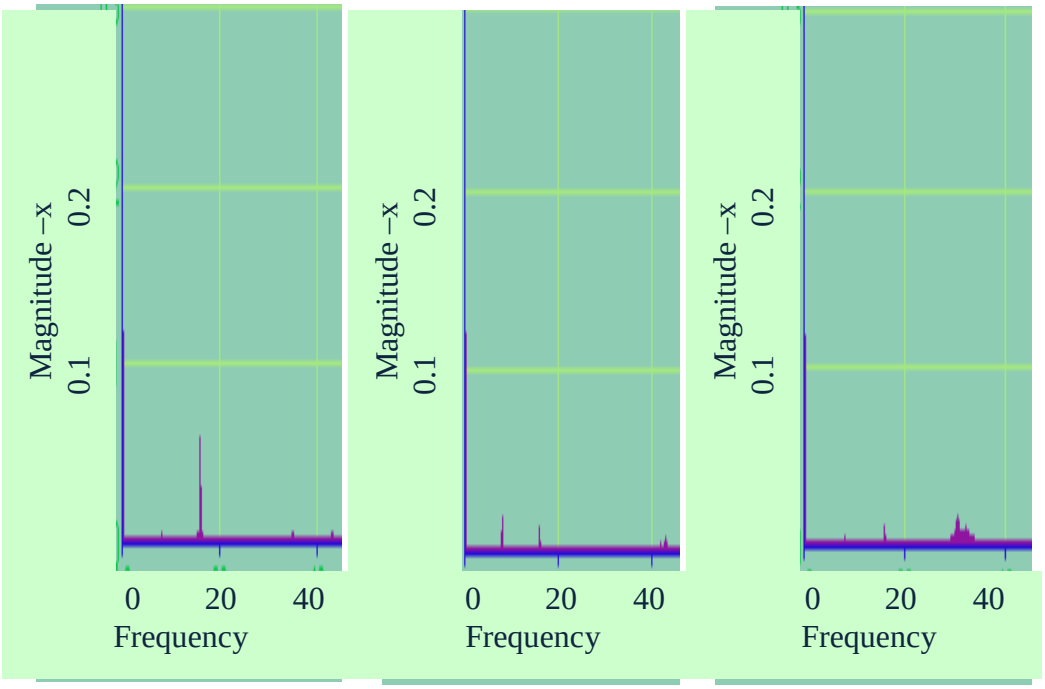

Figure 4.9: ODS FRF in x-, y-, and z- direction, at 8 Hz

From Figure 4.9, the peaks of the amplitudes within the 200 Hz range can be seen and compared to for all directions. It can be seen that the peak is not obvious at 8 Hz compared to the former resonant frequency.

The RMS value calculated for all directions shows a comparable result at 8.0 Hz. The energy content in all directions is almost the same. Apart from that, the vibration accelerations of the major points were also calculated and tabulated (Table 4.2).

Table 4.2: RMS Value of x-, y-, and z-direction at 8 Hz

Direction	x	y	z
RMS (ms^{-2})	0.007398181	0.007325355	0.00731386

By comparing the values from Tables 4.1 and 4.2, is it evident that resonance occurs when the motor is running at 12.1 Hz. The vibration acceleration at resonance frequency is more than 1000 times greater than at a non-resonance frequency. The natural frequencies obtained through EMA was able to be verified using ODS analysis. Although because the maximum operating frequency of the motor is only 50 Hz, the mode exceeding that value is not possible to replicate. From the three modes below 50 Hz, the first mode which is at 12.1 Hz were chosen for the replication of the resonance problem. From Figures 4.6 and 4.7, the structure can be clearly seen to resonate when the motor ran at 12.1 Hz since both the forced motion and the excitation frequency match the mode shape at 12.1 Hz. The same reasons should also apply to the other two modes which are at 16.0 Hz and 38.1 Hz but with different shapes depending on how the unbalanced flywheel would produce the deformation.

4.1.2 Finite Element Analysis (FEA)

There are two results from the FEA; one is from the model with weld elements (Figure 4.10 to Figure 4.13) and one without the weld elements (full solid model) (Figure 4.14 to Figure 4.17). The first model is of a better simulation of the real structure but takes a longer time to set up and analyze while the second assumes that the model is significantly accurate without the welds. The contours of the results only show a dimensionless eigenvalue magnitude of the behavior of the structure under the natural frequency. These values can then be interpreted as the mode shape of the model by taking the values as relative displacement. However, it must be noted that the value is not the displacement because no real force were added onto the model of the structure.

Figures 4.10 to 4.13 show the result for the model with welds. The natural frequencies and the corresponding mode shapes were obtained from the analysis. Only the first four modes were found because of the limitation employed to the analysis. The analysis was set to only find the first frequencies below 100 Hz. It is also shown in the figures that the mode shapes found from the FEA were close approximates for the mode shapes found from EMA.

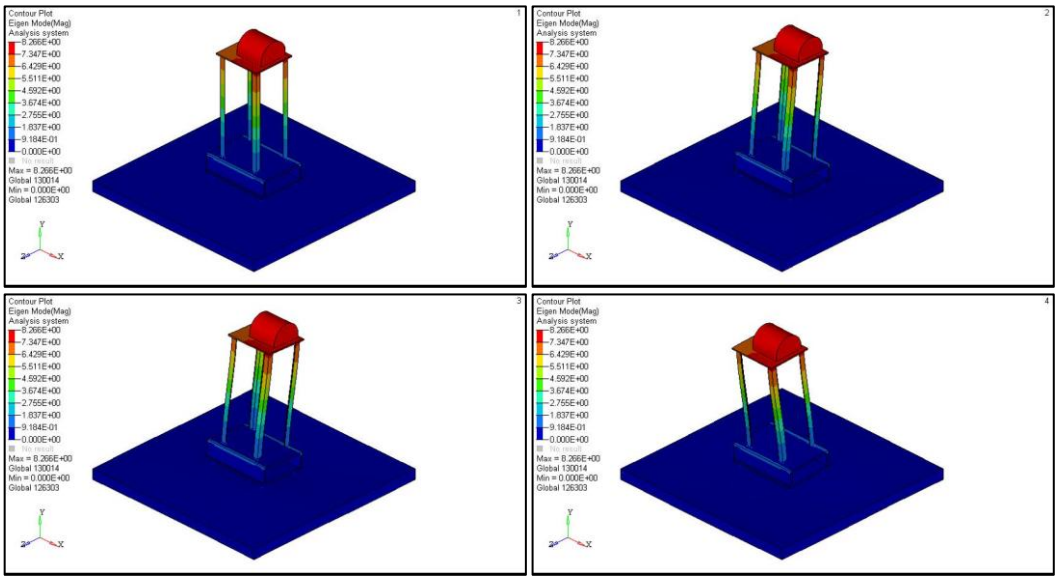

Figure 4.10: Mode 1 at 13.5 Hz of Rig with Spot Welds

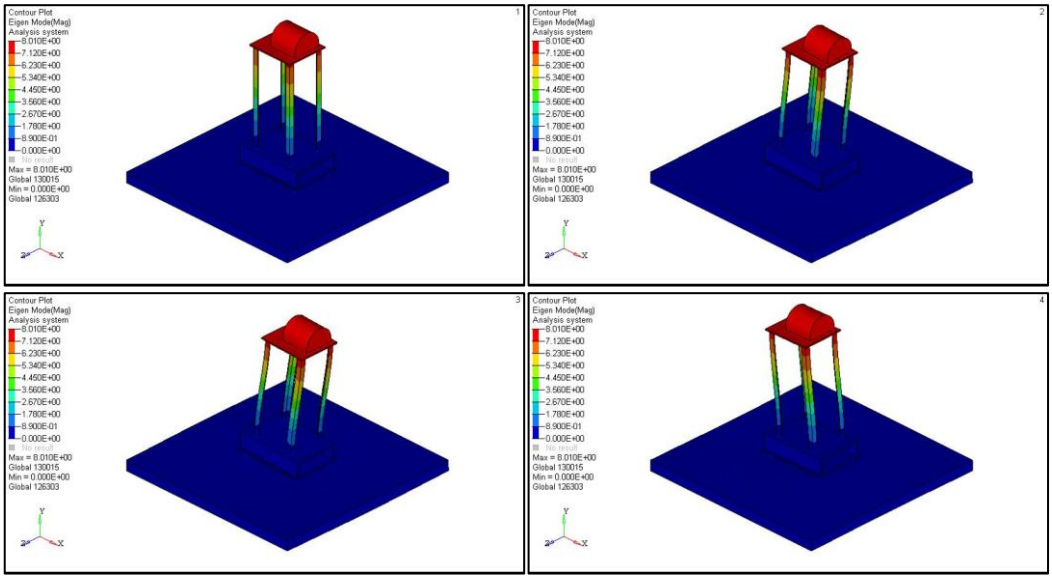

Figure 4.11: Mode 2 at 16.5 Hz of Rig with Spot Welds

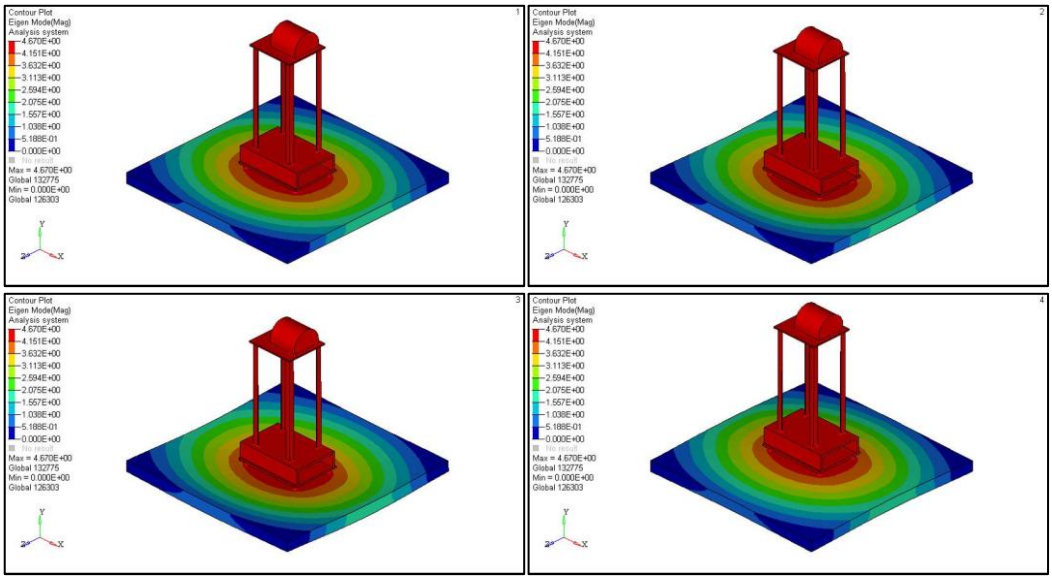

Figure 4.12: Mode 3 at 27.2 Hz of Rig with Spot Welds

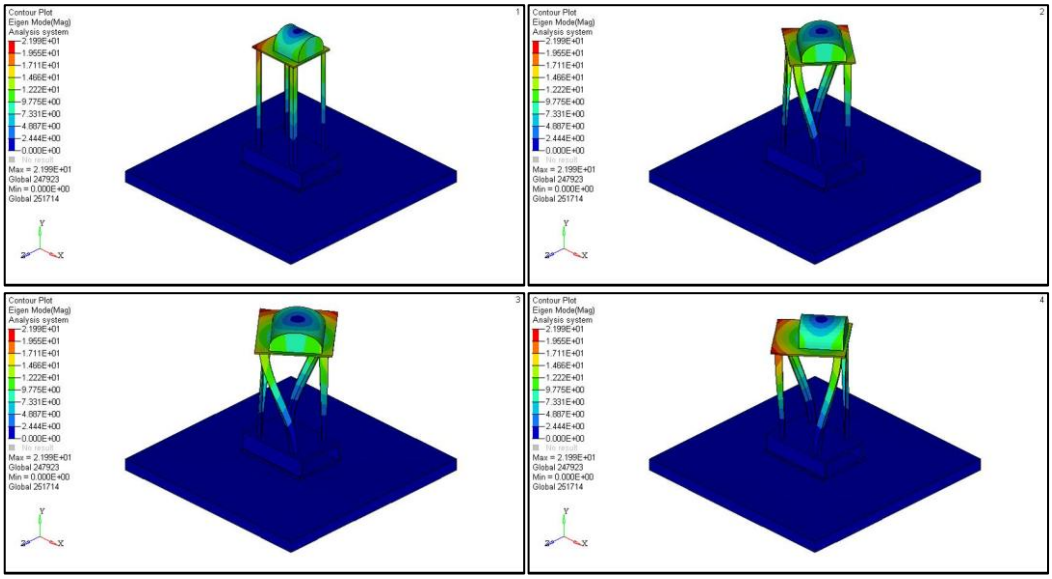

Figure 4.13: Mode 4 at 53.1 Hz of Rig with Spot Welds

Next, the Figures 4.14 to 4.17 show the result for the model without the welds. The values of the natural frequencies and also the corresponding mode shape for both FEA models were almost identical. Even without the weld elements, the results were shown to be quite accurate compared to the result from the experimental method. Hence, either model is able to precisely simulate the structure under dynamic loading.

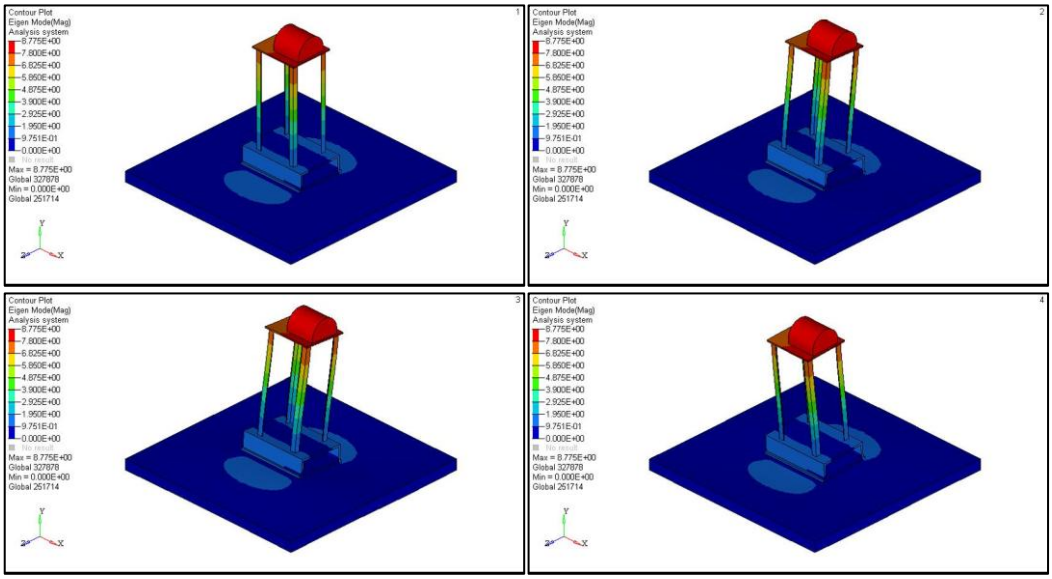

Figure 4.14: Mode 1 at 13.2 Hz of Experimental Rig

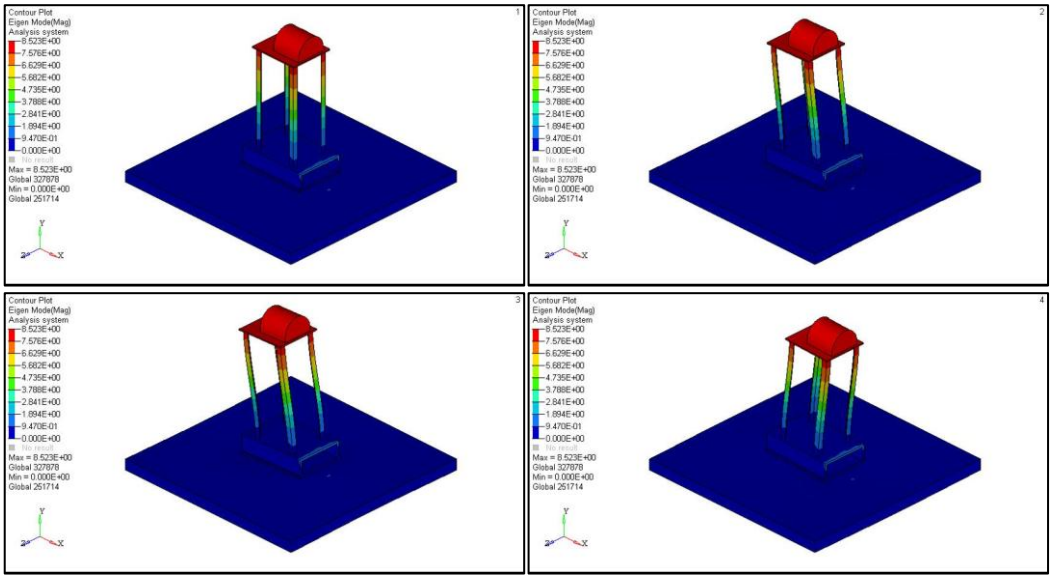

Figure 4.15: Mode 2 at 17.9 Hz of Experimental Rig

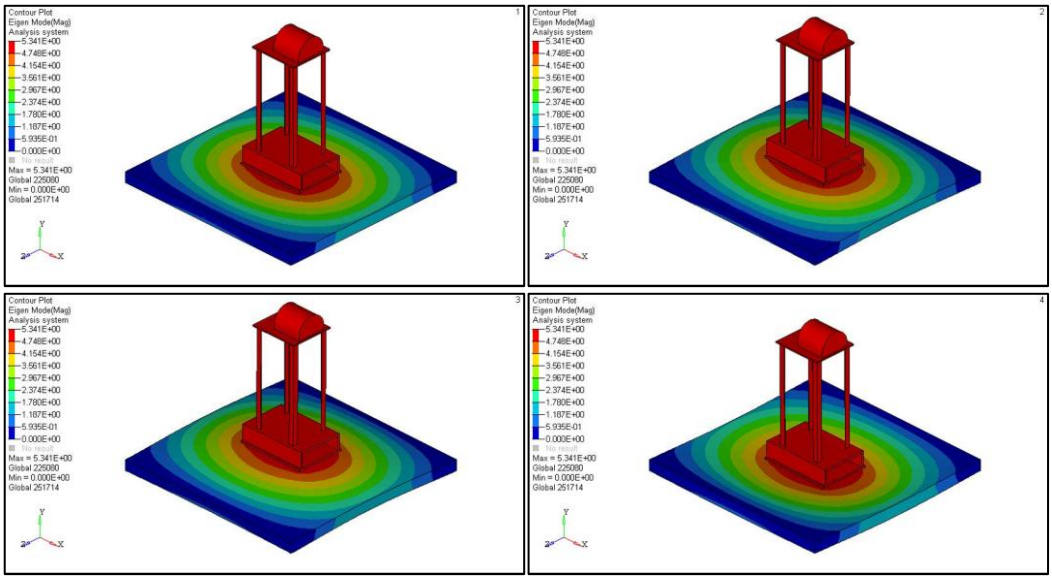

Figure 4.16: Mode 3 at 28.1 Hz of Experimental Rig

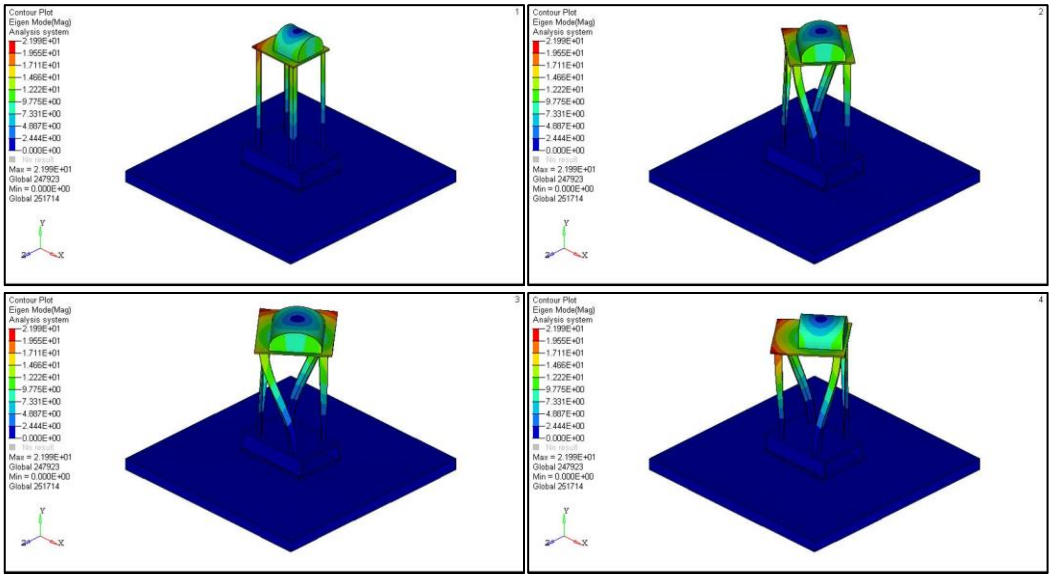

Figure 4.17: Mode 4 at 58 Hz of Experimental Rig

All four modes of deformation for the structure; front-to-back bending, left-to-right bending, bouncing up and down and z-axis torsion were simulated in FEA for both models.

4.1.3 Comparison

The four modes of the modal analysis from all the different methods were taken and used for comparison. This was done mainly to validate the result of the analysis done in FEA. The results from EMA shows natural frequency and the mode shapes of the real structure while the ODS validate that the structure would react the same way under the assumed loading conditions.

Then, the FEA results can be proven to be reliable by checking the result from EMA (Table 4.3). Both simulated model were compared to the EMA result to show the fair similarity of the result with and without the welds. These results show that the simulated analysis using real eigenvalue analysis in FEA is a good approximation of the real result.

Table 4.3: Comparison of Experimental and Computational Results

Modes	Shape	EMA	FEA			
			With Welds		Without Welds	
		Natural Frequency (Hz)	Natural Frequency (Hz)	% Diff.	Natural Frequency (Hz)	% Diff.
1	Bending, Left to Right	12.1	13.5	11.5	13.2	9.09
2	Bending, Front to rear	16.7	16.5	-1.19	17.9	7.19
3	Bouncing	31.4	27.2	-13.38	28.1	-10.51
4	Torsional	53.0	53.1	0.19	58.0	8.62

The main focus when running modal analysis using FEA is the mode shapes rather than the value of natural frequency. The frequency varies basically because of the arrangement of the elements in the model. As mentioned in Chapter 3.1, the validity of frequency value can be checked by plotting a graph of the experimental result against the computational result (Figure 4.18). It is shown that by plotting the values, the slope is very close to 1 proving that the there were no problems in the modal analysis test using FEA (Bernhard, 1943).

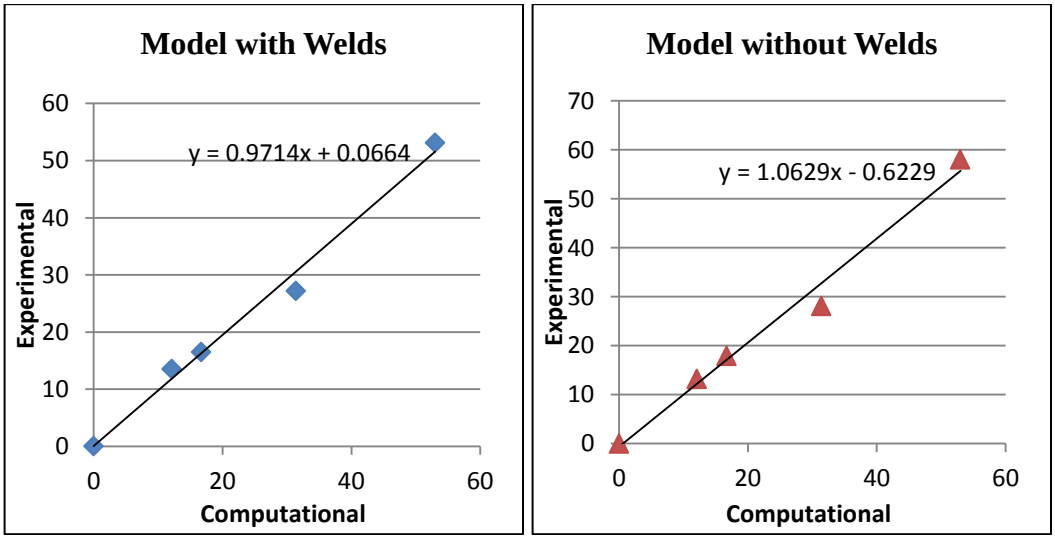

Figure 4.18: Validation Graph of Experimental against Computational Result

The second model was then used as the main model for FEA mainly because of the straightforwardness of the analysis for modal and also for the optimization process. The analysis was reduced to a more simple approach by using a simpler model that still present accurate result. With all the result from the modal analysis, the computational method was validated to be a reliable method of analysis for the structure. Therefore, the following steps of the research would only employ the second FEA model mainly for the structural optimization processes.

4.1.4 Structural Optimization

Using structural optimization, results from every possible input of design space, design constraints and objectives were studied. The results from the two design space used were divided into sections to properly show the differences of the optimized design. The objectives of the optimizations vary by changing the maximized frequency mode.

After 200 iterations, the final outcome of the optimization was shown using Hyperview with the contour result showing the element density. In topology, the color intensity or the value in the analysis would show if the element needs to exist at that position for the optimized design. The color varies from blue to red indicating the value from 0 to 1 of the material density. As the density value increases, the need for that particular element also increases. Therefore, elements with a density value of 1 are very important to the structure and must remain to obtain the best design.

Using Hyperview, the element density can be checked by viewing the model at gradually increasing number of iteration until it reaches 200. Optimization history can also be used and would show the changes in all the responses in relation to the number of iteration. The changes were viewed using the view panel for every sides of the pedestal. When the result

is satisfactory, the isosurface can be used to properly view the end outcome of the optimization. The isosurface was used by setting the value of the element density needed to achieve a good solution. The element density value used for all the result should be the same for consistency. The natural frequency of the result can also be checked prior to the redesigning to ensure the reliability of the results. The accuracy of the frequency value should be taken only as an approximate because of the lack of elements in the model after the optimization. For the best result, the design would need to be remodeled according to the isosurface. All the responses should be double-checked to satisfy all the constraints and objectives.

By using the isosurface model from the result, a new design for the rig can be redrawn using Solidworks. The results were observed at each side of the pedestal to find the pieces and elements that needs to be removed or retained for the new design. This can be done by measuring the dimensions of the isosurface to be used later. Then in Solidworks, the new dimension can be implemented to obtain the new design. Using the basic rig design space, the sketches of the new design were redrawn at each side of the readied structure and the unneeded sections can be cut.

After all four sides have been completed, the structure can be easily exported back to Hypermesh as an IGES file. The file will undergo the same treatment as before such as meshing using tetramesh and applying constraints. Modal analysis was done onto the new design to obtain the natural frequency of the modes. These new result were compared to the result of the original design. If satisfactory, the new design can then be taken as the best design for the given constraints.

4.1.4(a) SDM Using Structural Optimization – Existing Structure

For the experimental rig, where the physical build is already at hand, the optimization can be done directly as added reinforcement. It is reminiscent of SDM where modifications were made to improve the dynamic behavior of a structure by adding support materials. However, instead of using trial and error to identify the reinforcement, topology optimization will illustrate the change or modification that is needed on the structure through the model. Then, size optimization will further improve the reinforcement by searching the best dimension of the support structure.

Using a hollow region as the designable area would give a final design with constant thickness of 3 mm along all the sides. Nevertheless, the extra matter that was not in the original will undergo size optimization to obtain the thickness.

Figure 4.19 shows the result of the topology optimization to maximize the first natural frequency of the structure. The contour shows the element density of each element with the color red denoting valid areas and blue denoting void areas. Then, from the contour result, an isosurface where only the valid areas were taken into account can be extracted. The valid area was established to be when the elements occupying it have a density above 0.3. This model will then be the rough outline of how the new design for the model will look like.

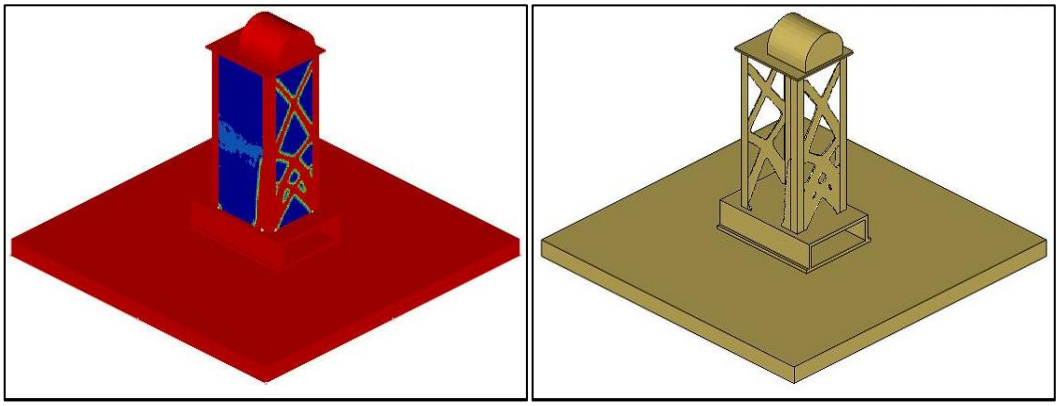

Figure 4.19: Contour and Isosurface of Hollow Region Reinforcement

The model was redrawn and remodeled in Solidworks according to the isosurface result. From Figure 4.20, it is shown that the reinforcements were mostly focused on the left and right side of the structure mainly due to the lack of lateral support at the base. For the front and back side of the structure, the only reinforcement needed is a slight increase of the width of the leg at the bottom. Modal analysis was performed for the new model on Hyperworks to show the new natural frequency.

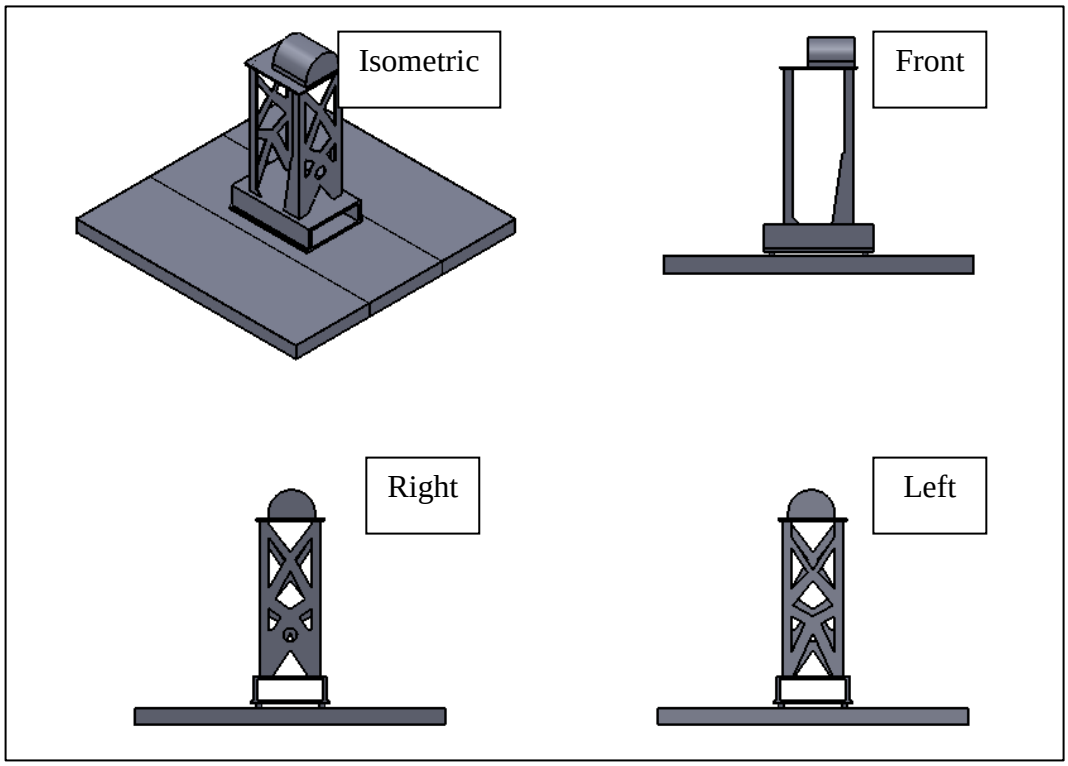

Figure 4.20: New Design of Hollow Region Reinforcement

To further the optimization process, size optimization was implemented onto the additional support structure. The thickness of the support was set as the variable for the optimization with the same objective and constraints as before. From the optimization, it is found that the thicknesses for front and rear sides are 2.12 mm, 1.47 mm for the right side and 1.41 mm for the left side.

Analyzing the dynamic characteristics of the new model by doing a modal analysis shows that the natural frequency did improve from the original model. Figure 4.20 shows the newly remodeled rig with Figures 4.21 and 4.22 showing the result of the analysis with the natural frequency and mode shape of the structure. The first mode is shown to have a frequency of 18.2 Hz and the second mode with a frequency of 24.3 Hz. Both show a fair increase from the original though still did not exceed the 20 Hz expected from a normal operation of the machine.

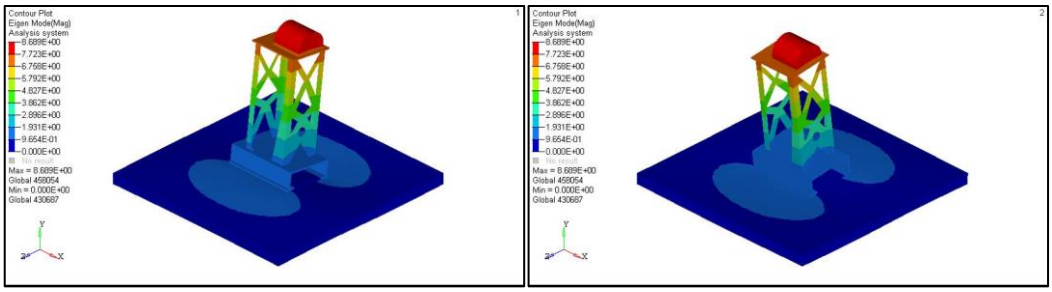

Figure 4.21: Mode 1 at 18.2 Hz

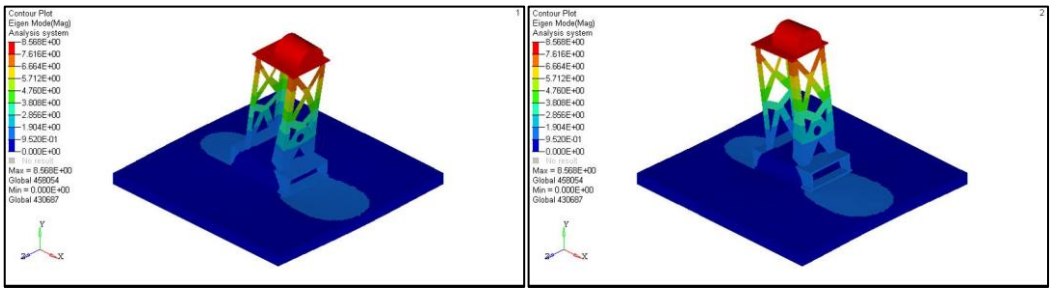

Figure 4.22: Mode 2 at 24.3 Hz

Next, the process was repeated using whole solid region as the designable space. The design obtained from this approach should demonstrate a slight difference in terms of varying the thickness of the parts in the structure.

The contour result in Figure 4.23 shows a similar pattern of the valid and void areas externally with the result from hollow region. In spite of this, the main difference is that with the whole solid region, it can be assumed that the internal material of the pedestal is not required and therefore can be removed entirely from the structure.

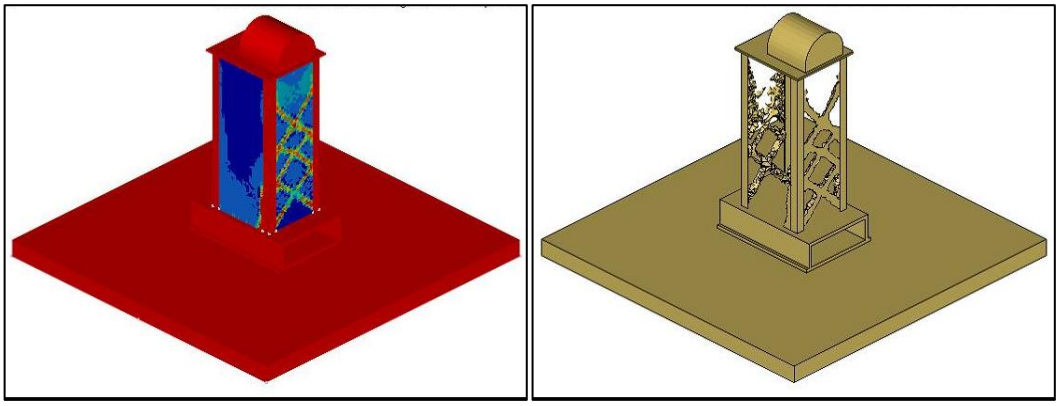

Figure 4.23: Contour and Isosurface of Whole Solid Region Reinforcement

However, this approach also proved that the original thickness of 3 mm is not the ideal value and needs to be discovered because of the concentration of the elements at each side. Therefore, size optimization was done to find the ideal value for the thickness of each component.

As shown in Figure 4.24, the new design obtained from using whole solid region is comparable to the result from hollow region. Both the left and right side require more support to increase the stiffness and in turn increase the natural frequency while only a little support is needed at the front and rear sides.

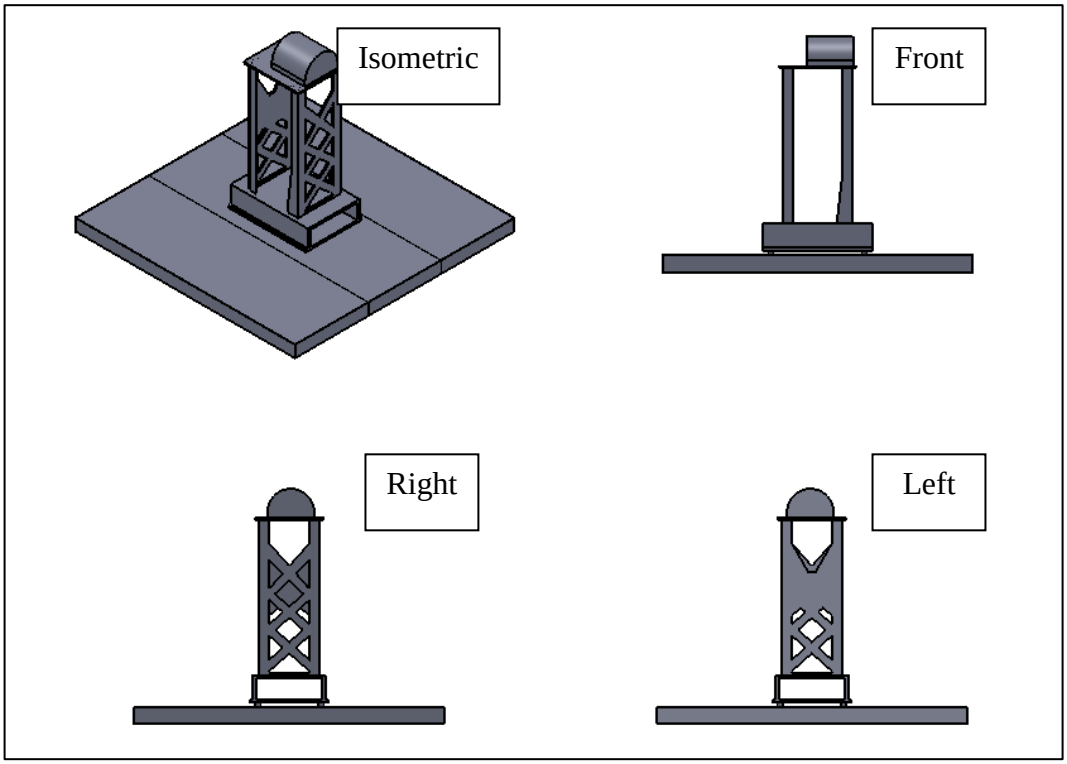

Figure 4.24: New Design of Whole Solid Reinforcement

The model was then imported into Hyperworks and undergone modal analysis to find the new natural frequency and mode shapes. Size optimization was done onto the sides excluding the 'legs'. The front and rear sides evened out to 8.79 mm, while the right and left side worked out to 0.94 mm and 1.63 mm, respectively.

Figure 4.25 and Figure 4.26 show the deformation shape for the first two modes. The natural frequencies for the modes have shifted to 17.7 Hz for the first mode and 21.0 Hz for the second mode. The shifted first mode was still under the target value of 20 Hz.

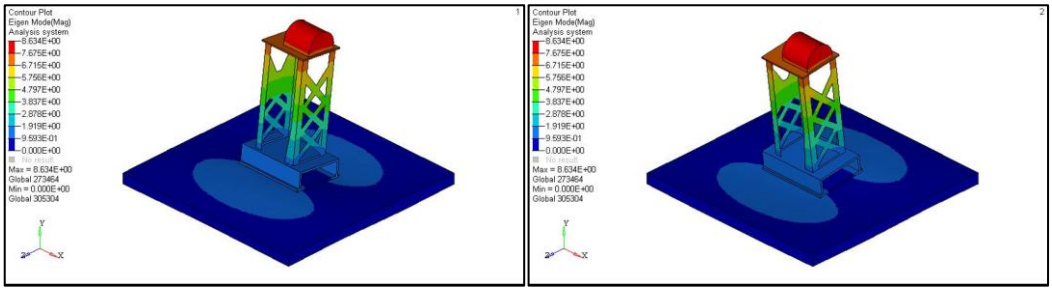

Figure 4.25: Mode 1 at 17.7 Hz

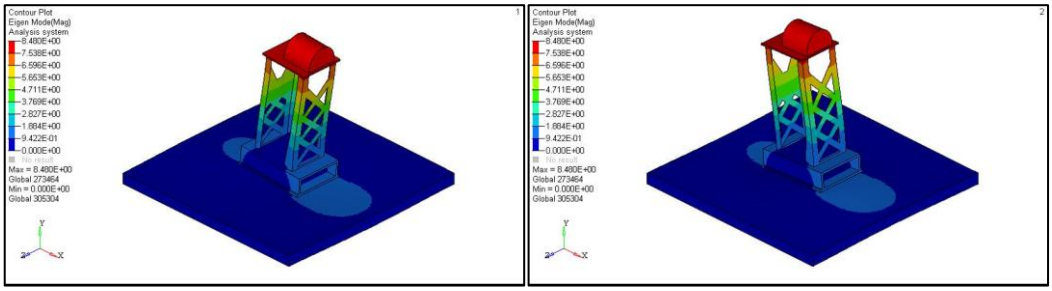

Figure 4.26: Mode 2 at 21 Hz

4.1.4(b) SDM Using Structural Optimization – Conceptual Design

Initial design stage is defined as the period where the design of the structure has not been finalized and therefore could be manipulated wholly without the repercussion on the original design. Though for this rig is already a functional structure, in theory it can still be improved at the design stage most likely for future use. So, to achieve the process, the approach for the designable variable was changed to accommodate for the additional development depending on the design space used. Even though the whole design can be changed to achieve the objective, it is advised to limit the design variable for any optimization process to simplify and lessen any complications that may occur. Thus, for the experimental rig, only the pedestal part was chosen as the design variable while ignoring the base. Moreover, rather than setting the original legs as non-designable parts, the whole pedestal between the base and motor base was set as the variable.

With the possibility of changing the final design of the rig, the whole hollow region was used as the designable space for the optimization. The result shown will be of maximizing the first mode. The volume and the mass were not constrained for this approach to show the different outcome of limiting (or not limiting in this case) the weight of the structure.

Figure 4.27 shows the contour result of the optimization with the first mode as the objective. The elements in red will be retained to extract the new design of the rig for this

approach. The model was redrawn using CAD and modal analysis was done for the new model. Using a level set 0.3 for the value of accepted element density for the optimization; the isosurface model of the rig was used as the basic form of the new design.

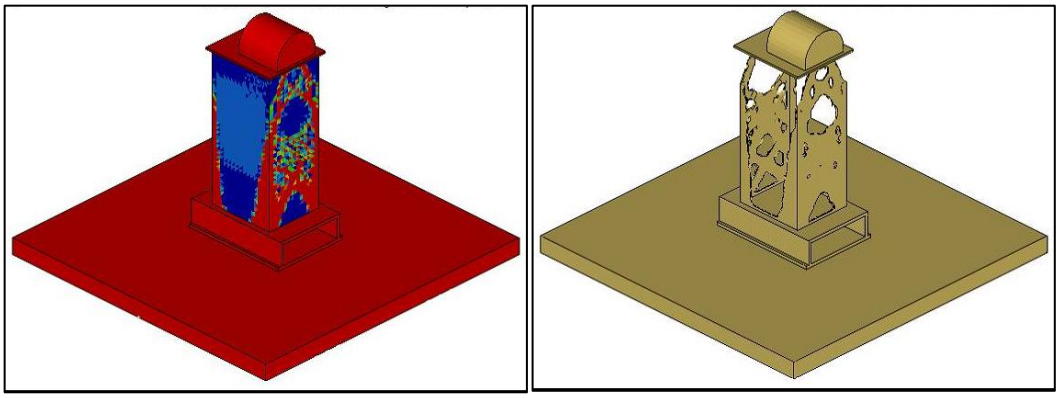

Figure 4.27: Contour and Isosurface of Hollow Region Design Change

From Figure 4.28, it can be seen that the left and right sides of the model shows a more elaborate change than the front and rear sides as in the previous approaches. This is mainly because of the shape of the deformation for the first mode that is being maximized which is bending from front-to-back. It also shows that the new design is much more intricate because of the lack of a basic scheme that the optimized design can be based on such as the inclusion of the legs.

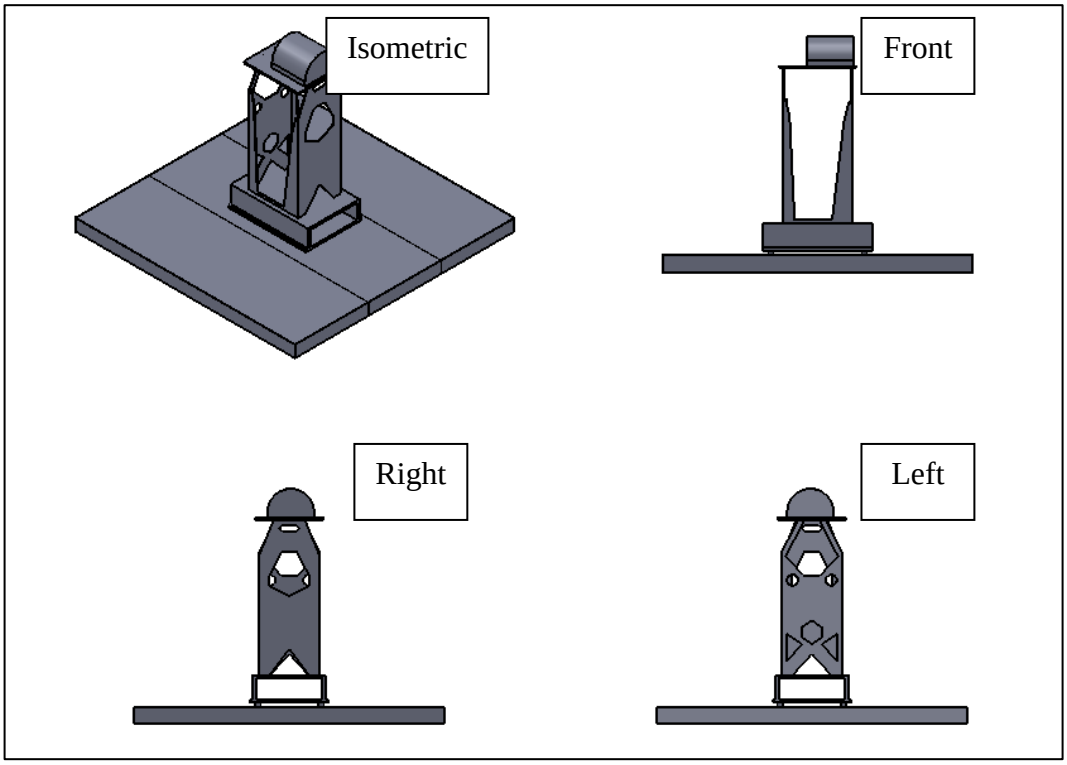

Figure 4.28: New Design of Hollow Region Design Change

For both left and right side, the “legs” were shown to curve towards the middle starting about the third of the length starting from the bottom. As for the front and rear sides, a simpler change can be seen where the width of the “legs” starts significantly large at the bottom and will decrease as it rises until it reaches the height where the right and left sides starts to curve. It can also be seen that the legs directly under the motor is larger than the other.

For the size optimization portion, unlike in the approach using the existing structure where the legs is kept unchanged with the thickness of 3 mm, in this approach the whole pedestal will go through size optimization. It was done by dividing the variable into the 4 sides so that the thickness for each side stays constant for easy manufacturability purpose. Front, rear, left and right side was found to be optimized with the thickness of 5.44 mm, 3.26 mm, 5.22 mm and 6.64 mm, respectively.

Analyzing the dynamic characteristics of the new model by doing a modal analysis shows that the natural frequency did improve from the original model. Figure 4.28 shows the newly remodeled rig with Figures 4.29 and 4.30 showing the result of the analysis with the natural frequency and mode shape of the structure.

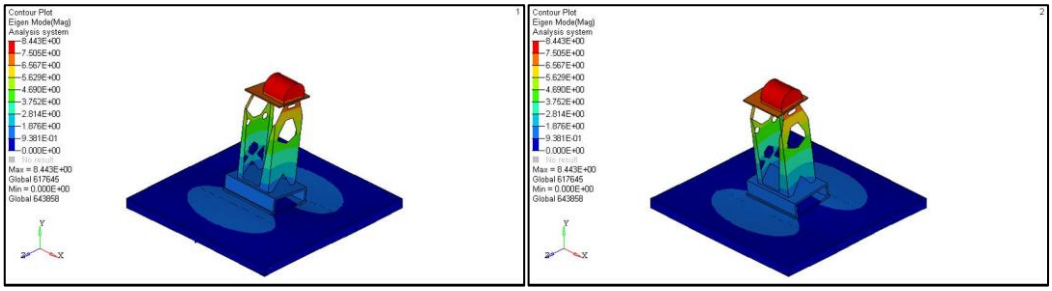

Figure 4.29: Mode 1 at 16.8 Hz

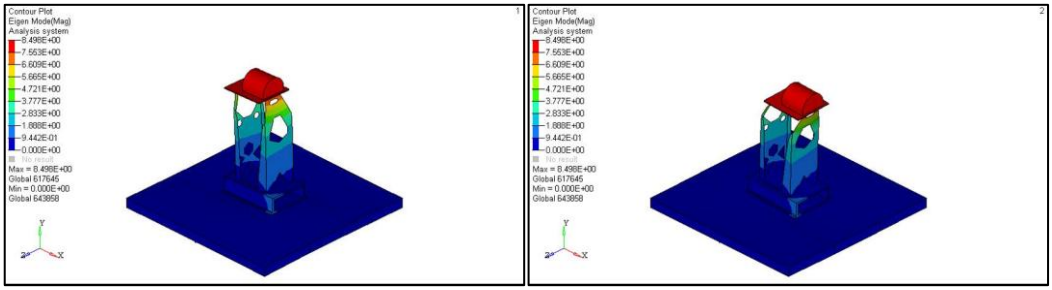

Figure 4.30: Mode 2 at 16.9 Hz

The first mode is shown to have a frequency of 16.8 Hz and the second mode with a frequency of 16.9 Hz. Both do show a fair increase from the original even if it is not ideal.

Then, the result of the optimization with the objective of maximizing the frequency of the first mode was repeated using the whole solid region. Figure 4.31 shows the contour of the optimization result and the isosurface of the result at a level of 0.3 element density. As explained previously, the optismooth model was extracted to obtain the same design as the isosurface model.

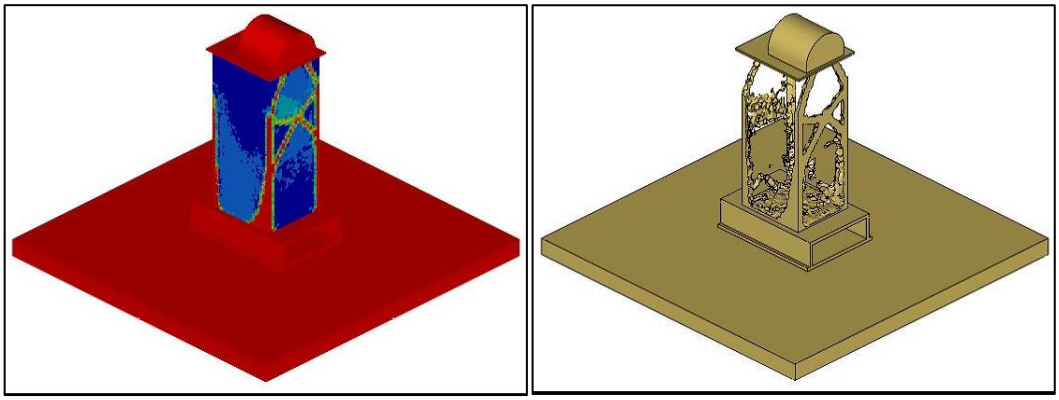

Figure 4.31: Contour and Isosurface Whole Solid Region Design Change

The left and right sides shows a more intricate change than the front and rear sides as generally seen when maximizing the first mode. The legs at both the left and right sides bend at two thirds of the length from the bottom up. A cross beam was also added on the right side while a plate was added on the left. The front and rear sides were only reinforced with triangular beams at the bottom. The newly-created model will undergo modal analysis to find the first and second mode.

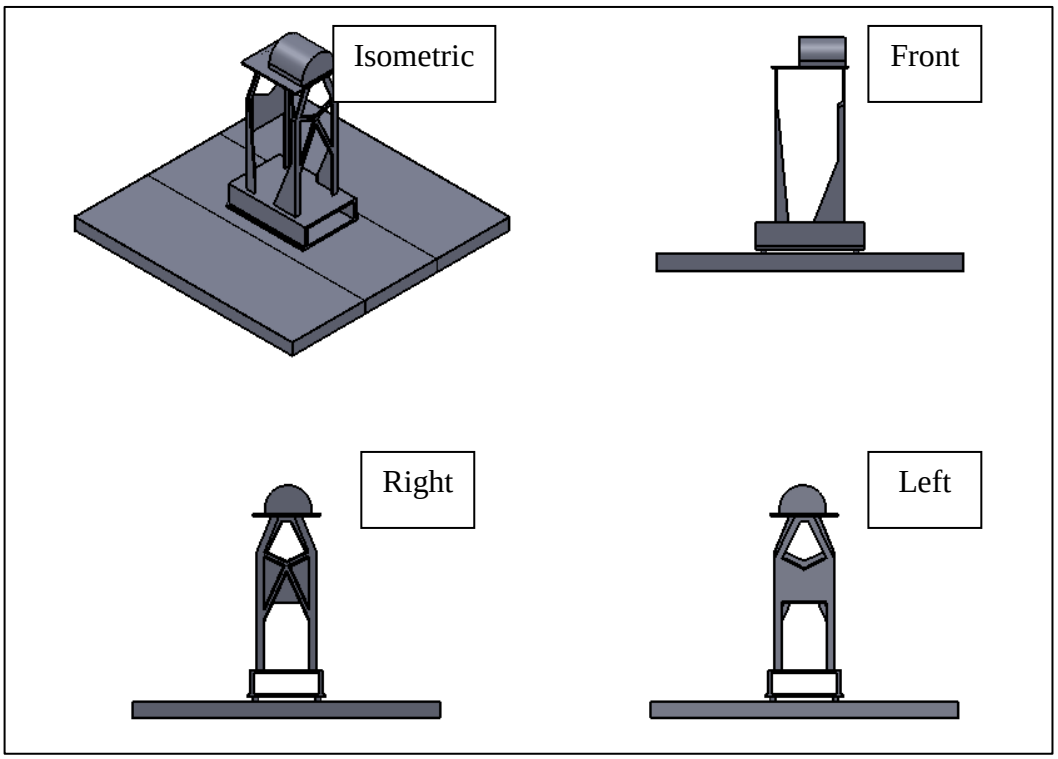

Figure 4.32: New Design of Whole Solid Region Design Change

Following the method used in the hollow region approach, size optimization was done on each side. The thickness was found to be 8.49 mm for the front side, 8.53 mm for the rear side, 8.54 mm for the left side and 8.44 mm for the right side.

The mode shape of the first and second natural frequency is shown in the Figures 4.33 and 4.34. The first mode frequency increases to 16.72 Hz and the second frequency increases to 16.73 Hz.

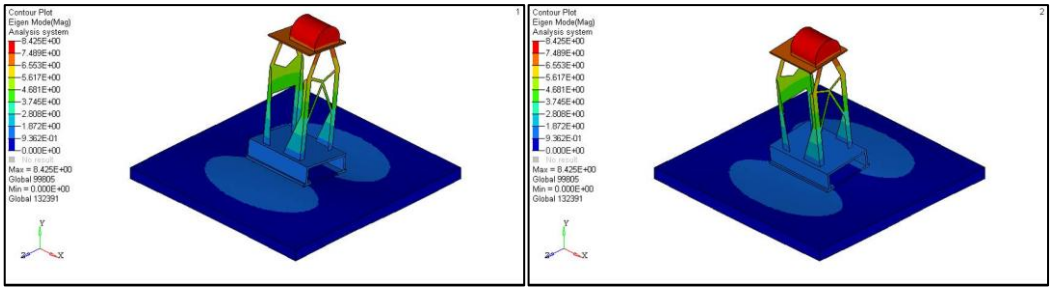

Figure 4.33: Mode 1 at 16.72 Hz

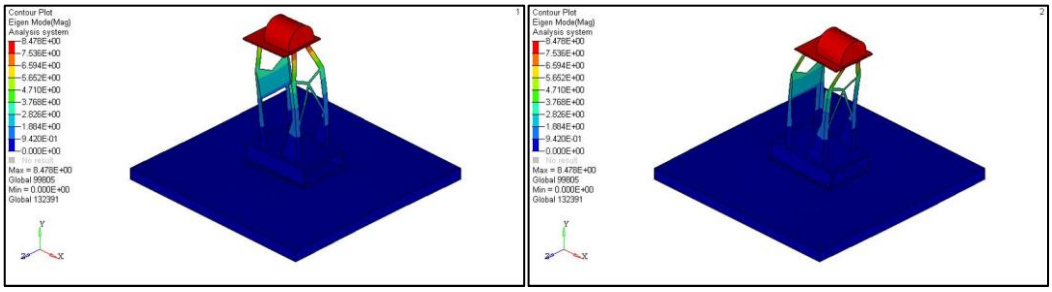

Figure 4.34: Mode 2 at 16.73 Hz

4.1.5 Optimization Result Comparison and Analysis

Finally, all the results can be assembled and weighed against each other for further analysis. The analysis involves the two first modes where the shape of the deformation is bending in the two different directions. The comparison also takes into account the added volume to show the practicality of the optimization process for other factors such as cost of material etc. In addition, another factor that is difficult to objectively evaluate was the complexity of

the design mainly for manufacturability reason which should be taken into consideration when comparing the methods.

Table 4.4: Result Comparison

Optimization Approach	Design Space	1st Mode Frequency (Hz)	Volume (m^3)	% Volume change
Existing Structure Reinforcement	Hollow	18.19	0.00967	1.896733
	Whole-solid	17.66	0.00951	0.210748
Initial Design Stage	Hollow	16.83	0.0095	0.105374
	Whole-solid	16.72	0.01025	8.00843

From the result comparison in Table 4.4, it is shown that all the result for the first mode natural frequency was increased from the original but still less than the target of 20 Hz. In addition, the volume added from the optimization is a cause for concern for the optimized design. Therefore, the best design from the optimization would need to have a frequency close to 20 Hz for the first mode while maintaining the volume added to a minimum.

For the process of reinforcing the existing structure, the results shows that the new frequency increased to about 18 Hz while increasing the volume by less than 2% for hollow design space and only about 0.2% for whole solid. Although the difference between the added volumes is quite large between the two design spaces, the changes are still very low compared to the original structure.

As for the initial design stage optimization, the result is fairly lower than the result from the existing structure optimization. This is probably due to the different initial design region used for the optimization. The design space affects the optimization process as the smaller the optimization region is, the better the result would be. The natural frequency obtained from the design stage optimization was only about 17 Hz but the volume added from the whole solid region optimization is exceedingly large.

4.2 Body-in-White (BIW)

As established from Chapter 4.1, SDM using structural optimization for a structure still in conceptual stage is fairly practical and convenient in finding an early design. Hence, for other more complicated structure, the method will be much more useful in finding a design at an early stage to try and weed out as many drawbacks as possible before any manufacturing process takes place. For structures such as the BIW, with as many as 155 components that will act differently under certain loads, structural optimization may improve the overall performance of the structure such as increasing the dynamic characteristics shown in this study.

The result from the BIW section of the research provides the frequencies for the first bending and torsion modes of the structure. Bending is defined when the whole body bends laterally as the front and back moves in the opposite direction of the middle. Torsion is defined when the whole body rotates with the front and the back rotating in the opposite direction. The two types of structural optimization used, which were the topology optimization and size optimization, will show the different pros and cons of each type. By understanding the positive and negative effect of the optimizations, the most suitable process can be considered as the final outcome for the conception of the design.

4.2.1 Static Test

Before acquiring the results for the dynamic characteristics of the BIW, the static test result would be taken first to relate the values obtained from the model with the result provided by the manufacturer. The static torsion and bending test results are shown in the following figures.

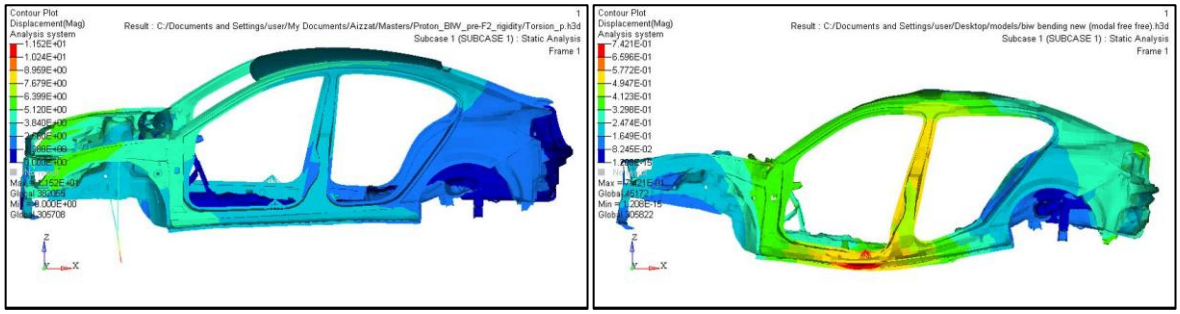

Figure 4.35: Static Torsion and Bending Test

As mentioned in chapter 3.21, the test was done by applying specific loads and calculating the corresponding deflection resulting from the analysis. The resultant value for static bending and torsion were 10395 N/mm and 5483.53 Nm/deg, respectively taken by calculating the ratio between the applied loads and the deflections at specific locations (Figure 4.35). These values were subsequently evaluated by comparing with the values given by the manufacturers which were 10663 N/mm for torsion rigidity and 5421.76 Nm/deg for bending rigidity.

The difference between the values, which were less than 3%, was mainly because of the different solvers utilized in this research and by the manufacturer (Entwistle, 2001). The model was updated, smoothed and cleaned from the original provided by the manufacturer to ensure the compatibility in terms of the solver. Therefore, the results from the model used for this research is slightly different from the manufacturer's though still acceptable.

4.2.2 Modal Analysis

After the validation was done, the results from the modal analysis were obtained from FEA. Only two modes were taken from the analyses which are the first bending and torsion modes. The bending mode frequency needs to be above 40 Hz and the torsion mode frequency needs to be above 60 Hz. These values were given by the manufacturer as a

benchmark considering the required structural rigidity under dynamic loading such as in crashworthiness rating.

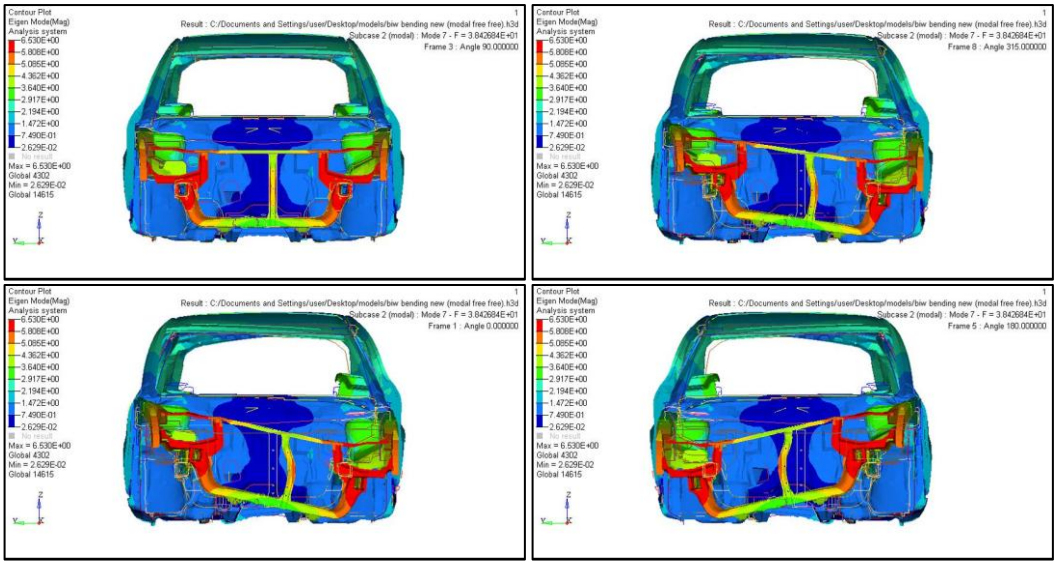

Figure 4.36: Torsion Mode at 38.4 Hz

Figure 4.36 shows the torsion mode of the structure expressed through deflections of the elements. The deflection however is dimensionless because no real load was applied but the basic mode shape was able to be determined from the result. The natural frequency for this mode was found to be 38.4 Hz which is still slightly lower than the target value which is 40 Hz.

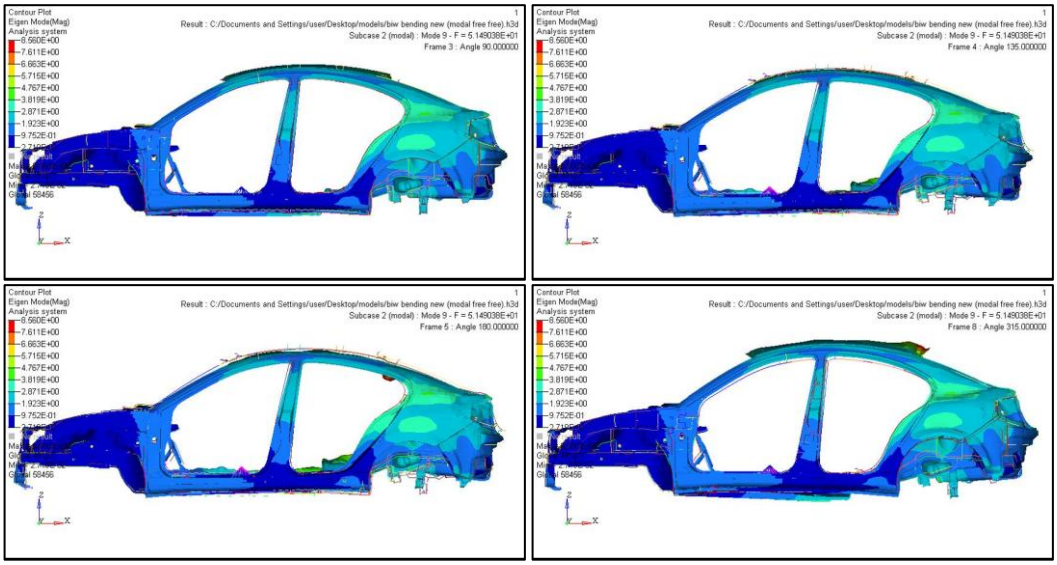

Figure 4.37: Bending Mode at 51.5 Hz

Next, the result for bending mode is shown in Figure 4.37 by distinguishing the deflection shape of the structure. The deflection is very subtle but can be observed at the frequency of 51.5 Hz. The natural frequency was found to be significantly less than the target value of 60 Hz.

So, structural optimization was applied to the model to increase the frequency for both modes by finding the locations that need reinforcements using topology optimization first and followed by size optimization. The optimization was also used to verify the necessity of any of the components in terms of the natural frequency.

4.2.3 SDM Using Topology Optimization

The design variable which is the thickness of the shell elements with the value of 0 represents the original thickness and the value of 1 would represent 4 mm of thickness in the first analysis. The locations of the reinforcements were pinpointed by interpreting the contour result of the optimization analysis. Using the contour of the result as a reference, spots in red would show where changes to the components would result in significant improvement to the natural frequency.

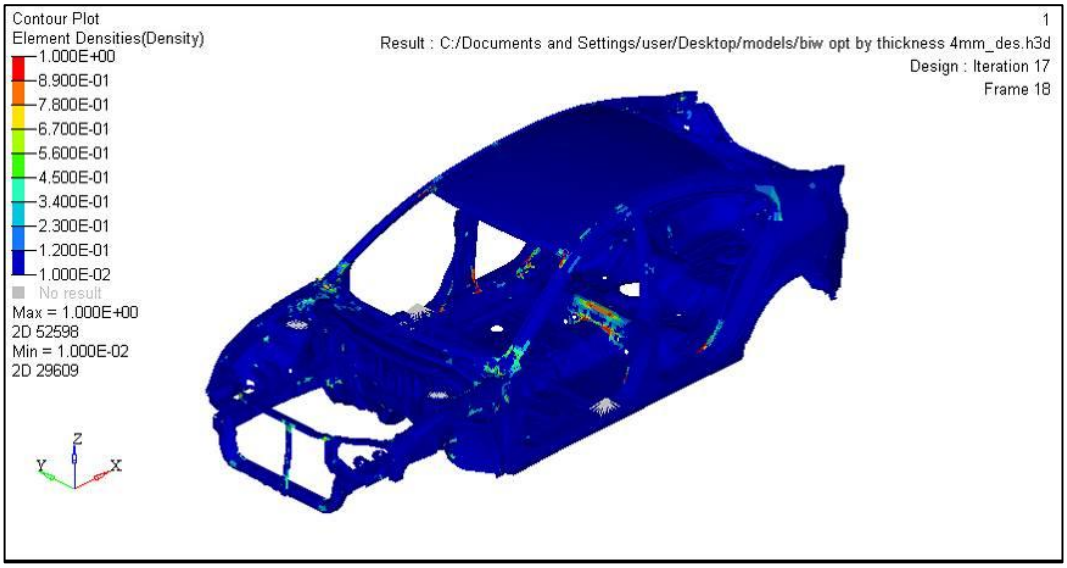

Figure 4.38: Optimization Result by Element Density

The positions of the modifications are shown in Figure 4.38 where the spots were illustrated by colors other than blue. A level set factor of 0.5 was used for the element density in the beginning. This means that only the elements that have a larger density than 0.5 would be chosen as elements that would be amended. The change needed is very small as only 4.87% of the total elements would need to be changed to satisfy the criteria.

With the changes done using the suggestion from the optimization, both the frequency for torsion and bending modes were increased to the proposed value. Furthermore, note that there is also an increase in the volume and mass of the structure, though it is of minimum value (Table 4.5). The extra load is the result of trying to increase the value of the frequency without presenting any significant changes in the design.

Table 4.5: Result Comparison of Original and Optimized Model

Parameter	Model		Value Difference	% Difference
	Original	Optimized		
Torsion (Hz)	38.4	42.6	4.2	10.9
Bending(Hz)	51.5	60.0	8.5	16.5
Mass (kg)	275.0	294.0	19.0	6.9

The static test was conducted again using the optimized structure to predict the behavior of the body for the other factors. The new results from the test were compared to the original to show that the changes to the structure are small in terms of static rigidity (Table 4.6). The decreased value of the deflection illustrates that the structure should now be stiffer and would also mean that the reliability of the structure is not compromised.

Table 4.6: Result Comparison of Static Analysis

Parameter	Stiffness		Value Difference	% Difference
	Original	Optimized		
Torsion	0.499	0.413	0.086	-17.2
Bending	0.742	0.675	0.067	-9.02

In retrospect, the added mass is not a welcoming solution to improve a body-in-white structure. The extra weight will affect the overall performance of the car. Therefore, the topology optimization was done again using different design variable to find the best arrangements for the optimization process and for the structure.

One possible way prepared in this research was by changing the maximum thickness of the new design. The use of 4 mm as the maximum thickness may not be the most ideal approximation for the optimization. The use of a lesser thickness may induce a change in the position of the reinforcement and hopefully would also reduce the added mass while still achieving the aim. The new value would still need to be above the largest original thickness of the components which is 3 mm, so the value of 3.2 mm and 3.5 mm were proposed as the new variable.

By changing the value of the design variable thickness, the result of the optimization would also change as can be seen in Figure 4.39 and Table 4.7, though the locations of improvements stay mainly the same. For the new thickness of 3.2 mm, 6.25% of the

elements need to be changed to satisfy the criteria, while the 3.5 mm variable thickness model resulted in 5.55% of altered elements.

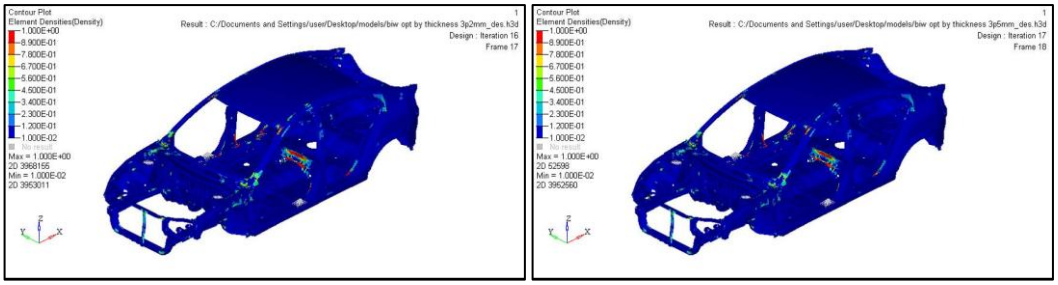

Figure 4.39: Optimization Result Using 3.2 mm (left) and 3.5 mm (right) Maximum Thickness Variable

Table 4.7: Result Comparison of Using 3.2 mm and 3.5mm Thickness Variable

Max. Thickness	3.2 mm		3.5 mm	
Parameters	New Frequency	% Difference from Original	New Frequency	% Difference from Original
Torsion (Hz)	42.5	10.7	42.6	10.9
Bending (Hz)	59.8	16.1	59.6	15.7
Mass (kg)	291.1	5.85	291.8	6.11

The same set factor of the element density which is 0.5 was used as in the previous optimization. This means that with a smaller value for the maximum thickness, more elements would need to be changed to achieve the optimization objective. However, the comparison does show a much better result of the optimization because of the lower added mass of the whole structure. This explains that the thickness of the reinforcement does not need to be large to achieve a good result. A more thorough investigation is needed to find the optimal thickness for the optimization to lower the added mass and improve the design.

4.2.4 Size Optimization

Initially, the process was done using all the components of the structure as the designable property and also uses the same criteria as in topology optimization. Since the structure comprises of 155 different components, the optimization process used sizable resource of

the processor to complete because each parts would need to be adjusted with different design-variable-to-property relationship.

Using this approach, the natural frequency of both modes increased successfully to 40 Hz and 60 Hz as well as a mass increase of 335.1 kg. Although the result shows a very reasonable consequence of the frequencies and the total mass, the substantial changes which involve adjusting the thicknesses of almost all components would mean that a lot of modifications and alterations would need to be applied to the original structure. This in turn would also shift the capability of the structure in other aspect such as crashworthiness and manufacturability.

Consequently, a method to avert this was to make use of the result from the topology optimization. The optimization criteria used were similar to the criteria set for the topology optimization previously except for the design variable used. Rather than using all the elements as the design variable, only the elements in the components that need reinforcements in the topology optimization were used. As a result, the number of elements or components that will be modified was reduced significantly for the subsequent size optimization processes.

From Table 4.8, the objective $f(x)$ was set as the minimization of the mass of the whole structure with a limit that the frequency of the first torsion and bending modes to be greater than 40 and 60 Hz, respectively. The thickness of the particular components will be the design variable with the original thickness as the initial value and 3.2 mm or 4 mm for the maximum thickness. The size was only set as 3.2 mm and 4 mm to check only the two end of the domain for component thickness. The two different thicknesses used for the

maximum thickness will assist in distinguishing the better combination of the two optimizations.

Table 4.8: Criteria of Size Optimization depending on Topology Optimization

Variable	Thickness of shell elements selected from topology optimization , T (Original Thickness < T <3.2 mm or 4 mm)
Constraints	First torsion mode > 40 Hz First bending mode > 60 Hz
Objective	Minimize mass

The result of the optimization using a level set factor of 0.5 from the topology optimization is shown in Table 4.9 where some components that have intermediate elements were also chosen as the design variable. Therefore, the components chosen are moderately more than if the elements selected are closer to 1. There are 54 and 46 components that will be adjusted for the 3.2 mm and 4 mm thickness optimization, respectively for 0.5 element density.

Table 4.9: Size Optimization Result

Max. Thickness	3.2 mm		4 mm	
Element Density	New Mass (kg)	% Difference from Original	New Mass (kg)	% Difference from Original
Factor of 0.5	335.6	22.04	337.4	22.7
Factor of 0.9	424.6	54.4	415.4	51.05

After changing the thickness of the components, the frequencies of both modes were increased to 40 and 60 Hz as intended. The mass also increased to 335.6 kg for the 3.2 mm and 337.4 kg for the 4 mm. These indicate that with the size optimization using 0.5 element density, a considerable number of components thicknesses would be changed and therefore would also alter the behavior of the whole structure quite significantly. For that reason, a

further optimization using the components where the elements has a density closer to 1 was done to show that the objective can be achieved by using less components.

Size optimization was done again using a level set factor of 0.9 as the element density. The number of components is significantly less than the previous approach with only 28 components for the 3.2 mm and 22 components for the 4 mm. From Table 4.9, it is shown that the mass of the new structure has increased significantly more than the structure optimized from using 0.5 for element density. While the objective of increasing the frequencies was achieved, the large increase in mass is too unfavorable in the construction of a vehicle body.

Using the result from all of the different approaches for size optimization, it is shown that the added mass is notably higher than from the topology optimization. This is mainly because rather than changing just the elements that will improve the rigidity, it changes the whole component that the element belongs to. By doing this, it may have increase the added mass but will also increase its manufacturing feasibility. By having a constant thickness throughout the parts, the same manufacturing process can be used to create the component without needing any new or additional process to add reinforcement to the initial component.

4.2.5 Static Test of Optimized Design

Static torsion and bending tests were performed again for the recent models to check the validity and quality of the optimization methods and results. The models will undergo torsion and bending static stiffness test as were done previously.

Table 4.10 shows that the new models after optimization when trying to improve the dynamic property of the structure, does not also denote that the static stiffness would also

increase. Two out of the three approach resulted in a decrease of static rigidity pertaining to either bending or torsion stiffness. The only approach that shows an increase in both is the model undergoing topology optimization with maximum thickness of 4 mm.

Table 4.10: Static Test of Models from Optimization Result

Optimization Method	Static Bending Test		Static Torsion Test	
	Result (N/mm)	% Change	Result (Nm/deg)	% Change
Topology – 3.2 mm max Thickness	11989.0	15.33	4821.67	-12.07
Topology – 4 mm max Thickness	10860.1	4.47	5916.68	7.9
Size – All components	10073.5	-3.09	6230.19	13.6

The result demonstrated from this test that the optimization may improve the dynamic characteristic while reducing the static stiffness. It is therefore recommended to check if the improvement may affect other related properties and factors as much as possible.

Chapter 5: Discussions

5.1 Differences between Design Spaces and Approaches

Based on the results obtained from all methods of optimization, the value of natural frequency, added mass and final design of the models shows significant differences in the improvement (Table 4.4). Therefore, an assessment was conducted to identify the cause of the variation in terms of design spaces and optimization approach.

The primary factor in the final design from the optimization depends on the initial design domain used. Since the model and the settings for designable and non-designable elements were different, the final result from the process yielded varying results. For example, when using hollow region where the thickness is small, the size of the elements would also be small and provided better outcome than when using whole solid region where the elements used were larger.

When assessing from the optimization approach perspective, introducing reinforcement to an already existing model will yield higher natural frequencies than completely redesign the structure. This could be due to the same reason where setting the designable space for reinforcements incorporate the use of smaller elements. The focus on fitting the reinforcing material onto the original model presented a more thorough meshing than just selecting the whole pedestal structure as in the approach of design change. Nonetheless, even with different approaches, there exist commonalities between the topology of the model designs.

5.2 Common Topology Occurrence

By examining all the results from the topology optimization of the structures, the new design suggests that there exist common topology designs between the results. A

comparison was conducted between the values obtained from each approach to objectively evaluate the designs. Then, by understanding the advantages and disadvantages of each design, the different final design options can be reduced. From the results, most corners are generally sharp, even though from previous researches, rounded corners and fillets should be a better in terms of structural integrity (ref). The reason most corners are sharp is because the elements used are tetrahedrons and quads that have sharp corners.

For the experimental rig structure, Figures 4.20, 4.24, 4.28 and 4.32 show that the new patterns for each side to have similar characteristics after the optimization process. These patterns can be used to basically determine the final design of the structure. Every side will have different designs depending on the approach from the topology optimizations. These patterns can also be used to make sure that the manufacturability of each design is acceptable and practical.

5.2.1 Right Side

The right side of the new designs for the experimental rig structure was analyzed. The new patterns were studied and compared to each other to find a general outline for the design.

Figure 5.1 shows the definitive result for the right side of the existing structure after the topology optimization. The designs illustrate the outline of the reinforcement between the legs. Since the original legs were left untouched (non-design) from the optimization, the main design for the fortification for the structure were shown to be more or less a cross plate connecting the two legs. By using plates in an X-shape, the amount of material used can be kept to a minimum while still improving the strength of the structure.

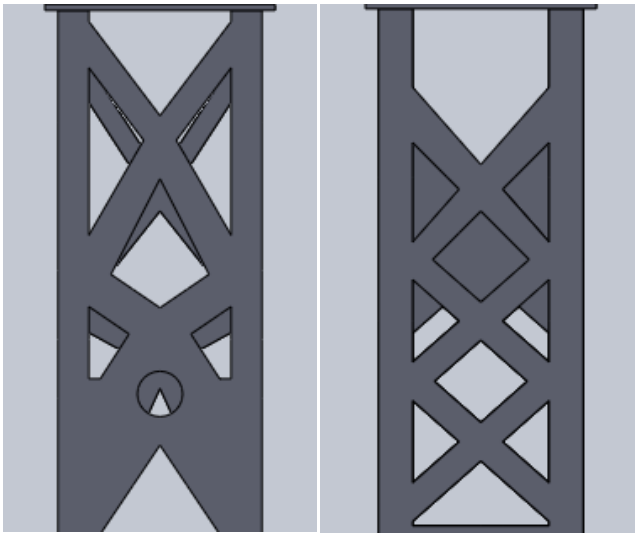

Figure 5.1: New Designs for Right Side of Model Reinforcement

Though there are areas where it is not exactly symmetrical X-shape, this may be due to the complexity of the mesh and optimization process and can be easily substituted with a more conventional shape or pattern such as an X-shape while still maintaining its effectiveness. The average width of each straight column of the pattern appears to be almost the same width as the original leg which was 25.4 mm. However, the position of the design differs for each method of optimization even though the area covered was similar where the top is mostly empty while the bottom is mostly concealed.

The results taken for changing the design during the initial design stage of the structure show that there were similar yet considerable different outcomes between using hollow model and whole solid model. The area of the effect from the optimization as shown in Figure 5.2, were almost the same with the edges enveloping the original width for three fourth of the length from the bottom. The top one fourth started bending towards the middle for both results.

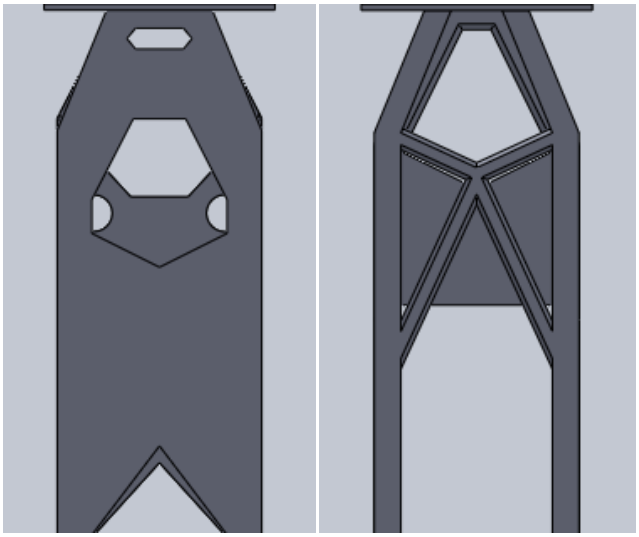

Figure 5.2: New Design for Right Side of Model Change

The key distinction between the two was the area covered with the coverage more sizeable for the hollow region than the whole solid region. This may have been due to the thickness used for the regions where thinner walls would mean more matter is needed to overcome the stress and load. This also explains the reason why the thickness of the new design varies significantly with 5.22 mm for the hollow space and 8.54 mm for whole solid space after size optimization was completed. Therefore, the dissimilarity demonstrates that either combination should work either lesser area with thicker beams or wider area with thinner plate.

5.2.2 Left Side

Next, the left sides of each result were analyzed and a comparison was done to find a complementary outcome for the new design of the structure.

The patterns found of the left side of the pedestal from the topology optimization of the existing structure were comparable to the right side of the same model. Then again, there were also noticeable differences for instance the reinforcing designs were positioned slightly lower than the right side. The X-shaped plate in this model is a little less refine for

the hollow model (Figure 5.3) and less apparent for the whole solid model (Figure 5.3). The thickness found from the size optimization which were 1.41 mm and 1.63 mm show that the amount of material to manufacture the reinforcing plates were not that different.

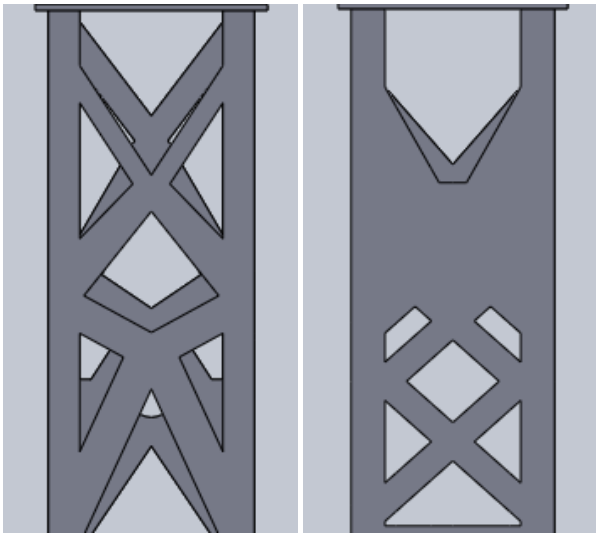

Figure 5.3: New Design for Left Side of Model Reinforcement

For the left side of the structure after optimization was executed at the design stage, the patterns show a similar configuration between the hollow (Figure 5.4) and whole solid region (Figure 5.4). The patterns were also comparable to the right side of the models but the bend at the top were slightly narrower.

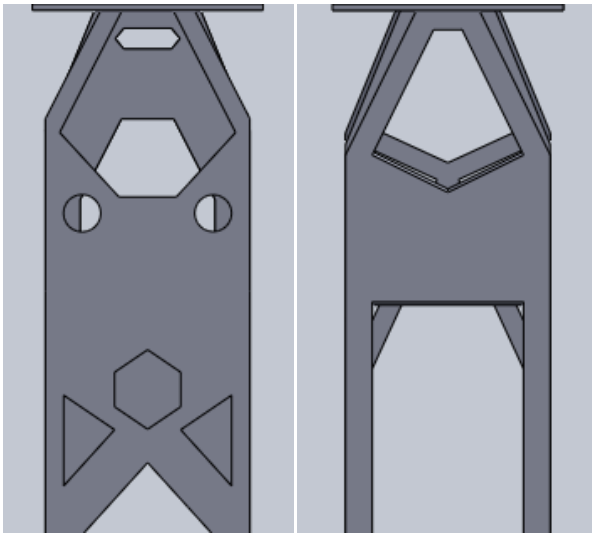

Figure 5.4: New Design for Left Side of Model Change

The areas covered were mostly different for each approach mainly due to the method used in the optimization process but generally the results were similar. The thicknesses of the design from size optimization were affected by the areas where larger areas produced smaller thickness which was 5.22 mm and smaller areas produced larger thickness which was 8.54 mm.

5.2.3 Front and Rear Sides

Following the designs for the left and right sides, the results concluded for the front and rear sides of the structure show simpler patterns overall. The front and rear sides were basically just mirrored design of the other for each approach. The reason was basically because of the asymmetrical outline of the structure in regards to the deflection shape of the modes. So, only the front sides were shown as the subject of the study of the patterns obtained from the topology optimization processes.

Figure 5.5 shows the front sides of the new model after optimization to reinforce the existing structure. The added support was very minor compared to the left and right sides. The main additions to the original structure were triangular supports that were attached to the more weighted side of the structure which was the right side from the front. The hollow region optimization also show some additional support on the left legs mainly due to the smaller thickness attained from the size optimization while only slight reinforcement was needed for the whole solid region optimization but also reveals a larger thickness.

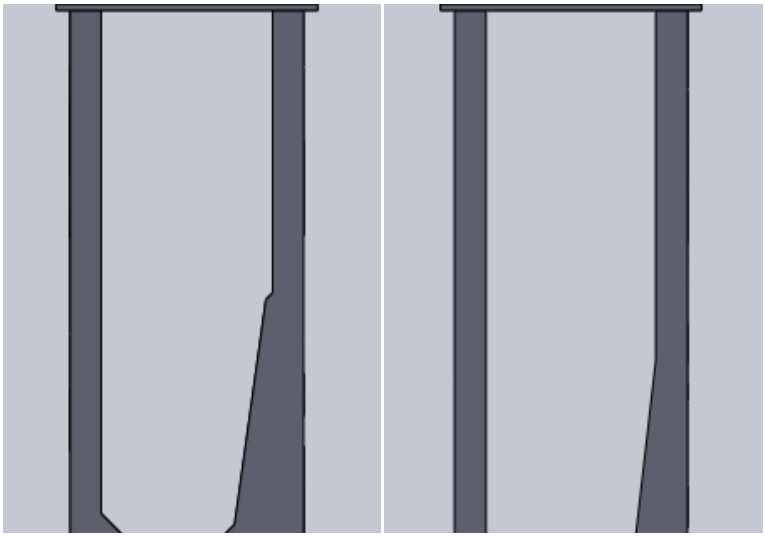

Figure 5.5: New Design for Front and Rear Side of Model Reinforcement

The changes in the front and rear side designs from the topology optimization at the design stage are shown in Figure 5.6. Without the original legs, the pattern of topology after the optimization follows a consistent outcome as in previous approach where the right part is wider than the left.

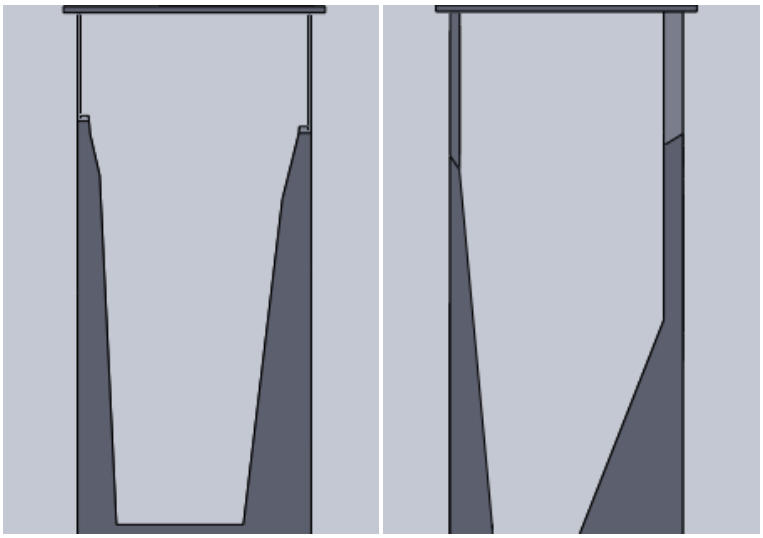

Figure 5.6: New Design for Front and Rear Side of Model Change

This is possibly because more material was needed to support the heavier side of the top where the motor is located. The outlines of the design were fairly triangular and end at

different position from the top. The whole solid model also shows a lower point of arrangement than the hollow model.

5.2.4 Common BIW Components

By examining the topology optimization results from Figures 4.38 and 4.39, it is shown that there exist components that need considerable change or modification. Some even show that a lot of the elements need to be changed in a single component. It is shown that by changing only specific areas of the component for reinforcement, the varied thickness on a single component will result in a stress concentration where the thickness changes Maceri, 2010). The concentration may then induce other problems such as fatigue crack initiation and growth (Huynh, Molent, & Barter, 2008). One possible way to reduce it is to change the thickness gradually as to not induce a significant stress concentration on the components. A smaller value of the maximum thickness should also decrease the concentration. Another method of preventing the concentrations that may be possible is to use additional reinforcing material rather than using components with varying thickness. These additional materials may be welded or bolted to the existing structure though this may allow other problems to occur such as weak welds (Gaul, Brauser, Weber, & Rethmeier, 2011) where cracks may initialize. So, a more thorough investigation is needed before any application is done.

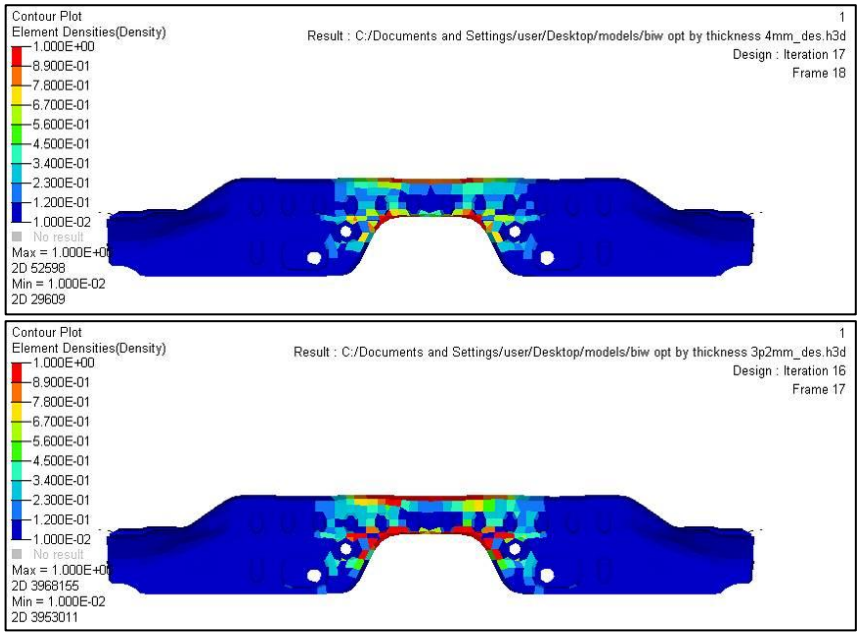

Figure 5.7: Highlight of Reinforcement Areas on Rear Seat Center Member and Rear Floor Extension 4 mm (top) and 3.2 mm (bottom)

For that reason, these components may establish a better solution if it only experience size optimization rather than topology. In this case, problem such as stress concentration from the varying thickness can be avoided. There are certain parts where the area of strengthening covers noticeably more such as on the rear seat center member and the rear floor extension. The area covers almost one third of the whole components as shown in Figure 5.7. Hence for these sorts of components, it is possibly a much better idea to use size optimization to improve the component properly. Therefore, to achieve the objective while still maintaining the practicability of a body-in-white of a car, the best method would be to incorporate the result from both topology and size optimization according to the effectiveness of the modification in regards to the manufacturability of the change.

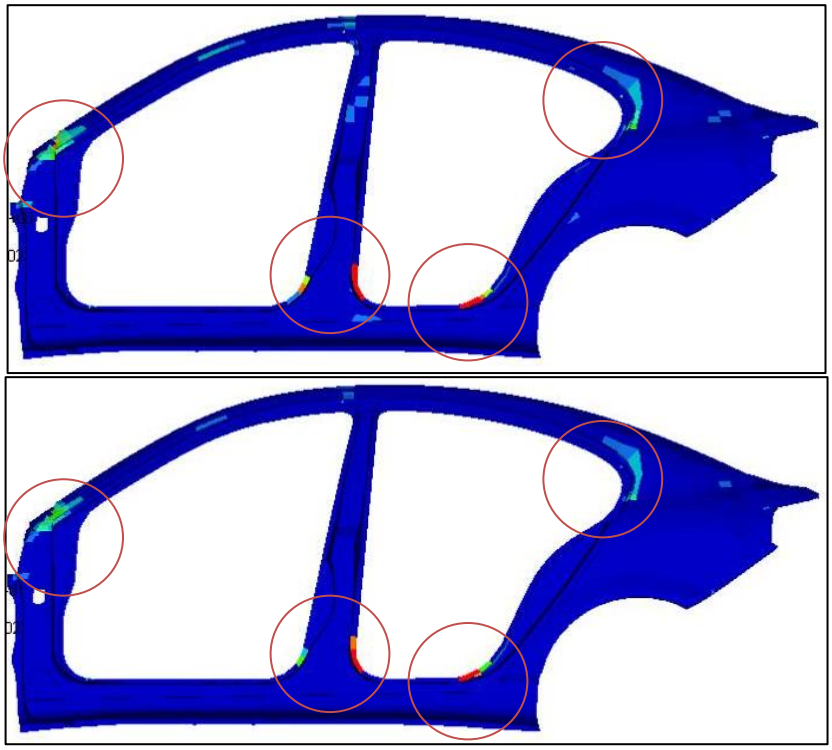

Figure 5.8: Highlight of Reinforcement Areas on Outer Quarter Panel for 4 mm (top) and 3.2 mm (bottom)

However, there were also components from the result of the topology optimization that shows that the placement of the reinforcement is relatively small compared to the size of the component such as the outer quarter panel (Figure 5.8). Thus by implementing size optimization and increasing the thickness of the entire component may result in an unnecessary additional mass. So, it is wise to consider the implication of either using size optimization on certain components or just reinforcing the components at specific area according to the topology optimization such as shown in Chapter 3.4.

5.3 Additional Optimization Approach

Some alternative optimization approach was introduced based on the result from the conventional optimization technique. Two additional approaches that will be used are changing the order of approach and combination of different optimization processes.

5.3.1 Order of Approach

The optimization process used in this study as shown in the previous chapters were the typical approach where topology optimization was done first to remove any unnecessary material and followed by size optimization of the preserved parts. However, analysis and optimization involving dynamic applications are not as clear-cut, so a different order of approach was suggested and may provide different and better result for the design.

First was to only optimize the legs of the platform. All four will undergo topology, size and free-size optimization to find a new design. The domain was kept unchanged so the range for which the alteration can be made is very limited.

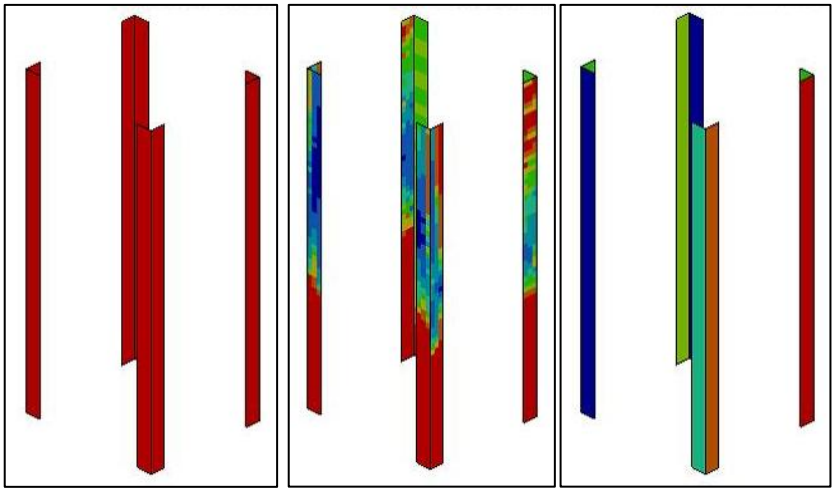

Figure 5.9: Optimization Result for Topology (left), Size (middle) and Free-size (right)

In Figure 5.9, the color of the contour represents the element density for the topology and the thickness for size and free-size optimization. It is shown that no design change occurred when running topology optimization using only the legs as the domain. Any modifications that can be successfully introduced through this method would be the change in thickness either with free-size which is very impractical or normal size optimization.

Table 5.1: Legs Optimization Results

	Topology	Size	Free-size
Modifications	No change in the design or thickness	• Front and rear = 10 mm and 5.78 mm • Left = 14.76 mm • Right = 10.97 mm	• Min = 0.18 mm • Max = 10 mm
Frequency (Hz)	13.2	16.08	16.34
Volume (m^3)	0.00949	0.01020	0.00982

Next, the design domain used is the hollow region as in the previous analysis but with a slight change in the order. Rather than starting with topology optimization, size optimization was used first to find the thickness of the walls. So, the thickness would not be 3 mm as in the thickness of the original legs. Two different thicknesses were found using different method. Firstly, the thicknesses found from the size optimization of the legs (Table 5.1) were used.

Secondly, the thicknesses of the optimized hollow region wall were used, where size optimization was done for the wall of the hollow region. It is found to be .541 mm for front and rear sides, 0.488 mm for left side and 0.619 mm for the right side. Then after obtaining the value for the thickness, topology optimization can be done onto the hollow domain.

Table 5.2: Result of Topology Optimization after Size Optimization

Optimization Approach	Natural Frequency (Hz)	Volume (m^3)
Size (legs) – Topology (Design Change)	16.83	0.01024
Size (walls) – Topology (Design Change)	16.21	0.00939
Size (walls) – Topology (Reinforcement)	16.04	0.00964

The results obtained were shown in Table 5.2 where the frequency has been raised to about 16 Hz which is still under the normal operating frequency. However, with the wall size

optimization done before undergoing topology, the added mass was significantly lower compared to the design obtained from the conventional optimization process.

5.3.2 Implementation of Free-sizing

Another additional aspect that can be added to improve the result but may come with other disadvantage is by implementing free-size optimization on most of the new design instead of normal size optimization. The main downside of free-size is the impracticality or the difficulty in manufacturing the parts based on the optimization results. Free-size optimization will change the thickness of each element on a component independently and will therefore produce a component with varying thickness throughout the structure which will be very difficult to manufacture.

Table 5.3: Result of Designs After Free-size Optimization

Optimization Approach	Natural Frequency (Hz)	Volume (m^3)
Hollow Region Topology (Design Change)	17.24	0.0102
Hollow region Topology (Reinforcement)	18.32	0.00975
Whole Solid Region Topology (Design Change)	16.96	0.01034
Whole Solid Region Topology (Reinforcement)	18.11	0.00951

All the result registered higher natural frequency than the original value after the optimization as shown in Table 5.3. The added mass from the modification was also within similar range of values as in the size optimization for each of the approaches. Therefore, objectively, this approach offer the best improvement in terms of maximizing first mode frequency while minimizing added mass, though with some manufacturability issue from the varying thickness. Alternatively, the result from the free-size optimization can also be used as a basis to identify the points where extra reinforcements are needed.

5.3.3 Combination of Size and Topology

From the results of the optimization using the different strategies proposed previously, a new method can be introduced in an attempt to further utilize the configuration of the optimization processes. While the main objective of the study was to maximize the first natural frequency, there are other factors that are important to users in terms of improving the structure and the processes involved. In this discussion, two main factors that were taken into account were the volume of the new design and the manufacturability of the parts.

The value of both natural frequency and volume was easy to identify throughout the process as shown in the results but for manufacturability, where it is more subjective, was much more complicated. Therefore, to simplify the focus of controlling the manufacturing of parts in the models, the method utilizes the optimization process to monitor the potential modification of the components. Since topology optimization would mean that the basic shape of a component would be altered because of voided areas, it was not the best approach as this would indicate that new parts or components would need to be fabricated.

Thus, by just using size optimization on a basic shape of a component was more fitting in terms of manufacturability as only the dimensional value would be changed. However, according to the results obtained and the observation of the strategies used prior, topology optimization shows a better maximization of the frequency and minimization of the volume. Ideally, there are other more advanced methods for which to gauge the manufacturability of certain components (Gupta, Regli, Das, & Nau, 1997). The method proposed is debatable as the amount of change cannot directly contrast the

manufacturability of a component. This was done solely because of the simplicity and objectivity of the method.

Therefore, to properly include all three main factors of the optimization, a combination of size and topology optimization is proposed. This hybrid method basically checks the result from an optimization and objectively verifies the next step for each component to compensate for any diminishing value or worth in any of the three main factors.

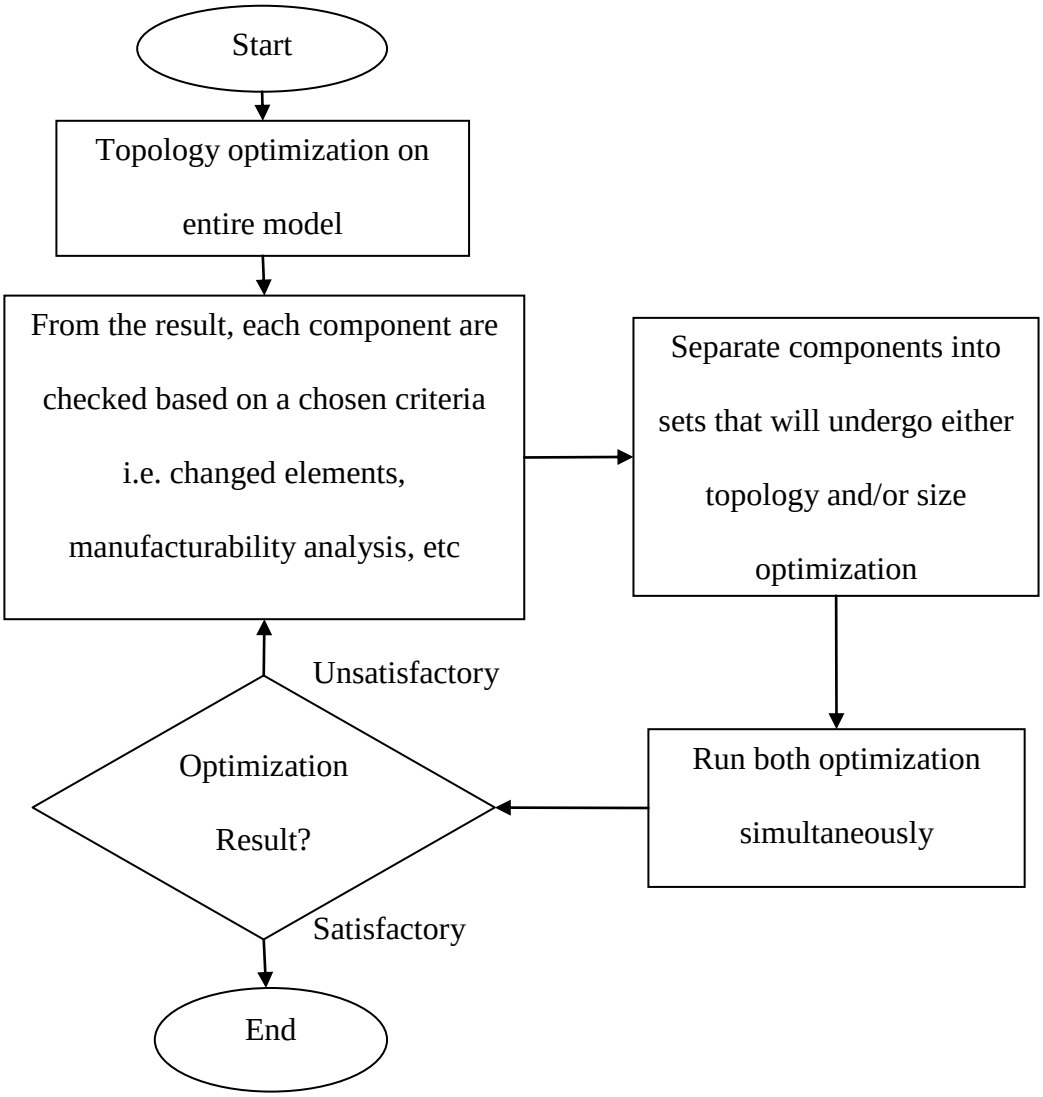

Figure 5.10: Combination of Optimization Strategy

The structure will first need to be set to accommodate the optimization processes, which were size and topology optimization, and also the methods used to fulfill the objective as shown in Figure 5.10. So, additional material may be added as further reinforcement of the original structure. Since the method will need to run both size and topology optimization, all the elements used for this method will be shell elements. The structure will then be separated into different components where each may be of structural importance or act only as additional reinforcement depending on the structure itself.

First, for the experimental rig, because the analysis that had been done previously was by using solid elements, so a new model was created using only shell elements. The whole structure will undergo topology optimization first basically to check the amount of changes of modification needed to improve the model. Each of the components can now be distinctively inspected by verifying the elements that will be omitted or left unchanged from the process. The result of each elements was extracted especially the element density.

The tabled result will show if the design of the components are required to be modified according to the topology results or show be left unchanged by inspecting the amount of alteration of each components. The ratio of the number of elements with element density of close to 1 (valid material), $E_{unchanged,}$ and the total number of elements, E_{total}, of every components is calculated. From this, the ratio will be compared to a threshold value, where the component may forego topology optimization and left as the original design.

$$Component\ modification\ ratio = \frac{E_{unchanged}}{E_{total}} \tag{5.1}$$

The next step of the method will depend on value of the ratio in terms of the threshold value. The outcome will be either the component will be left unchanged or will undergo only size optimization or undergoing both topology and size optimization. This is done to objectively set the optimization process to control the change in the design of the components to cater for manufacturing constraints.

The threshold value can be set from 0% to 100% of changed elements in a particular component with 0% means full size optimization and 100% means full topology optimization. The value would be set depending on the aim of the whole optimization mainly on the manufacturability of a design in its most simplistic way. The higher the number of elements needed to be altered would possibly mean that a lot of modification is needed to be implemented onto the component. Hence, a high threshold value would produce a design where most components would be modified according to the topology optimization result.

A trial run was done to understand the extent of the method and the results obtained. For simplicity sake, one value of the threshold was used which is 30%. This was done to nominally separate the components into the two categories; ratio value higher and lower than the threshold. While the best threshold value remains to be seen, it is wise to first experiment with only one specific value.

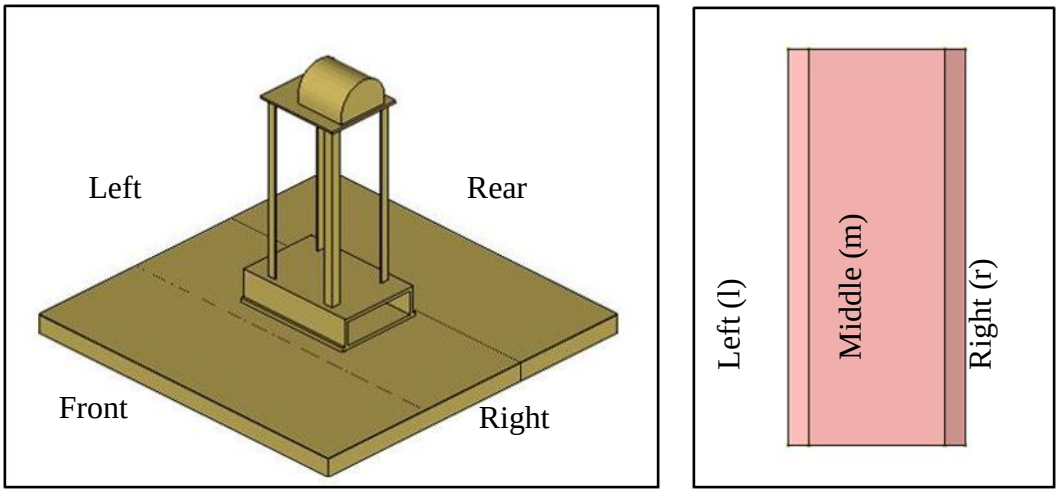

Figure 5.11: Labels Schematics of the Experimental Rig

The model will need to be first split into different components depending on the configuration of the initial parts and also the added supporting parts. Each component was labeled accordingly as shown in Figure 5.11. For this structure, every side was separated into three parts; left, right and middle. Both left and right are part of the angle beam legs while middle parts are the extended formation of additional material. So each component will be referred to by combining the name of the side and the initial of the part of each side (either l,r, or m) such as “rightl” for left part of the right side or “frontm” for middle part of front side.

The topology result will show the element density of each elements ranging from 0 to 1. The new design does not go through a remodeling in CAD yet, as it will undergo another set of optimization process before finalizing the design. From the result, the data were extracted and tabled for further analysis. The data needed were the element ID, component ID and element density.

Table 5.4: Results Obtained from First Topology Optimization

No	Element ID	Comp ID	Element Densities
1	700579	leftl	1.00E+00
2	700580	leftl	1.00E+00
3	700581	leftl	1.00E+00
4	700582	leftl	1.00E+00
5	700583	leftl	1.00E+00
……..			
8926	721048	rightm	9.96E-01
8927	721049	rightm	9.88E-01
8928	721050	rightm	1.00E+00

Then, the data from Table 5.4 will need to be organized for the next step of the method. The data were arranged according to the unique component ID and the numbers of elements were checked. Both total number of elements and number of elements with density close to 1 is determined. The ratio or percentage of the changed element was calculated for every component which will be the component modification ratio (equation 5.1).

Table 5.5: Component Modification Ratio Calculations

Comps	Total Elements	Elem density > 0.7	Modification Ratio	1 if >30, 0 if <30
leftl	288	138	47.92	1
rearr	288	134	46.53	1
frontl	288	134	46.53	1
leftr	288	138	47.92	1
rearl	288	188	65.28	1
rightr	288	157	54.51	1
rightl	288	157	54.51	1
frontr	288	188	65.28	1
frontm	1800	140	7.78	0
leftm	1512	160	10.58	0
rearm	1800	140	7.78	0
rightm	1512	366	24.21	0

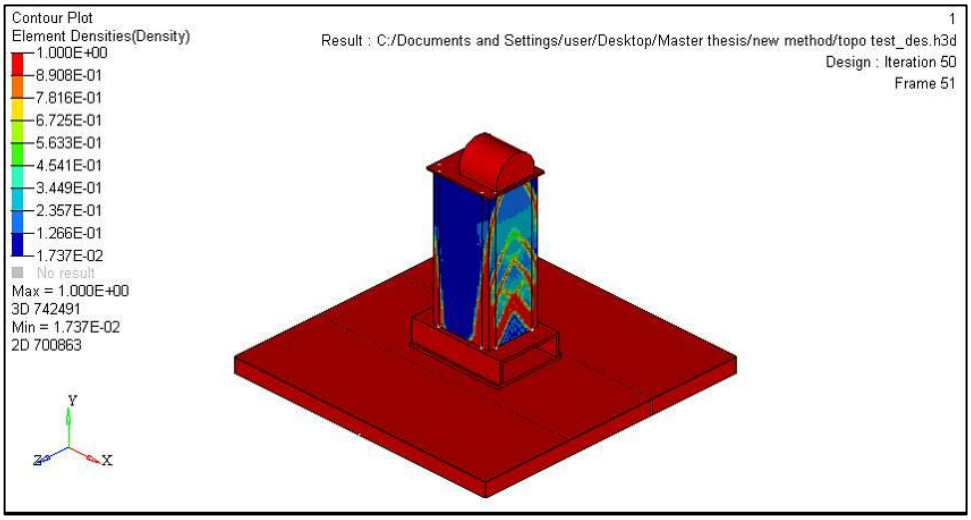

Figure 5.12: Contour Result for First Topology Optimization

With the calculated value, all the components will go through the subsequent step accordingly. For this trial run, the threshold value was set to 30%. Therefore, if the chosen element densities to be acknowledged as valid are elements with more than 0.7 densities, each component will then be inspected accordingly using the component modification ratio. Table 5.4 shows the result of each element (only some were shown) mainly displaying the density and Table 5.5 shows the ratio check of each component. From the inspection, it is found that 8 components have more than 30% of the elements that will experience change which were leftl, leftr, rightl, rightr, frontl, frontr, rearl, and rearr. As a result, the next step for the two groups of components will differ greatly depending on the chosen procedure.

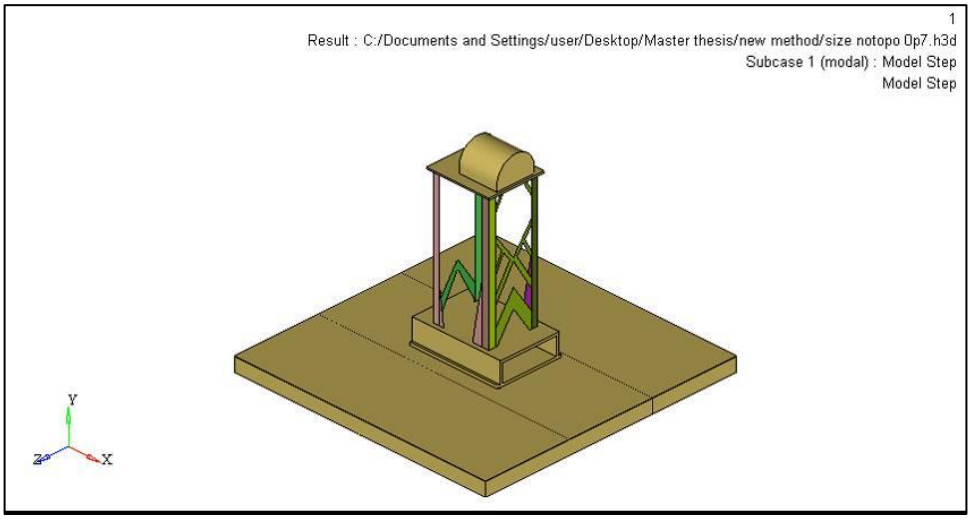

Figure 5.13: New Design with Unchanged Components

First attempt was done by directly applying the result from the topology optimization onto the components with ratio above the threshold value (Figure 5.13) without any subsequent optimization. The other components will not be altered from the original at all. The main advantage from this attempt is that only some component will be changed rather than the entire design space. No new parts or modification is needed for all the legs, though the middle components would still need to be fabricated and applied onto the original model. The first natural frequency and the volume obtained from the new design were 17.73 Hz and 9.646×10^6 mm^3, respectively.

Another approach is to utilize size optimization onto the unchanged components. By doing this, improvement on the stiffness of the structure can be done while still maintaining the form of a common angle beam only with different thickness.

At this point, another drawback that arises is that the component that was redesign from the topology optimization result will be rendered impractical as results from FEA optimizations tend to be very specific in regards to the initial design space and arrangement. Since some of the components was set not to change from the topology optimization or in other words

was set as a non-designable space, a better approach is to run topology optimization again on the components with ratio above the threshold value (Figure 5.14). Thus ensuring that the new result will be applied according the new configuration of the optimization.

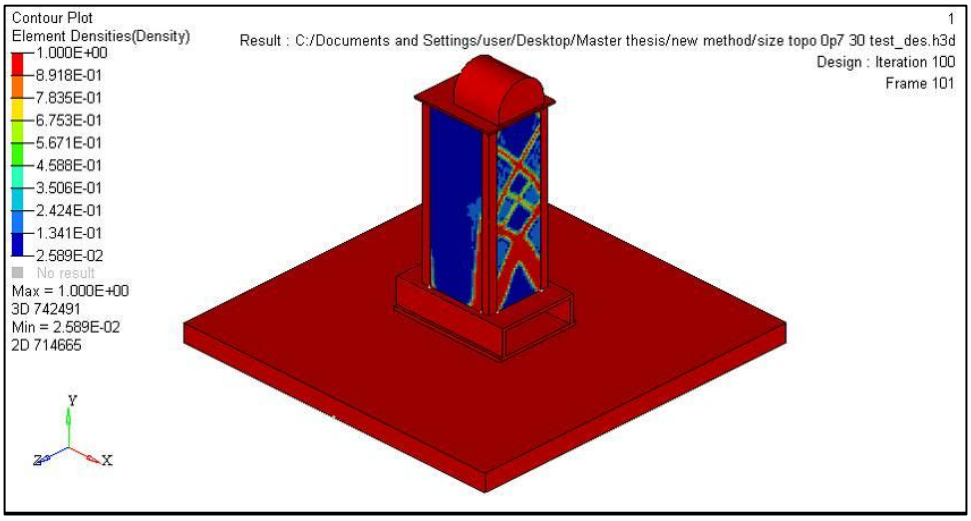

Figure 5.14: Second Topology Optimization after Component Check

To finish off the optimization method, all the components will either go through another size optimization to find the best thickness or left unchanged on the original thickness which is 3 mm. This is done to satisfy both occurrence of altering the original angle beam with a new thickness while also finding the thickness of the new reinforcement material added through the middle part after undergoing topology optimization.

Table 5.6: Results from Each Approach

Comp < Threshold	Comp > Threshold	First ω_f (Hz)	Volume (m^3)
Left Unchanged	Follow design according to topology result	16.14	0.00981
Size Optimization		16.18	0.00985
Left Unchanged	Redo Topology with new design space	17.56	0.00970
Size Optimization		17.72	0.00956

From the result of all the steps after singling out the components according to the modification ratio, the result of natural frequency of the first mode and the volume of the structure were recorded in Table 5.6. It is shown that by redoing the topology optimization

and combining it with size optimization, a much better result of both the frequency and volume can be found.

Then, the same method was applied onto the second structure which is the BIW. The previous analysis only involves shell element, so no other revision were made to the earlier model. So, the model will then go through the combination of optimization process where some components only go through topology optimization while others will only go through size optimization. The set components were split by calculating the percentage of the changed element in a single component after topology optimization using the component modification ratio (Equation 5.1). Hence, components with a large change of elements will only undergo size optimization.

As a trial run, the setup for the topology optimization used with maximum thickness of 4 mm was used as the basis. From the topology run, the components were separated into the two categories with which optimization process will be used. The components with the most practical change were Comp 5012021, Comp 5018020 and Comp 5018022 where these three will only go through size optimization without any change to the design.

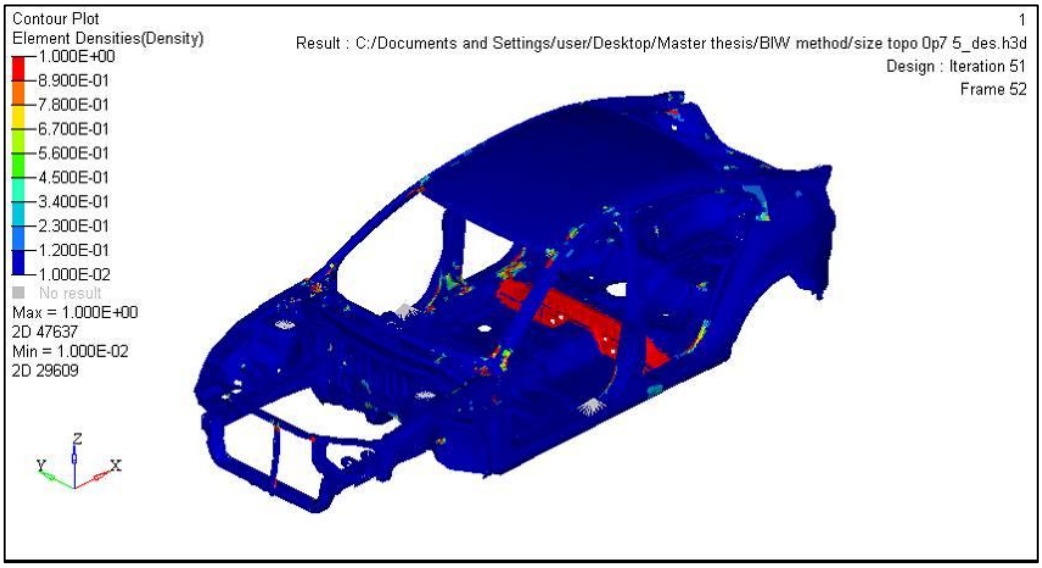

Figure 5.15: Combination of Size and Topology Optimization Result

Figure 5.15 shows the result from the optimization where both size and topology was used. The new model illustrate the points where reinforcement is needed except at the three components where size optimization was employed. The thickness of the three components changes are:

- Comp 5012021: 0.75 mm to 2.544 mm
- Comp 5018020: 1.2 mm to 1.99 mm
- Comp 5018022: 1.5 mm to 0.5297 mm

The new natural frequency for torsion mode and bending mode were successfully increased to satisfy the objective with value of 42 Hz and 60 Hz, respectively. The whole mass also increased from 275 to 295.7 kg which is about 7.5%. This reveals that the method of combining both optimizations is acceptable as it does satisfy the objective while maintaining the low mass. Then, the static stiffness test was also done to show feasibility of the approach. The result for bending stiffness shows an increase of 4.16% to 10827.2 N/mm while torsion stiffness shows an increase of 0.25% to 5497.23 Nm/deg in terms of rigidity. Thus, by combining the optimization method and in turn with using a better approach, the model should be able to be improved more in regards of its dynamic characteristics.

Chapter 6: Conclusion and Recommendations

The results from this study show that the main aim and each objective were significantly satisfied. The optimization process managed to improve the design of the structure according to the intended outcome. In addition, future recommendation to advance the work further will be suggested.

6.1 Conclusion

The modal analysis for both structures was conducted with significant accuracy after comparing the values from experimental and computational methods. For the experimental rig, where the structure is readily available, the EMA and FEA modal analysis resulted in the natural frequency values for the first 4 modes which were within the acceptable range. However, only the first natural frequency was used for the corresponding structural optimization process. Subsequently, for the BIW structure, the natural frequency for the first torsion and bending mode was found at the 7^{th} and 9^{th} mode, respectively. These two values were then used in the structural optimization process.

Using structural optimization, the first natural frequency of the experimental rig which is the first lateral bending, was maximized in order to shift the value to be larger than the normal operating frequency. Although the value did came short from the intended result, the success of increasing the value shows that the method is satisfactory. The process was conducted by either changing the design or adding reinforcement onto the original structure. For the BIW, the frequency for both the first torsion and bending mode were increased to the set value of 40 Hz and 60 Hz, respectively, by reinforcing certain part of the structure. In each case, there exist a few drawbacks from the process such as added

volume or mass, manufacturing constraints, and stress concentrations that can be resolved by introducing additional methods.

The structural optimization methods also show the distinction of using computationally focused methods versus using conventional methods that relies on the knowledge of the user such as trial and error. The structural optimization methods have been shown to reliably present an optimum design in each case within a predictable timeframe while trial and error method would only provide a pseudo-optimum design within an indefinite amount of time depending on the skill of the user.

There were a number of different strategies employed in order to further improve the design of the structures. Even though these approaches resulted in various values for the frequency, each has their own advantages and disadvantages. Moreover, more advanced optimization process such as combining optimization techniques and running them simultaneously. Therefore, with all the different strategy, the final design for both structures can be decided based on the results.

6.2 Recommendations

There are certain possible manners in which the optimization approach can be improved upon such as using multi-objective optimization. The study also only involved single flexible structure that is rigidly connected so the process of optimizing the structure is much simpler. By introducing flexible multi-body dynamic structure into the optimization process, the method can be performed for more complex structure such as machines with moving components.

References

Ahmadian, M. (2010). Closed-Form Analysis of Vehicle Suspension Ride and Handling Performance. *Non-Smooth Problems in Vehicle Systems Dynamics*, 29-40. doi: Doi 10.1007/978-3-642-01356-0_3

Arora, J. S. (1993). Sequential linearization and quadratic programming techniques. *Structural Optimization: Status and Promise, AIAA*, 71-102.

Bendsoe, M. P., & Rodrigues, H. C. (1991). Integrated Topology and Boundary Shape Optimization of 2-D Solids. *Computer Methods in Applied Mechanics and Engineering, 87*(1), 15-34.

Bendsøe, M. P., & Sigmund, O. (2003). *Topology optimization : theory, methods, and applications*. Berlin ; New York: Springer.

Bernhard, R. K. (1943). *Mechanical vibrations, theory and applications; an introduction to practical dynamic engineering problems in the structural field*. New York, Chicago,: Pitman Publishing Corporation.

Billah, K. Y., & Scanlan, R. H. (1991). Resonance, Tacoma Narrows Bridge Failure, and Undergraduate Physics Textbooks. *American Journal of Physics, 59*(2), 118-124.

Bletzinger, K. U., & Ramm, E. (1993). Form Finding of Shells by Structural Optimization. *Engineering with Computers, 9*(1), 27-35.

Bower, A. F. (2010). *Applied mechanics of solids*. Boca Raton: CRC Press.

Brandt, A. (2011). *Noise and vibration analysis : signal analysis and experimental procedures*. Chichester: Wiley.

Cawley, P. (1986). The Accuracy of Frequency-Response Function Measurements Using Fft-Based Analyzers with Transient Excitation. *Journal of Vibration Acoustics Stress and Reliability in Design-Transactions of the Asme, 108*(1), 44-49.

Cea, J., Garreau, S., Guillaume, P., & Masmoudi, M. (2000). The shape and topological optimizations connection. *Computer Methods in Applied Mechanics and Engineering, 188*(4), 713-726.

Cempel, C., & Tabaszewski, M. (2007). Multidimensional condition monitoring of machines in non-stationary operation. *Mechanical Systems and Signal Processing, 21*(3), 1233-1241. doi: DOI 10.1016/j.ymssp.2006.04.001

Chen, B. C., & Kikuchi, N. (2001). Topology optimization with design-dependent loads. *Finite Elements in Analysis and Design, 37*(1), 57-70. doi: Doi 10.1016/S0168-874x(00)00021-4

Chu, D. N. (1997). Evolutionary Structural Optimization Method for Systems with Stiffness and Displacement Constraints. [PhD]. *Victoria University of Technology, Melbourne, Australia*.

Diaz, A. R., & Kikuchi, N. (1992). Solutions to Shape and Topology Eigenvalue Optimization Problems Using a Homogenization Method. *International Journal for Numerical Methods in Engineering, 35*(7), 1487-1502.

Duffy, J. E. (2009). *Auto body repair technology* (5th ed.). Australia ; United States: Delmar Cengage Learning.

Duysinx, P., & Bendsoe, M. P. (1998). Topology optimization of continuum structures with local stress constraints. *International Journal for Numerical Methods in Engineering, 43*(8), 1453-1478.

Ebrahimi, R., Esfahanian, M., & Ziaei-Rad, S. (2013). Vibration modeling and modification of cutting platform in a harvest combine by means of operational modal analysis (OMA). *Measurement, 46*(10), 3959-3967. doi: DOI 10.1016/j.measurement.2013.07.037

Enblom, R. (2006). Two-level numerical optimization of ride comfort in railway vehicles. *Proceedings of the Institution of Mechanical Engineers Part F-Journal of Rail and Rapid Transit, 220*(1), 1-11. doi: Doi 10.1243/095440905x33279

Entwistle, K. M. (2001). *Basic principles of the finite element method*. London: Maney.

Fan, P. Q., & Zhao, B. (2009). Analysis of Dynamic Comfort of Automobile Seats. *Icicta: 2009 Second International Conference on Intelligent Computation Technology and Automation, Vol Iii, Proceedings*, 483-486. doi: Doi 10.1109/Icicta.2009.582

Gaul, H., Brauser, S., Weber, G., & Rethmeier, M. (2011). Methods to Obtain Weld Discontinuities in Spot-Welded Joints Made of Advanced High-Strength Steels. *Welding in the World, 55*(11-12), 99-106.

Gulyaev, V. I., & Markovskaya, E. O. (1982). Optimum Control of Non-Linear Mechanical Systems by the Method of Gradient Projection to Constraints. *Dopovidi Akademii Nauk Ukrainskoi Rsr Seriya a-Fiziko-Matematichni Ta Technichni Nauki*(11), 25-28.

Gupta, S. K., Regli, W. C., Das, D., & Nau, D. S. (1997). Automated manufacturability analysis: A survey. *Research in Engineering Design, Volume 9*(Issue 3), pp 168-190.

Haftka, R. T., & Grandhi, R. V. (1986). Structural Shape Optimization - a Survey. *Computer Methods in Applied Mechanics and Engineering, 57*(1), 91-106.

Haftka, R. T., Gürdal, Z., & Kamat, M. P. (1990). *Elements of structural optimization* (2nd rev. ed.). Dordrecht ; Boston: Kluwer Academic Publishers.

Haiba, M., Barton, D. C., Brooks, P. C., & Levesley, M. C. (2002). Review of life assessment techniques applied to dynamically loaded automotive components. *Computers & Structures, 80*(5-6), 481-494.

Hale-Heighway, B., Murray, C., Douglas, S., & Gilmartin, M. (2002). Multi-body dynamic modelling of commercial vehicles. *Computing & Control Engineering Journal, 13*(1), 11-15.

Happian-Smith, J. (2002). *An introduction to modern vehicle design*: SAE International, Butterworth-Heinemann.

Hermans, L., & Van der Auweraer, H. (1999). Modal testing and analysis of structures under operational conditions: Industrial applications. *Mechanical Systems and Signal Processing, 13*(2), 193-216.

Holzleitner, L., & Mahmoud, K. G. (1999). Structural shape optimization using MSC/NASTRAN and sequential quadratic programming. *Computers & Structures, 70*(5), 487-514.

Huang, L. P., & Yue, W. H. (2009). Reliability Modeling and Design Optimization for Mechanical Equipment Undergoing Maintenance. *Proceedings of 2009 8th International Conference on Reliability, Maintainability and Safety, Vols I and Ii*, 1029-1034.

Huang, X. D., & Xie, Y. M. (2010). Natural frequency optimization of structures using a soft-kill BESO method. *9th World Congress on Computational Mechanics and 4th Asian Pacific Congress on Computational Mechanics, 10*.

Huynh, J., Molent, L., & Barter, S. (2008). Experimentally derived crack growth models for different stress concentration factors. *International Journal of Fatigue, 30*(10-11), 1766-1786. doi: DOI 10.1016/j.ijfatigue.2008.02.008

Jamal, R., & Pichlik, H. (1999). *LabVIEW : applications and solutions*. Upper Saddle River, NJ: Prentice Hall PTR.

Jang, G. W., Choi, Y. M., & Choi, G. J. (2008). Discrete thickness optimization of an automobile body by using the continuous-variable-based method. *Journal of Mechanical Science and Technology, 22*(1), 41-49. doi: DOI 10.1007/s12206-007-1005-x

Jenkins, W. M. (1991). Towards Structural Optimization Via the Genetic Algorithm. *Computers & Structures, 40*(5), 1321-1327. doi: Doi 10.1016/0045-7949(91)90402-8

Jog, C. S. (2002). Topology design of stpuctures subjected to periodic loading. *Journal of Sound and Vibration, 253*(3), 687-709. doi: DOI 10.1006/jsvi.2001.4075

Kim, K. C., & Kim, C. M. (2005). A study on the body attachment stiffness for the road noise. *Journal of Mechanical Science and Technology, 19*(6), 1304-1312.

Kim, Y. S., Kim, E. Y., Shin, Y. W., & Lee, S. K. (2010). Vibration Transmission Reduction from a Centrifugal Turbo Blower in a Fuel Cell Electric Vehicle. *International Journal of Automotive Technology, 11*(5), 759-765. doi: DOI 10.1007/s12239-010-0090-5

Kundra, T. K. (2000). Structural dynamic modifications via models. *Sadhana-Academy Proceedings in Engineering Sciences, 25*, 261-276.

Liu, G. R., & Quek, S. S. (2003). *The finite element method : a practical course*. Oxford ; Boston: Butterworth-Heinemann.

Lu, J., & DePoyster, M. (2002). Multiobjective optimal suspension control to achieve integrated ride and handling performance. *Ieee Transactions on Control Systems Technology, 10*(6), 807-821. doi: Doi 10.1109/Tcst.2002.804121

Ma, Z. D., Cheng, H. C., & Kikuchi, N. (1994). Structural Design for Obtaining Desired Eigenfrequencies by Using the Topology and Shape Optimization Method. *Computing Systems in Engineering, 5*(1), 77-89. doi: Doi 10.1016/0956-0521(94)90039-6

Maceri, A. (2010). *Theory of elasticity*. Heidelberg ; New York: Springer.

Maia, N. M. M., & Montalvão e Silva, J. M. (1997). *Theoretical and experimental modal analysis*. Taunton, Somerset, England: Research Studies Press ;Wiley.

Michell, A. G. M. (1904). The limits of economy of material in frame-structures. *Philosophical Magazine Series 6, 8*(47). doi: 10.1080/14786440409463229

Miro, A., Pozo, C., Guillen-Gosalbez, G., Egea, J. A., & Jimenez, L. (2012). Deterministic global optimization algorithm based on outer approximation for the parameter estimation of nonlinear dynamic biological systems. *Bmc Bioinformatics, 13*. doi: Artn 90 Doi 10.1186/1471-2105-13-90

O'Connor, P. D. T., & Kleyner, A. (2012). *Practical reliability engineering* (5th ed.). Hoboken, NJ: Wiley.

Ou, J. S., & Kikuchi, N. (1996). Integrated optimal structural and vibration control design. *Structural Optimization, 12*(4), 209-216. doi: Doi 10.1007/Bf01197358

Prager, W., & J.E., T. (1968). Problems of optimal structural design. *Journal of Applied Mechanics-Transactions of the Asme*(35), 102-106.

Ramsey, K. A. (1983). Experimental Modal-Analysis, Structural Modifications and Fem Analysis on a Desk-Top Computer. *Sound and Vibration, 17*(2), 19-27.

Ravindran, A., Reklaitis, G. V., & Ragsdell, K. M. (2006). *Engineering optimization : methods and applications* (2nd ed.). Hoboken, N.J.: John Wiley & Sons.

Reddy, J. N. (1999). *Theory and analysis of elastic plates*. Philadelphia, PA: Taylor & Francis.

Renwick, J. T. (1984). Condition Monitoring of Machinery Using Computerized Vibration Signature Analysis. *Ieee Transactions on Industry Applications, 20*(3), 519-527.

Richardson, M. H. (1997). Is it a mode shape, or an operating deflection shape? *Sound and Vibration, 31*(1), 54-61.

Rong, J. H., Liang, Q. Q., Guo, S., & Mu, R. K. (2008). A topological optimization method considering stress constraints. *International Conference on Intelligent Computation Technology and Automation, Vol 1, Proceedings*, 1205-1209. doi: Doi 10.1109/Icicta.2008.223

Ruszczynski, A. (1980). Feasible Direction Methods for Stochastic Programming-Problems. *Mathematical Programming, 19*(2), 220-229. doi: Doi 10.1007/Bf01581643

Schedlinski, C., Wagner, F., Bohnert, K., Frappier, J., Irrgang, A., Lehmann, R., & Muller, A. (2005). Experimental modal analysis and computational model updating of a car body in white. *Proceedings of ISMA 2004: International Conference on Noise and Vibration Engineering, Vols 1-8*, 1925-1938.

Schmit, L. A. (1960). Structural design by systematic synthesis. *Proceedings of the 2nd conference on Electronic Computation, New York.*

Spall, J. C. (2003). *Introduction to stochastic search and optimization : estimation, simulation, and control*. Hoboken, N.J.: Wiley-Interscience.

Sugahara, Y., Kazato, A., Koganei, R., Sampei, M., & Nakaura, S. (2009). Suppression of vertical bending and rigid-body-mode vibration in railway vehicle car body by primary and secondary suspension control: results of simulations and running tests using Shinkansen vehicle. *Proceedings of the Institution of Mechanical Engineers Part F-Journal of Rail and Rapid Transit, 223*(6), 517-531. doi: Doi 10.1243/09544097jrrt265

Thorby, D. (2008). *Structural dyncamics and vibration in practice : an engineering handbook*. Boston, MA: Elsevier.

Xu, C. S., Yi, H. H., & Huang, C. X. (2006). Experimental study of vehicle modelling and ride comfort simulation based on the topology structure analysing. *ISDA 2006: Sixth International Conference on Intelligent Systems Design and Applications, Vol 3*, 197-201.

Yagawa, G., Aizawa, T., & Ando, Y. (1981). Linear and Non-Linear Elastic Analysis of Cracked Plate - Application of a Penalty-Function and Superposition Method. *International Journal for Numerical Methods in Engineering, 17*(5), 719-733. doi: DOI 10.1002/nme.1620170506

Zheng, Z. C., Guo, D., Zhang, Y. J., & Hou, Z. C. (2001). Dynamic analysis of large-scale flexible systems for free-free space structures. *Philosophical Transactions of the Royal Society of London Series a-Mathematical Physical and Engineering Sciences, 359*(1788), 2209-2229.